Copy No. 6

FINAL REPORT

UTILIZATION OF RADAR IN SHORT RANGE FORECASTING

Contract No. N189s-88164

5 August 1953

ILLINOIS STATE WATER SURVEY

AT

UNIVERSITY OF ILLINOIS

URBANA, ILLINOIS

FINAL REPORT

UTILIZATION OF RADAR IN SHORT-RANGE WEATHER FORECASTING

Contract No. N189s-88l64

The research reported in this document has been made possible through support and sponsorship extended by the Bureau of Aeronautics Project AROWA, Naval Air Station, Norfolk, Virginia, under Contract No. N189s-88164. It is published for technical information only, and does not necessarily represent recommendations or conclusions of the supporting agency.

Prepared by

H. W. Hiser and S. G. Bigler

G. E. Stout, Group Leader

A. M. Buswell, Chief

5 August 1953

UTILIZATION OF RADAR IN SHORT-RANGE WEATHER FORECASTING

TABLE OF CONTENTS

PART III CASE STUDIES

PREFACE

This manuscript is to be considered the final report covering one ??ear'sresearch by the Illinois State Water Survey on the operational use ??f radar as a weather forecasting aid under BuAer contract number ??189s-88l64. The material is presented in a manner so that the sponsoring agency may publish it as an Aerology bulletin.

Additional research is needed for further development and refinement of techniques in the field of radar weather forecasting. More accurate determinations of echo intensity as related to other weather phenomena should be pursued.

It was decided to include the first section of the report even though there are several other articles available. Only those factors affecting the use of radar in meteorological work are discussed. The , forecaster must.become thoroughly familiar with the characteristics of his radar set before proper interpretations of the scope can be made.

The authors are indebted to Floyd A. Huff for editing, to Glenn E. Stout for valuable assistance and to Duane Yetter and Donald Worden for much of the plotting and calculations. The authors are also indebted to Dr. H. R. Byers of the University of Chicago, Department of Meteorology, for reviewing the report.

All scope photographs appearing in this report were made with the Water Survey's APS-15 radar.

ABSTRACT

The radar data used in this report were collected with a modified APS-15, 3-cm radar during the period 1950-52. This radar set was equipped with an automatic gain reduction device which afforded a method of measuring echo intensity. Surface and upper air observations by the U. S. Weather Bureau stations in Illinois and rainfall records from a 95 square mile raingage network were used for correlation purposes.

Radar characteristics, radar scope interpretations, radar performance factors and limitations, and desired radars and operational aspects are discussed in Part I.

Part II of the report deals with the study of the utility of radar in: the determination of upper-level winds; the prediction of rainfall intensity; the calculation of visibility during rainfall; and the determination of squally winds.

Sixty-nine cases of radar echo movements were correlated with the winds aloft. The echoes were classified into two groups: one of elements of squall lines and one of isolated echoes. The movements of the echoes were correlated with the mean wind for three layers: 2000-20, 000 ft; 2000-26, 000 ft; and 6000-30, 000 ft; and with winds at three specific levels: 6000 ft, 10, 000ft, and 20,000 ft. Standard errors of estimate were computed for each of the layers and levels to obtain an estimation of the accuracy of the wind determinations. A list of rules for increased accuracy of wind determinations is presented. Nomograms for operational use are also included.

A graph based on theoretical calculations by Wexler was constructed which gives the theoretical rainfall intensity produced by an echo at a given range. Quantitative comparisons were made between the theoretical graph values and the actual measured rainfall produced by echoes over the raingage network. Results indicate that more research is needed on effects of drop size distribution and attenuation on 3-cm wavelength radar in order to develop accurate equations for rainfall determination from such radar.

Percentage reductions in visibility produced by various intensities of showers and thundershowers were computed from surface observations taken at nine Weather Bureau and Air Force stations in Illinois. Percentage reductions in visibility can be applied to showers of different intensities as observed on the radar. In this manner, the visibility reduction to be expected with the passage of a shower of a given intensity can be determined from radar.

The determination of squally winds from radar echoes remains largely qualitative due to the lack of good wind data associated with echoes of measured intensity. Comparisons of wind gusts and shower intensities were made from Weather Bureau surface observations taken at stations in the range of the radar. The results as expected indicate that the average and

??eak gusts from heavy showers and thunder showers are considerably ??igher than those from light or moderate intensities of showers and ??hunder showers. The findings of the Thunderstorm Project (8) were ??f great value as supplementary information in this study.

Part III of this report gives special case studies of specific storms which were made to aid in training aerologists in the use of radar. These studies show the good relationships which exist be- ??ween synoptic conditions and radar data, and illustrate how each ??an aid in proper interpretation of the other. These cases also show ??hat considerable weather can exist undetected by the present networks ??f surface observation stations, such as those in the Midwest. By the ??se of radar the forecaster is able to keep a constant vigilance over, ??he weather in areas lacking reporting stations and to watch for new levelopments.

INTRODUCTION

The advent of radar has provided the field of Aerology with one of its ??st useful tools for keeping continuous vigilance over the weather in time ?? space. As an analysis and forecasting aid to aerologists, who are quently exposed to operational forecasting with very limited synoptic a, radar has proved to be extremely valuable.

The possibilities for application of radar to Aerology were recognized World War II soon after the equipment became generally available. In the ??t few years it has become a regular part of weather observing and fore- ??ting systems; however, development of specific forecasting techniques ?? not yet been pursued sufficiently to permit effective utilization of radar the operational forecaster.

The purpose of this report is to demonstrate quantitative techniques the operational use of radar in weather forecasting. The examples are ??ited to the use of PPI (Plan-Position Indicator) radar.

PART I

RADAR CHARACTERISTICS

principles of Radar

A radar set emits a short, intense pulse of electro-magnetic energy ch is confined within a narrow beam as it travels outward. If a target ??rcepts the beam, some of the energy contained in the pulse is reflected. mall portion of the reflected energy returns as an "echo" to the point of transmission, where it is received, amplified, and presented on differ- types of scopes. The range of the target is determined by the elapsed e between transmission of the pulse and its return as an echo. The muth of the target, with respect to the radar set, is given by the direction vhich the beam is pointed. Raindrops act as scatterers of the radar beam her than direct reflectors; each individual drop returns a part of the iated pulse to the radar. (1) (2) The process is sometimes called Rayleigh ttering after Lord Rayleigh who studied the effect in great detail 40 years

scope Presentations

There are three common types of scope presentations of radar echoes ch are valuable for aerological use. These are the Plan-Position Indicator (I), Range-Height Indicator (RHI), and "A" scope. The PPI scope gives a izontal plane projection of the echoes so that a map can be drawn with the ar station at the center. As the radar antenna turns in azimuth, a syn- onous sweep line rotates on the PPI scope. When the beam intercepts a get, a bright spot appears on the sweep line at a radial distance corre- nding to the range of the target. The face of the scope is coated with a sphorescent material, which continues to glow for a few seconds after the ??ep has passed, thus preserving between sweeps the impression of the get on the scope.

The RHI scope presents a vertical cross section of the echo along the muth on which the antenna is pointed. This type of presentation requires antenna which scans in the vertical as well as sweeping in azimuth.

The third type is an "A" scope in which the electron stream sweeps ??rally, tracing out a fixed ho rizontal time base on a screen. If a signal letected by the radar receiver at any instant during the sweep, the elec- n stream is deflected vertically by an amount corresponding to the signal ength. Targets which are intercepted by the beams appear as vertical tuberances (pips) on a horizontal base line. The base line is calibrated ectly in range. "A" scopes are generally used to accompany PPI and RHI pes, and are useful in detecting very weak echoes, and in tuning the radar eiver.

??ar Equation

The following equation gives the average power received from a ??ttering-type echo which completely fills the radar beam with spheres ??niform diameter (3) (4):

$$. 1) \quad P_r = \frac{C[P_t G^2 \lambda^2 \phi \theta h K a]}{R^2} \quad \text{or} \quad \frac{P_r R^2}{P_t} = C'[ND^6]$$

·re $C' = C(G^2 \lambda^2 \phi \theta hK)$ and $(ND^6) = a$ = function of rainfall intensity in inches/hr.

ıbol	Quantity	Values for* Modified APS-15
R	Range of the targets	.....Km
ı	Reflectivity per unit volume of storm	.....Cm^{-1}
K	Attenuation factor depending on media	Dimensionless Const.
C	Constants of proportionality for units used	6.1×10^{-16}
P_t	Power transmitted	9 to 14 x 10 watts
P_r	Minimum detectable signal	5 x 10-13 watts
ı	Pulse length	300 meters
N	Number of drops/unit volume	
D^6	Sixth power of drop diameter	
λ	Wave length	3.2 cm
ϕ	Beam width (horizontal)	2.5 degrees
θ	Beam width (vertical)	2.9 degrees
G	Antenna gain	Dimensionless

This equation is applied later under "Precipitation Intensity Measure- ??ts", where values for R, Pr, and Pt are used to solve for the reflectivity ??n raindrops.

Targets in the form of scattering particles such as rain clouds have ??aracteristic not common to other types of targets, namely, they can be ??etrated by the radar beam. Thus it is possible to view the rain-cloud ??oes in depth and to see one behind the other. The precipitating clouds do ??ever, attenuate, that is, reduce the intensity of the beam so that there ??limit to the penetration. This attenuation will be discussed in detail in ??tersection.

It is interesting to note that the smallest cloud particles detectable ??adar methods at ordinary ranges and at 3-to 10-cm wavelengths are ??r those that have an appreciable fall velocity and are therefore classified ??recipitation.

---

values are for the radar set used by the Illinois State Water Survey in this ??search.

??ar Wavelengths for Weather Use

The military services and other organizations have used both 3-cm 10-cm wavelength radars for storm detection. The 3-cm is more sitive than the 10-cm for this purpose. The 3-cm wavelength presents ??-defined echoes but attenuates too much when solid lines of heavy echoes present and when widespread light rain exists. This attenuation some-??es results in a failure to detect showers behind a solid line of echoes ??ring toward the radar station, or failure to detect the extent of widespread ??train. The 10-cm radar has the advantage of penetrating through heavy ??es and extensive areas of rain. It is favored for hurricane and thunder-??m tracking. However, it fails to give the desired definition in many ??es and fails completely to detect light showers.

Probably the best wavelength for weather radar operations lies in 5-6 cm band because attenuation is negligible and good definition can be ined. Research and development of these more desirable wavelengths ?? progress in the military services.

RADAR SCOPE INTERPRETATIONS

??king by Obstructions

Radar sets operating from both shipboard and land stations might be ??ect to blocking. Nearby superstructures, buildings, or mountains pro-??ing into the beam result in blank segments or shadows in which weather ??ot be detected. In Figures la and lb, blocking effects can be noted due ??eesto the south and to another radar antenna to the southwest.

Return and Ground Clutter

Echoes from the sea near the radar set show a greater resemblance recipitation echoes than those from solid fixed land targets. Visual ob--ation at close range from the ship will usually afford a means of checking ther the echoes are sea echoes or precipitation.echoes. Sea echoes ??lly show random variation to a more marked degree than precipitation ??es (5).

Buildings, trees, hills, and even slight undulations in topography in ??vicinity of the radar station appear as "ground clutter" when the antenna ??inted horizontally or at low elevations. Ground return is usually more ??e and has more well-defined edges than precipitation echoes on a PPI ??e. On the "A" scope ground clutter gives strong, steady pips rather the fluctuating variety produced by precipitation. After precipitation occurred, the ground clutter is often more extensive. Some of the more ??ant isolated ground targets are ideal for orienting radars on land if these

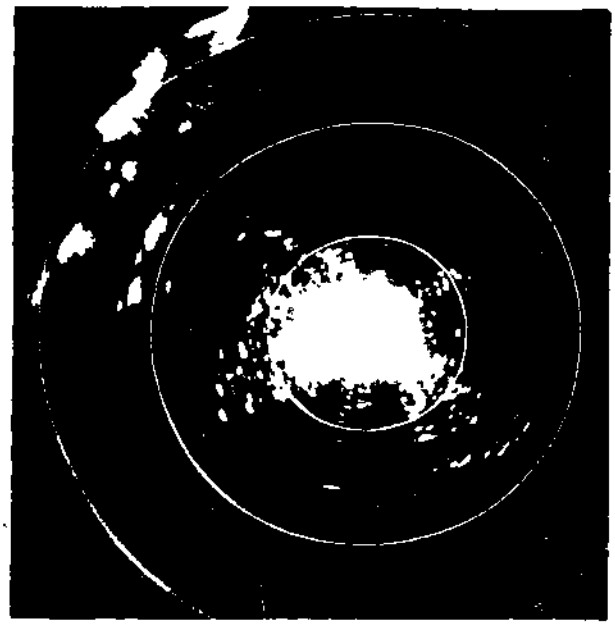

A. GROUND CLUTTER 8/9/52, 10 MILE RANGE MARKERS. PRECIPITATION W. AND NW. 20 TO 30 MILES.

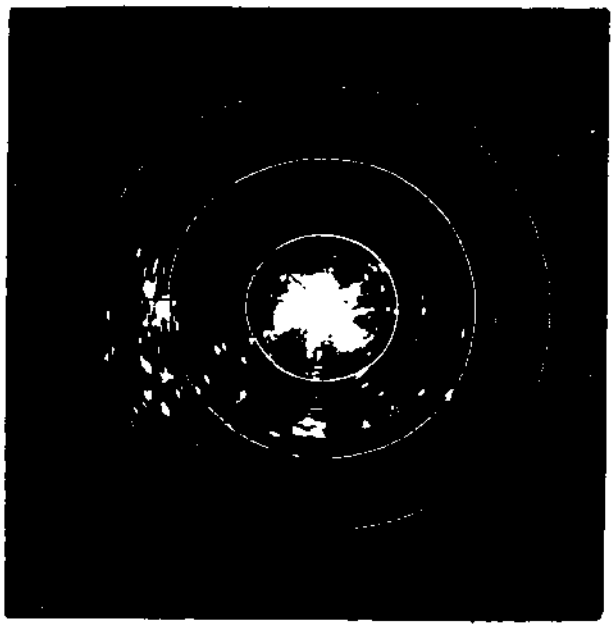

C. ANOMALOUS PROPAGATION 7/21/52, 20 MILE RANGE MARKERS. GROUND CLUTTER IN CENTER WITH BLOCKING S. AND SW.

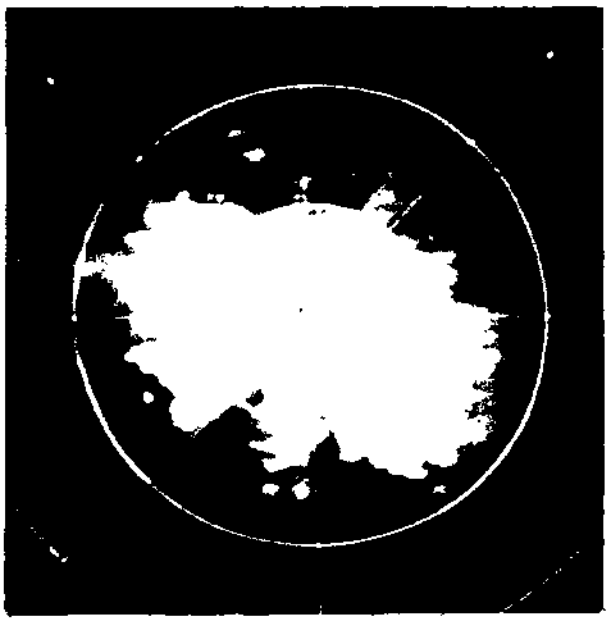

B. PRECIPITATION ATTENUATION 4/24/53, 10 MILE RANGE MARKERS. LOCAL OBSTRUCTIONS BLOCKING S. AND SW.

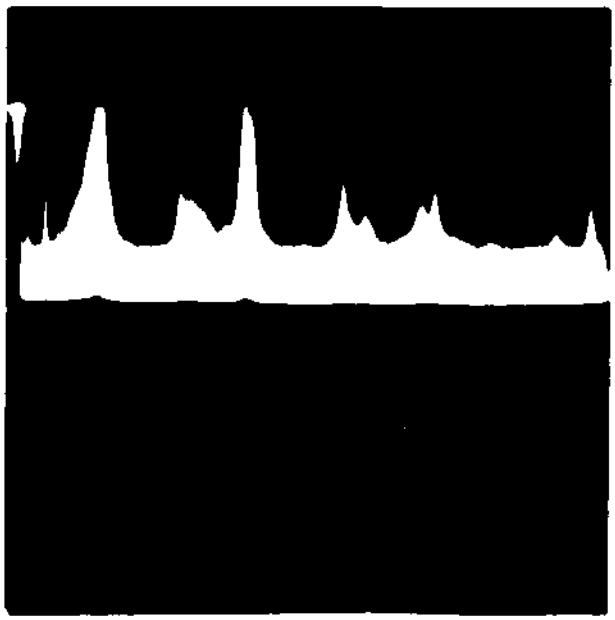

D. "A" SCOPE SHOWING SHORT FUZZY PRECIPITATION ECHOES MOSTLY ON THE RIGHT AND TALLER HEAVY PIPS PRODUCED BY GROUND TARGETS TO THE LEFT.

FIG. I RADAR SCOPE PHOTOS

targets can be identified on a map of the area. Figure la shows the ground clutter around the Water Survey's radar station. Some small precipitation echoes appear 20 to 30 miles west and northwest of the station.

Attenuation

Attenuation is the loss of energy by the radar beam due to absorption or scattering while traveling to and from the target. There are two types: one due to precipitation and the other due to range.

Precipitation. The greatest attenuation is produced by the raindrops themselves. When the radar beam passes through a distribution of water drops, some of the energy is scattered in all directions and some is absorbed. The amount of scattering and absorption depends upon the size, concentration of the drops and upon the frequency of the radar signal. Scattering is necessary if the disturbance is to be detected, but absorption decreases the depth of penetration.

When the attenuation is small, it is possible to see through nearby precipitation areas and to observe heavier precipitation echoes beyond these. When pronounced attenuation occurs on a 3-cm wavelength radar, a precipitation area may be obscured by another which lies between it and the radar set, or a given disturbance may not be detected to its full radial depth. Figure lb is an example of precipitation attenuation when a rainfall rate of 0. 24 in/hr was occurring at the radar station. Attenuation can usually be distinguished by the feathered edges and faded-out appearance of the edge of the echo with increasing range.

Range. Range attenuation results from divergence of the transmitted beam so that the beam is not filled in cross section by an echo at considerable range. If the target has uniform reflectivity throughout its cross section, the total reflected power remains constant over the range in which the beam is completely filled. Beyond this range, the fraction of the beam occupied by a target of given size decreases as the square of the distance. The energy scattered by the target also diverges so that the power density along the return path from the target decreases as the square of the distance.

Range attenuation must be taken into account when estimating storm intensities. This factor will be discussed under "Precipitation Intensity Measurements".

The portion of a storm which lies below the horizon increases with range and becomes significant at long range. The fraction of the beam filled by a storm at any given range is thereby further diminished by this earth curvature factor as the range increases.

Anomalous Propagation

Under very stable atmospheric conditions with low-level temperature inversions or high concentrations of moisture near the earth's surface, a bending of the radar beam may occur. This results in anomalous propagation when the curvature of the beam becomes equal to or greater than that of the earth. The attenuation of power with distance is noticeably diminished since the energy is not allowed to spread out (diverge) in the vertical plane. Consequently, targets which lie within the trapping layer or "duct" can be detected at unusually great ranges as in Figure 1c. In this figure small, sharply defined, elongate echoes, typical of anomalous propagation, are detected to a range of 60 miles to the west and 40 miles to the south and east.

"Sea return" may also be observed at extended ranges under such conditions. Sea return unfortunately appears very much like precipitation on either the PPI or "A" scope.

Elevation of the antenna 2 or 3 degrees will usually eliminate anomalous propagation involving land or sea echoes, or cause enough change in their position to distinguish them from precipitation echoes. Also, ground targets (solid objects) detected under such conditions can usually be distinguished from precipitation echoes by use of the "A" scope. The "V scope "pips" produced by precipitation echoes show considerably more short-period fluctuations and have a fuzzier appearance than those produced by ground targets. (Figure 1d)

Any process which tends to destroy or oppose horizontal stratification of the atmosphere is unfavorable for anomalous propagation. Therefore, anomalous propagation is not likely to occur on days when conditions are favorable for well-developed showers or thunderstorms, except after thunderstorm rain has stratified the low level air (6).

Receiver Noise

A certain amount of electronic noise is produced by the thermal activity in the electronic components of a radar set. As the receiver gain is increased, the noise level increases and appears as small randomly fluctuating pips or "grass" on the "A" scope. Any received signal is superimposed on the noise and the sum of the signal and noise must be somewhat greater than the noise alone in order to be detected. Weather echoes on the "A" scope show a random fluctuation much like the noise, except that the pips have greater amplitude. The fuzzy base line across the "A" scope in Figure 1d is produced by receiver noise.

This noise also shows on the PPI and RHI scopes as background light. This background light intensity can be controlled by the receiver gain and the scope brilliance. The receiver gain should be turned down and the scope brilliance adjusted so that the sweep is faintly visible. Then the receiver

gain should be increased until the "grass" shows on the "A" scope and a slight amount of background light appears on the PPI or RHI scope.

RADAR PERFORMANCE FACTORS AND LIMITATIONS

Stability and Calibrations

When radar is used for quantitative measure of storm intensities, occasional measurements should be made of the transmitted power and the receiver sensitivity. If the transmitted power and the receiver sensitivity of the radar vary as much as 3 decibels, then quantitative measurements of storm intensities require frequent calibrations of the radar. The ratio of receiver power to transmitted power should be calculated for different received gain settings (this will be discussed later under "Precipitation Intensity Measurements"). It is recommended that measurements of receiver sensitivity and transmitted power be made before or after each rain in order to obtain reliable data.

Refraction

As a result of refraction in the lower atmosphere, the radar beam is gradually and continuously bent from a straight line path. The bending is usually downward so that energy reaches below the geometrical horizon. The extent to which the radar beam is bent depends upon the gradients of temperature and moisture in the lowest layer of the atmosphere.

Under average weather conditions the curvature of the rays is less than that of the earth and the horizon distance is increased by about 15 per cent. Line OB in Figure 2 illustrates this bending of the beam for a radar antenna located on the earth's surface with the beam directed horizontally. OA is a horizontal line and the upper curve shows the bending of a radar beam tilted upward 1 degree.

Beam Width

From the earlier discussion of range attenuation resulting from divergence of the beam, it became obvious that a radar for quantitative weather use should have a beam as narrow as possible (3 degrees or less) so that relatively small storms will fill the beam at long ranges. The radar equation assumes the beam to be filled. For qualitative weather surveillance wider beam widths are nevertheless usable.

DESIRED RADARS AND OPERATIONAL ASPECTS

Usage of PPI, RHI, and "A" Scope Presentation

The PPI type of presentation has the widest range of uses in Aerology. Because it gives a horizontal plane or map-type projection, the areal extent,

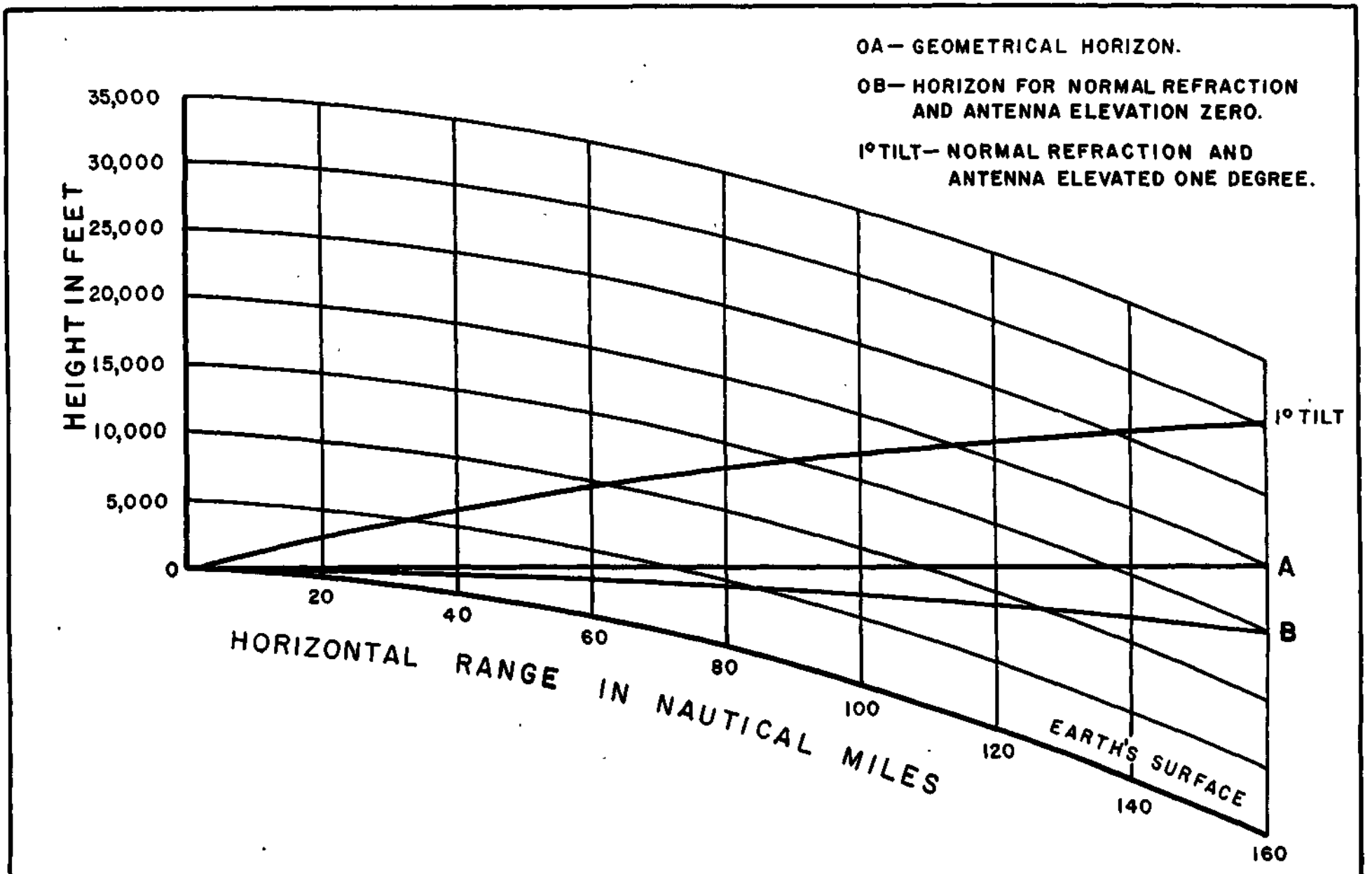

FIG. 2 RANGE—HEIGHT DIAGRAM FOR CENTER OF RADAR BEAM

except as sometimes affected by attenuation, and the direction of movement of precipitation can be ascertained with reasonable accuracy. The formation and dissipation of storms can be readily observed. Also, by the use of a variable-position, receiver-gain control or an automatic gain-reduction device, (to be described later) the intensity of the precipitation, the expected associated visibility reduction, and changes in precipitation intensity with time can be ascertained.

The RHI type of presentation has great value, especially when used in conjunction with a PPI scope. RHI radar gives the tops of echoes at extended ranges, provided the echoes are tall enough to compensate for the earth's curvature and to protrude into the radar beam. The base can also be determined at close ranges; but often when precipitation reaches the ground, the base appears at or below ground level. The use of the base and height data will be discussed under "Upper Wind Data from Radar Echoes". The vertical growth rates as indicated on RHI give some indication of the violence of the storm. RHI radar provides a useful means of identifying cumulo-nimbus clouds hidden from view by areas of light precipitation of the more stable types, as commonly associated with warm frontal overrunning. It is probable that the largest gusts experienced by aircraft in flight are associated with the edges of strong and sharply-defined columns of weather echo as shown on RHI. Also, the evidence strongly supports the belief that well-marked columns of echoes as shown on RHI are associated with strong updrafts, while well-marked troughs in the echo are indicative of downdrafts (7). Updrafts at the top can be measured roughly by noting the rate of upward growth. . It is believed that rapidly-growing tops are associated with hail(8).

The "A" scope is ideal for use in conjunction with either an RHI or PPI scope. As pointed out previously, it is a valuable aid in tuning and in identifying precipitation echoes and ground targets.

When tuning the radar receiver manually, the antenna should be stopped while pointing at some fixed ground target. The receiver tuner should then be adjusted so that the "pip" on the "A" scope produced by the ground target is at its maximum height.

Receiver-Gain Controls

The receiver-gain controls the intensity of the echo image on the PPI scope. By reducing the receiver-gain, the weaker echoes can be obliterated from the scope, thus affording a method of measuring the storm intensity.

Prior to the development of the automatic receiver-gain control, only two methods of obtaining echo intensities were known to be in general use. One method employed a manually controlled calibrated gain dial; the other used video-inversion circuits. (3) (9).

Calibrated Receiver-Gain Dial. This method merely requires replacing the regular receiver-gain control knob with a calibrated dial so that the receiver-gain could be accurately controlled. The dial was calibrated in terms of echo power necessary for the threshold of visibility on the PPI scope. The radar operator changes the gain to various settings in order to measure the relative intensity of the storm (9).

Video Inversion. The video inversion method of measuring storm intensity presents the storm structure as alternate bright and dark bands. The light rain around the outside of the storm appears bright, while the heavier rain appears as a dark area in the center of the storm (9).

Automatic Receiver-Gain Control. The basis of the automatic gain control circuit is a multiple-positioned "stepping switch" that reduces the receiver-gain by fixed steps (10). An antenna switch is used to control the stepping switch and can be used to trigger a scope camera if desired.

A selector circuit enables the radar operator to select the number of steps the circuit will automatically scan. The stepping circuit provides a maximum of 10 steps. With increased range, fewer steps will be required to reduce a given rainfall rate to the threshold of detection on the radar scope due to the range effect on scattering of the energy.

This automatic system is particularly valuable for use with a scope camera, whereby a continuous record of the storm intensity can be made with short intervals of time between photographs. Figure 3 shows a series of photographs of a squall line using j 7 gain steps.

Regardless of the gain-reduction method used, there should be a fixed initial setting for the receiver-gain to aid in proper interpretation of the s cope.

Plotting Devices

Research in radar Aerology usually makes use of photographs of the scopes which are enlarged for processing at some later date.

Operational usage of radar makes it mandatory to plot the scope data in some fashion in order to keep a current record and to check on the movement and development of echoes. Because most radars use small PPI and RHI scopes, some device for enlarging these presentations is desirable. This is especially true for PPI presentations when it is desired to track echoes for determining upper level winds. Four methods that might be employed are:

First, freehand plottings of the radar echoes can be made in pencil on some type of plotting chart using range and azimuth as a means of orientation. A plastic overlay can be used which shows surrounding towns and

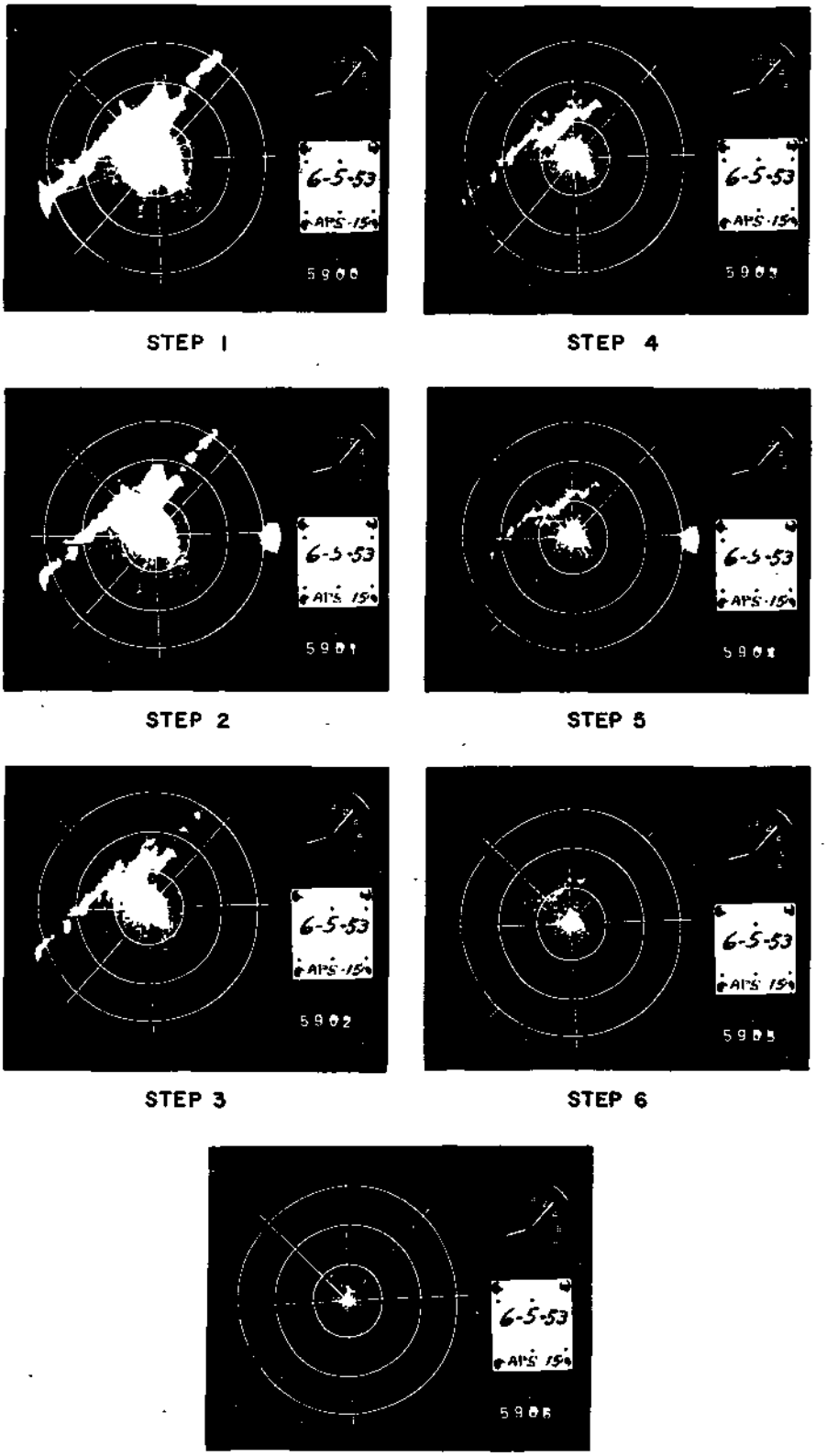

FIG. 3 RAIN INTENSITY PATTERNS AS PRESENTED ON THE PPI SCOPE WITH THE AUTOMATIC SENSITIVITY CONTROL

other land marks which aid in interpretation if the radar station is on land. The main objections to this system are the possibilities for error in orientation, and the difficulty of showing the details which often indicate growth or decay.

Secondly, an optical comparator can be used which permits the operator to view the scope and plotting board independently by means of lenses, prisms, and eye pieces which make the scope face and plotting board appear synonymous (11). A plotting board adjusted for at least a 24-inch projection of the scope presentation is desirable. This will allow for tracing of details and make it easy to track echoes for determining upper wind data. With this system the tracings can be made in pencil and filed for future reference. This system is somewhat simple in construction and avoids the maintenance problems of an electronic device.

A third method employs a polaroid oscilloscope camera, such as the Fairchild Model F-284, which will produce a finished black and white scope photograph in about one minute. These can be blown up to more desirable sizes by use of an opaque projector. This method permits quick comparisons of detailed shapes and positions of echoes from photo to photo.

The fourth and most desirable type of operational projector makes use of a dark trace oscilloscope tube and has a complete control panel for its operation. The Projection Plan Position Indicator, type CG-55AFN (VG-3 Repeater), used with Navy Radar Model SP-1M, is an example of a desirable type of dark trace projector. This system provides a large plotting surface and improved accuracy with sufficient brilliance to permit detailed tracings of the weakest echoes.

Cameras for Training Purposes, Research, and "Hindcasting"

A 16-mm or 35-mm scope camera should be used at least part of the time on some shipboard radars in order to acquire good training films of storms at sea. Also, these would provide excellent material for "hindcasting" to improve techniques and for research.

The Navy type "A" scope camera is ideal for this purpose since it has a built-in clock and data card which are recorded on the film. (Figure 3). The data card also has six small lights which may be used in various combinations for recording gain step numbers. This camera can be triggered automatically by a switch on the rotating antenna. A camera control box is provided so that pictures can be taken on every scan, every second, every fourth, or every twelfth scan. For most antenna speeds, every second or every fourth scan gives sufficient details.

PART II

UPPER WIND DATA FROM RADAR ECHOES

Introduction

Forecasters are sometimes faced with the problem of determining upper wind structures when soundings are not available. Also, land stations and ships at sea, equipped for. taking upper air soundings, often cannot make balloon releases due to high winds or other adverse weather conditions at the station,, The use of radar makes limited upper wind data available under such circumstances.

Since the clouds producing showers and thundershowers are embedded in atmospheric layers of considerable thickness, both specific level winds and layer mean winds are significant. Layer mean winds are particularly valuable for operation of jet aircraft when a flat parabolic path is flown, and for firing of projectiles which travel a parabolic path, because the parabolic paths tend to integrate wind conditions through a layer.

Scope and Techniques Used

A study was made to determine the relationships between localized echo movements and the large scale wind structure as portrayed by streamline charts covering several midwestern states. The cases of echo movement were selected without regard to synoptic conditions favorable for correlation purposes in order to introduce the problems that might be encountered when only PPI radar information is available.

The study was limited to an investigation of squall lines and air mass showers during summer and fall. About 25 per cent of the cases studied occurred in the fall. Radar echo movements, as portrayed on the PPI scope, were correlated with the upper air circulation as indicated by streamline charts constructed from 6-hourly Pibal and Rawin observations made by Weather Bureau and Air Force stations over the Middle West.

Sixty-nine cases of radar echoes were investigated. The radar echoes were traced from 35-mm photographs of the PPI scope onto a base map using a recordak microfilm viewer. The echoes were classified into two groups consisting of isolated echoes and elements of squall lines. Isolated echoes are those which are not associated with a definite squall line. These frequently represent air mass showers and thunderstorms. Elements of squall lines are the individual echoes which are a part of a line or a narrow squall zone.

Figure 4 shows the vectors used to describe the motion of elements of a squall line. "A" is the component of motion parallel to the line. "B" is the normal component which gives the forward motion of the squall line. "C"

FIG. 4 SQUALL LINE
OF AUGUST 9, 1952.

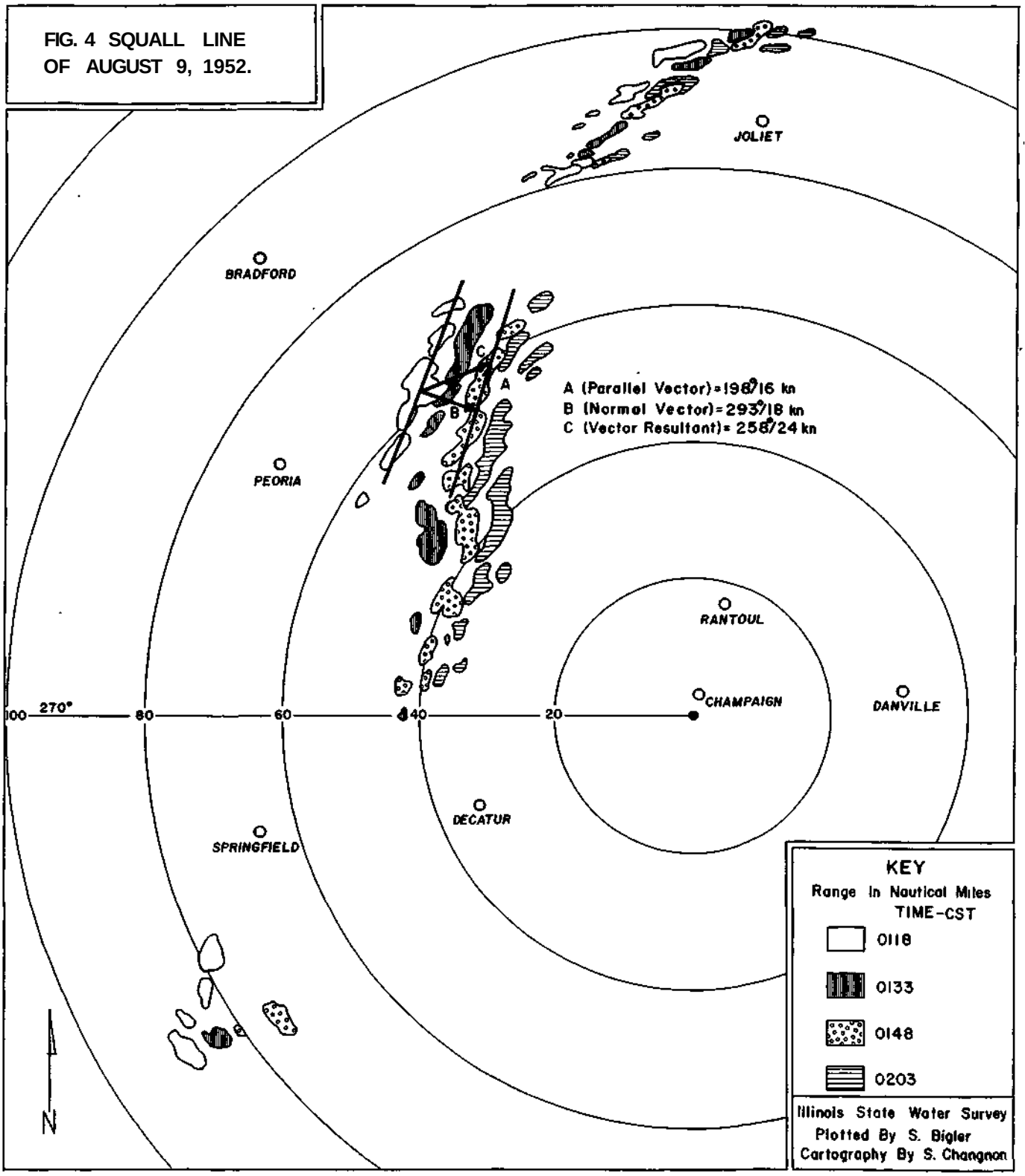

is the resultant vector which describes the actual path of an element as observed on radar. Vector "C" was correlated with the upper level winds. The echoes were identified at successive times by following the heaviest cores, as shown by the automatic gain-reduction device, or by prominent features of the echo, if gain reductions were not made.

Streamline charts, as illustrated in Figure 5 were prepared for each 2000-ft level from 2000 ft to 20, 000 ft and for the 25, 000-ft and 30, 000-ft levels. For convenience of statistical analysis data for the 2000-ft levels between 20, 000 ft and 30, 000 ft were obtained by interpolating from the charts for the 20, 000-ft, 25, 000-ft and 30, 000-ft levels.

The movements of both isolated echoes and elements of squall lines were correlated with the mean wind direction and speed for three layers: 2000-20, 000 ft, 2000-26, 000 ft, and 6000-30, 000 ft; and with the wind direction and speed for three individual levels; 6000 ft, 10, 000 ft, and 20,000 ft.

Correlation of Layer Mean Winds With Echo Movement

Thirty-four cases of the movement of isolated echoes were analyzed. Results showed about equal correlation for the combination of speed and direction for the layers, 2000-20, 000 ft and 2000-26, 000 ft. The 6000-30, 000-ft layer showed correlation with direction as good as the other layers but somewhat poorer correlation with speed (Table 1).

Figure 6 shows scatter diagrams for the relation between the movements of isolated echoes and the mean wind for the three investigated layers. The slope of the regression lines indicates that for the 2000-20, 000 ft layer, the echoes moving faster than 20 knots are moving faster than the mean wind,, For the 2000-26, 000-ft layer, the echoes moving faster than 30 knots are moving faster than the mean wind. It must be remembered that this study was concerned with the overall wind field obtained from streamline charts, and that the wind field in the vicinity of the thunderstorm may be somewhat different from the over all wind field. It is possible that local maxima of wind speeds exist in the vicinity of fast moving echoes.

Thirty-five cases of the movement of elements of squall lines were compared with the mean winds. Results show the correlation coefficients for all three layers to be about the same (Table 1).

A set of scatter diagrams similar to those in Figure 6 was constructed to show the relation between the layer mean winds and the movements of elements of squall lines. The complete set of diagrams was presented in the technical report covering the wind study (12). As in the case of isolated echoes, the elements of squall lines move faster than the winds at the higher wind speeds. In this case, propagation of the squall line may cause observed speeds to be too fast; however, in this study attempts were made to follow an individual element and to avoid following other echoes that may have developed nearby.

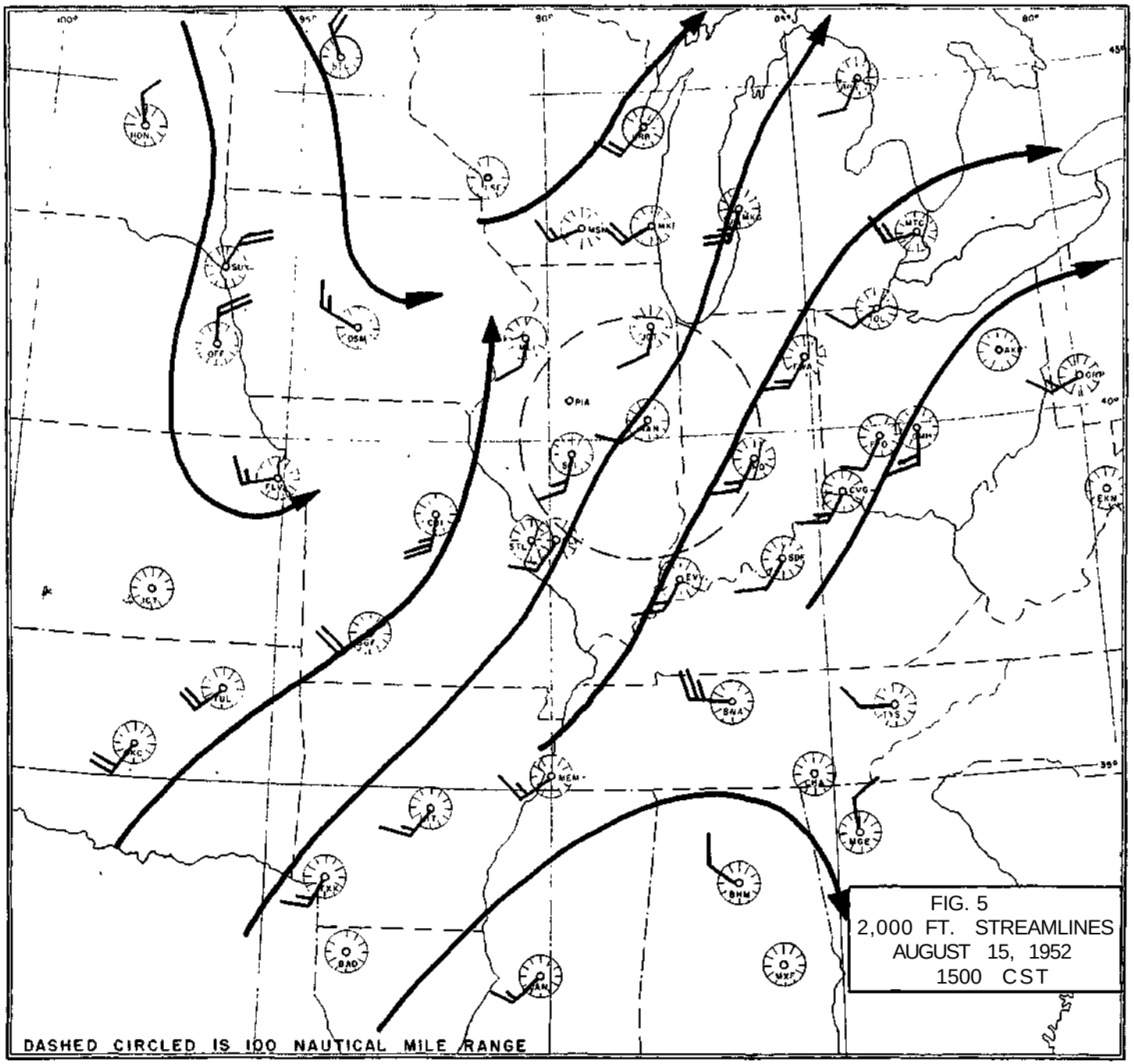

FIG. 5
2,000 FT. STREAMLINES
AUGUST 15, 1952
1500 CST

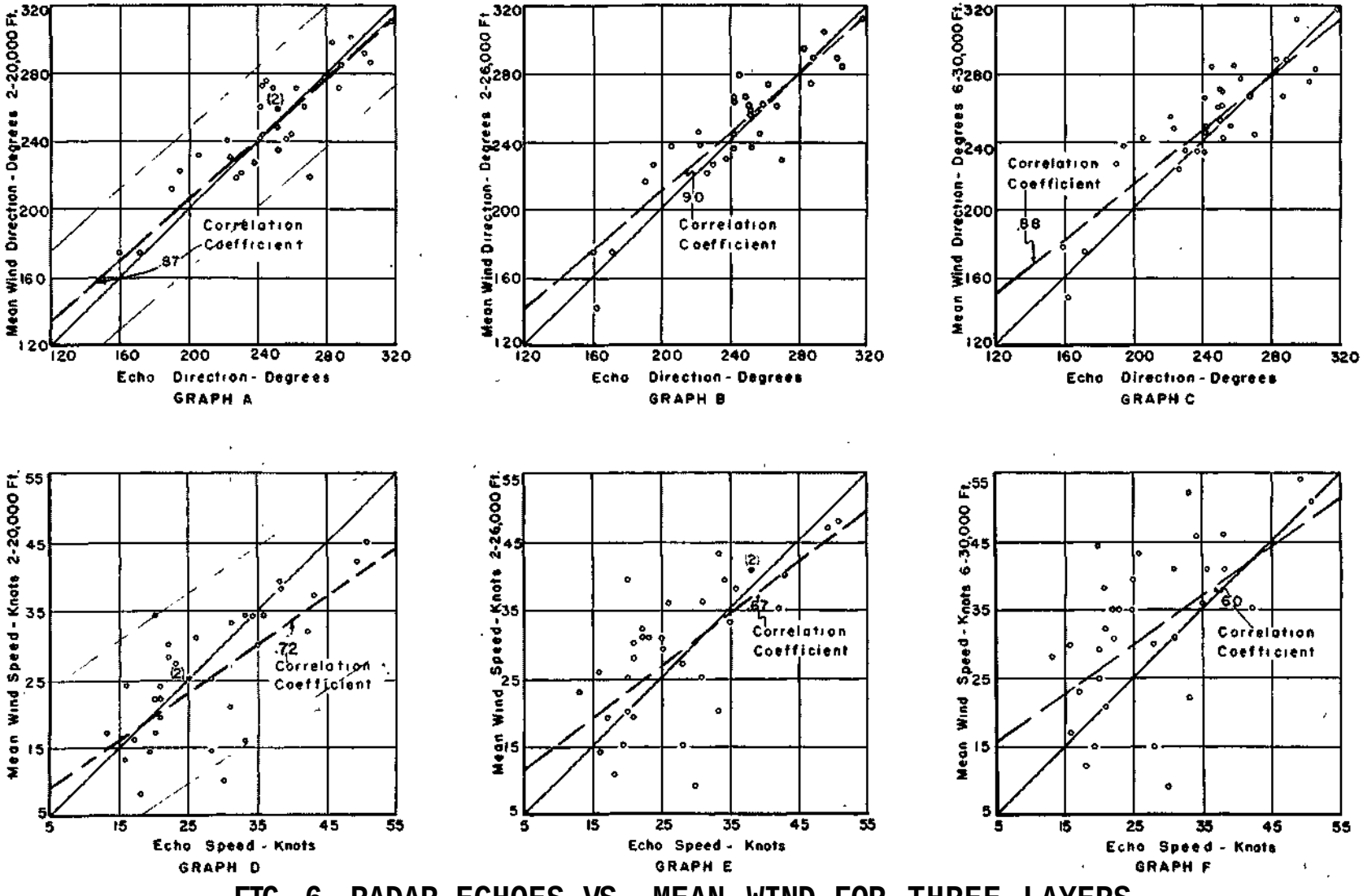

FIG. 6 RADAR ECHOES VS. MEAN WIND FOR THREE LAYERS
ISOLATED ECHOES

—— 1:1 LINE --- REGRESSION LINE

Accuracy of determinations. Standard errors of estimate were computed for each of the layers to obtain an estimation of the accuracy of the wind determinations. Values of two standard errors, or the accuracy to be expected 95 per cent of the time, are given in Table 1 along with the correlation coefficients.

These correlation coefficients and standard errors were computed from all the data and include some cases that could have been eliminated since the echoes had either high-bases or low tops. For example, a thunderstorm based at 6000 ft and extending to 35, 000 ft could not be expected to correlate well with the 2000-20, 000-ft layer.

TABLE 1

RELATION OF THE MOVEMENT CF ISOLATED ECHOES AND ELEMENTS OF SQUALL LINES WITH LAYER MEAN WINDS

		Correlation Coefficients		Two Standard Errors	
	Layer (ft)	Dir.	Speed	Dir. (deg)	Speed (Knots)
Isolated Echoes	2000-20, 000	.87	.72	±40	±13
	2000-26, 000	.90	.67	±34	±16
	6000-30, 000	.88	.60	±34	±19
Elements of Squall lines	2000-20, 000	.79	. 72	±32	±13
	2000-26, 000	.84	.73	±26	±13
	6000-30, 000	.82	. 72	±26	±15

Presenting the data in this manner shows the maximum error to be expected if only PPI radar data are used for upper wind determinations. It is to be expected that greater accuracy will be achieved when supplementary data from RHI radar and surface *weather* observations are available.

Correlation of Winds at Specific Levels with Echo Movements

The correlation of the movement of isolated echoes with the wind at specific levels was not as good as with the layer mean winds. This is not surprising since the cumulus-type cloud is embedded in a somewhat thick atmospheric layer and should be steered by the winds in this entire layer rather than by the wind at one specific level. The winds at 10, 000 ft gave the best correlation considering both speed and direction (Table 2). The 6000-ft and 2 0, 000-ft winds show good correlations with direction but poorer correlations with speed.

Figure 7 shows the scatter diagrams for the relation between the isolated echo movement and wind velocity at the three investigated levels. These diagrams exhibit the same general distribution as the diagrams in Figure 5. At speeds exceeding 20 knots, the echoes generally move faster than the wind at the 6000-ft and 10, 000 ft levels but slower than the v/ind at the 20, 000-ft level.

As with isolated echoes, the correlation of the movement of elements of squall lines with the wind at specific levels was not as good as with the layer mean winds. The correlation coefficients indicate that these echoes are better suited to determining the 10, 000-ft winds than the 6000-ft or 20, 000-ft winds. (Table 2)

The scatter diagrams for these relationships will not be reproduced here since they are similar to those in Figure 7, and are available in the technical report covering the wind study (10). The diagrams indicate the same relationship between echo speed and wind speed, as in Figure 7. The echoes traveling at more than about 20 knots move faster than the wind speeds in the overall wind field. The propagation of the squall line, already mentioned, may be the eause of these faster speeds.

Accuracy of determinations. Standard errors of estimate were also computed for each of the levels to obtain an estimation of the accuracy of the wind determinations. Table 2 gives the values of two standard errors of estimate and the correlation coefficients.

T ABLE 2

RELATION OF THE MOVEMENT OF ISOLATED ECHOES AND ELEMENTS OF SQUALL LINES WITH WINDS AT SPECIFIC LEVELS

	Levels (ft)	Correlation Coefficients		Two Standard Errors	
		Dir.	Speed	Dir. (deg)	Speed (Knots)
Isolated Echoes	6 000	.84	.44	±53	±15
	10, 000	. 75	.62	±54	±16
	20, 000	. 82	. 54	±44	±24
Elements of Squall Lines	6000	.56	.44	±75	±2 0
	10,000	. 80	.68	±25	±14
	20, 000	.63	.64	±45	±2 0

An examination of the standard errors shows some quite large values. These were also computed without a qualitative inspection of the cases to

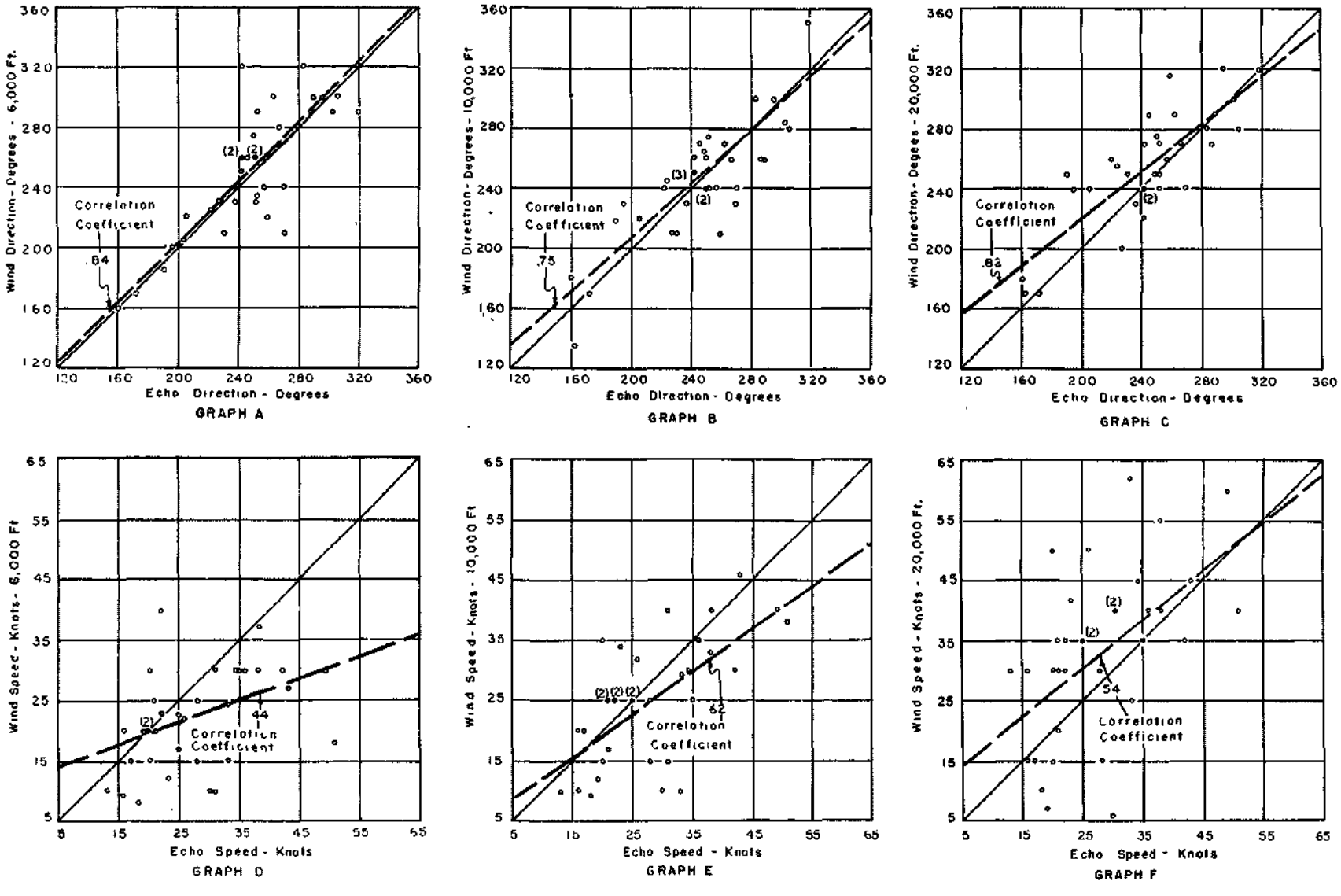

FIG. 7 RADAR ECHOES VS. WIND FOR THREE LEVELS
ISOLATED ECHOES

—— 1 1 LINE --- REGRESSION LINE

determine the ones that could be eliminated. There were only a few cases where the echo movement and winds did not correlate well with any of the three layers or levels, indicating further that if attention had been given to the height of the bases and tops, the correlation could have been improved.

The high standard error and low correlation coefficient for the 6000-ft level for elements of squall lines indicates that frequently the squall lines used in the study were above the frontal surface, while the 6000-ft wind was beneath the frontal surface and had no effect on the movements of the elements of the squall lines.

Comparison of Results

Some comparisons of results were made with the findings of H. B. Brooks in 1945, the Thunderstorm Project in 1946-47, and recent work by Ligda, (13, 8, 14).

Brooks used 46 storms and found that "large storms" move most frequently with the 11, 000-ft winds, while "small storms" move most frequently with the 5000-ft winds. Ligda used data for one 12-month period, which probably included a considerable amount of stable air mass precipitation types. His results indicate that convective cells in the New England area moved essentially with the velocity of the 700-mb geostrophic wind. In this study, the winds at the 6000-ft and 10, 000-ft levels were correlated with echo movements to give some form of comparison with the findings of Brooks and Ligda. The results obtained for the 10, 000-ft level are in fair agreement with Ligda's work. Brooks defined small storms as echoes having diameters less than 7. 5 miles. If isolated air mass showers can be considered "small" storms, since their diameters were usually less than 7. 5 miles, then these results are not in agreement with the findings of Brooks, because the echoes were found to move considerably faster than the 6000-ft winds.

The Thunderstorm Project, using wind observations from their own network in the vicinity of the echoes, found that clouds move slower than the mean wind for the layer from the gradient level to 20, 000 feet. Also, this difference was found to increase with increasing wind speeds. The two studies are in agreement for slow moving echoes but in this study the fast moving echoes usually had speeds greater than the mean wind speed for the layer, 2000-20, 000 ft. It must be remembered that this study was concerned with the large scale wind structure, as it is related to the movement of radar echoes. It is possible that local maxima of wind speeds exist in the vicinity of fast moving echoes. These local conditions would have been measured by the Thunderstorm Projects' micro-network of upper air soundings, with 10 upper wind stations in about 350 square miles. Also, some of the disagreements are probably due to differences in the heights of bases and the vertical extent of the echoes studied by each investigator, which would have a bearing on their movement.

Nomograms For Determining Winds

All of the nomograms shown are based on summer-time observations. Figure 8 shows nomograms for determining winds from isolated echoes. The bracketed values are two standard errors of estimate, or 95 per cent confidence limits. The regression lines were taken from the original graphs of echo movements versus winds, as shown in Figures 6 and 7. It is interesting to note in the upper right hand nomogram how much the speed of isolated echoes usually exceeded the 6000-ft wind speed. This was mentioned earlier in comparing results of this study with those of Brooks in which he found that small storms moved most frequently with the 5, 000-ft winds. Figure 9 shows a set of nomograms for determining winds from elements of squall lines.

Some of the nomograms can be expected to give better results than others, as indicated by the confidence limits. For purposes of comparison, nomograms were prepared for all layers and levels studied. However, the nomograms with the broadest 95 per cent confidence bands should be used with caution.

The nomograms were constructed using all of the cases studied in order to arrive at conservative estimates of the accuracy of wind determinations to be made from them. Likewise, there was no initial selection of cases for study. The following rules for increasing the accuracy of wind determinations will result in more accurate wind determinations than indicated by the confidence limits on the graphs. The graphs present the overall accuracy to be expected when all echoes are used regardless of their adaptability to wind determinations.

Rules for Increased Accuracy of Wind Determinations

An inspection of the cases where poor correlations existed resulted in the establishment of the following set of rules for increasing the accuracy of the wind determinations:

1. Use RHI data to determine the base and top of the echo where possible, and use such observations to choose the proper layer for correlation.

2. If RHI data are not available, plot the heaviest cores of echoes on the PPI scope. These are more likely to have sufficient vertical extent to reflect upper level wind conditions.

3. Areas of more intense precipitation within areas of light rain should be avoided. These more intense areas may be a result of natural seeding (14) (15) from higher clouds,

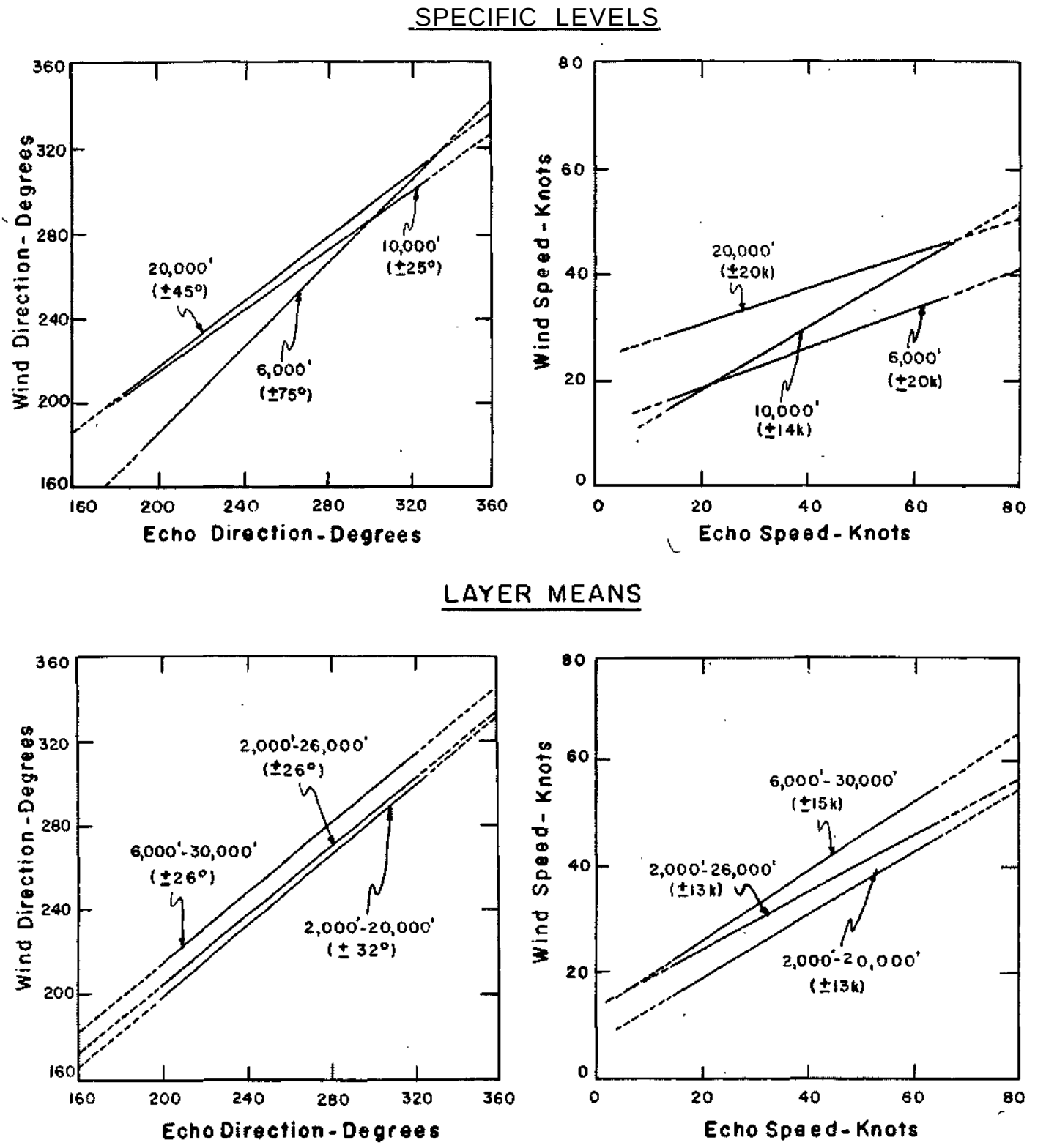

FIG. 9 NOMOGRAMS FOR DETERMINING WINDS, FROM ELEMENTS OF SQUALL LINES

and the precipitation areas will move with a velocity-similar to the clouds at the seeding level.

4. If thunderstorm bases are likely to be high, e. g. in the case of warm air over-running a cold dome, a higher-based layer, such as from 6000-30, 000 ft, should correlate best.

5. Use echoes within about 50 miles range when choosing an element of a squall line. At longer ranges, it is often quite difficult to separate the echoes and keep track of a particular one.

It must be emphasized that great care must be taken in making successive plots of the same echo to avoid identification errors. The operator should pick an echo that is isolated or is easily distinguishable from its neighbors either by its shape or size. The tracking of a particular echo requires almost constant vigilance of the scope because of rapid fluctuations in the appearances of echoes.

PRECIPITATION INTENSITY MEASUREMENTS

To make full use of radar for measurements of storm intensities for predicting the associa ted surface wind gusts and visibilities, it is necessary to know what rainfall rates or water drop concentrations produce a given intensity of echo. An areal method and a radial method have been employed for comparing rainfall rates with radar echo intensities.

Areal Method

A quantitative study of the areal relationships between one minute radar isoecho maps and one minute isohyetal maps drawn from raingage records from a micronetwork was made in order to compare theoretical with observed values and to establish operational techniques.

The one-minute rainfall amounts used in drawing isohyetal maps were obtained from fifty Bendix-Friez dual traverse, rain gages located on a 96-square-mile network centered 18 miles west-northwest of the radar station.

The isoecho maps have contours enclosing areas of precipitation echoes equal to or greater than a certain intensity as determined by an automatic receiver gain-reduction device (Refer to the discussion of the Automatic Receiver-Gain Control). The isohyetal maps have contours enclosing areas with amounts of precipitation equal to or greater than the chosen contour value. Graphs were plotted of areas versus intensities from both the isohyetal and isoecho maps. Rainfall equivalents of the radar echo intensities were then obtained by comparing like areas on these graphs.

Radial Method (Point)

Earlier work (16) made use of a radial method of analysis which gave results comparable to the areal method and afforded additional data for comparison with the theoretical values. In the radial method each gain step on the radar isoecho map was matched with a certain isohyet on the rainfall map.

To compensate for the fall time and drift of raindrops from the average height of 2000-3000 feet observed by the radar, successive one-minute maps of radar contours and surface rainfall were used. The one-minute rainfall rates were determined from the slopes of the curves on the raingage charts.

The direction and amount of drift were approximated from the movement of the radar cores for several consecutive minutes. The radar and rainfall profiles were matched by comparing a chosen one-minute radar profile along an appropriate radial from the radar station with consecutive one minute surface rainfall profiles along the same radial, after applying a drift correction to the surface rainfall pattern,,.

Only those cases where the indicated time lag was less than five minutes with drift not greater than 1. 5 miles were used in this analysis. Cases involving intervening rain and core centers moving off the network were excluded. Where the operator's log showed the possibility of instrumental error or other observational inconsistencies, the data were discarded. Examples of very light shower activity were not considered.

Previous studies by other investigators have indicated that the received power from rainstorms should closely follow the Rayliegh scattering effect. According to Spilhaus' information on drop size (17), the received power should be exponentially related to rainfall intensity. A proportionally greater received power has been noted with the APS-15 from higher rainfall rates than from the lower rates. These proportionally greater received-power values at higher rainfall rates may be a result of changes of the mean drop size and shape. The Illinois State Water Survey is currently collecting data on raindrop sizes and drop shapes at different rainfall rates.* The results of this work will be published at a later date.

Nomograms for Rainfall Estimates

Figure 10 presents a method of determining the intensity of precipitation and the corresponding visibility reduction from radar echoes. This graph is based on theoretical calculations rather than quantitative data from independent measurements by radar and raingages. The radar equation (Eq. 2) used in constructing the graph is that of Wexler (4). The equation was applied with the radar parameters for the Illinois State Water Survey's modified APS-15 radar. (Refer to the basic radar equation and APS-15 parameters under "Radar Characteristics") This gives:

*Under sponsorship of Evans Signal Laboratory, Contract No. DA-36-039 SC 42446

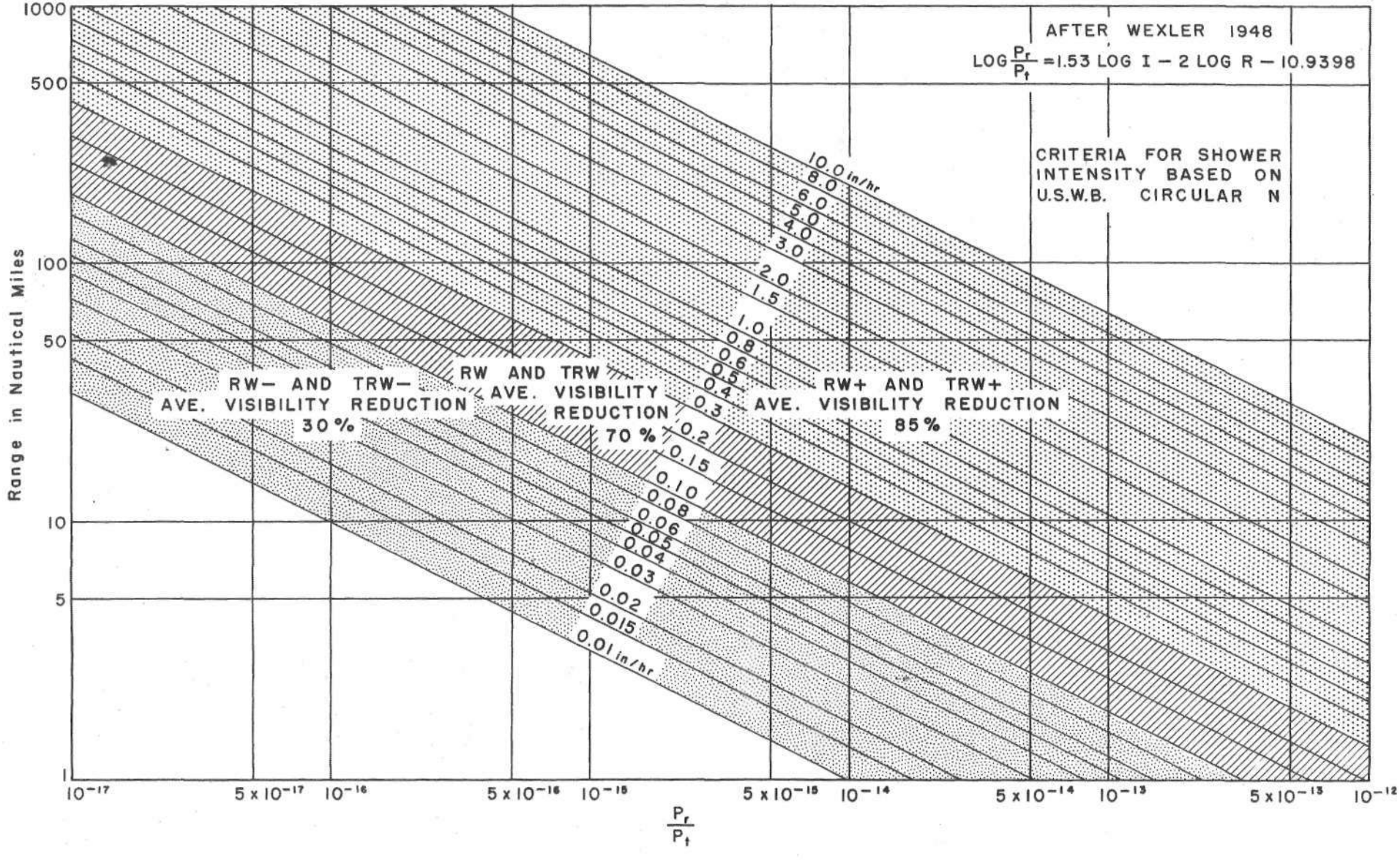

FIG. 10 THEORETICAL RAIN INTENSITY AND ASSOCIATED VISIBILITY REDUCTION — APS-15 RADAR

$$\text{(Eq. 2)} \quad \text{Log } \frac{P_r}{P_t} = 1.53 \text{ Log } I - 2 \text{ Log } R - 10.94$$

where P_r is power received in watts
P_t is power transmitted in watts
I is intensity of rainfall in in./hr.
R is range in nautical miles.

The constant, 10. 94 represents the radar set used and compensates for horizontal and vertical beam widths, antenna aperture, pulse length, wave length, and the refractive index of water. The constant 1. 53 relates rainfall intensity to drop size distribution, and according to W'exler (4) corrects to some extent the deviation from the Rayleigh scattering for 3-cm wavelength radar when large raindrops are present.

The abscissa on the graph in Figure 10 can be plotted in two forms. The P_r/P_t ratio works to best advantage for radar sets with varying transmitted power (Pt). For these sets, P_r and P_t measurements should be made as often as possible and at certain selected values of receiver gain. Echoes on the PPI scope can be reduced to their threshold of visibility by reducing the receiver gain manually or by use of an automatic gain reduction device. These reduced gain settings can be converted to P_r/P_t ratios, and used in conjunction with the echo range to determine the rainfall rate in inches per hour from Figure 10. The per cent reduction in visibility is then determined from the rainfall rate. This will be discussed in the following section on visibility. The rainfall rates in inches per hour in Figure 10 have been classified as light, moderate, and heavy showers according to Weather Bureau Circular N standards.

For a radar set with a constant transmitted power, the abcissa of Figure 10 can be plotted directly in terms of receiver gain, and less frequent checks of received and transmitted power will be necessary. With either set of abscissa values, the shower intensity may be determined directly from the graph.

This particular graph is applicable only to the Illinois State Water Survey's modified APS-15 radar set and is presented as an example. Each radar would require its own graph because received and transmitted power values are different for each set and the radar parameters (beam width, pulse length, etc.) are different for each model.

Also, drop size and shape distributions probably affect the received power (P_r) of 3-cm wavelength radar to a greater extent than the chosen constant 1. 53 in Equation 2 takes into account. The result is that on numerous occasions the graph in Figure 10 did not check by the "Areal Method" or the "Radial Method" of correlation between radar and raingage measurements.

A graph such as Figure 10, set up with Equations 1 and 2 and using the parameters for a 10-cm radar set, should give better rainfall intensity-estimates than the 3-cm radar-rainfall graph because the ratio of maximum raindrop diameter to radar wavelength is much smaller for 10-cm radar than for 3-cm radar. Consequently, the Rayleigh scattering law holds much better for the 10-cm wavelength. Also attenuation of the signal by the raindrops, which is appreciable at 3-cm, is negligible for 10-cm radar.

Additional research on attenuation and on raindrop size and shape distributions as they affect scattering at 3-cm wavelengths is needed in order to develop more accurate equations for determining rainfall rates from 3-cm radar echo intensities.

VISIBILITY DURING RAINSHOWERS

Introduction

Knowledge of visibility reduction during rainfall is pertinent to the planning and accomplishment of certain fleet operations. A measure of the intensity of rainfall can be obtained from the radar echo intensity as observed on the PPI scope. Since visibility reduction during rainfall is related to the intensity of the rainfall, it should be possible to establish quantitative empirical relations between rain intensity and visibility reductions. With the establishment of such relations, radar could be utilized for determining visibility reductions during rainfall when weather station observations are not available. Also the visibility reduction values can be used for forecasting visibilities once the expected shower intensities have been forecast by any method other than radar.

This section summarizes the results of a limited investigation to establish quantitative relations between the intensity of shower-type precipitation and visibility reduction. The results are based upon data from nine Illinois weather stations for the summers of 1951 and 1952. Consequently, the results are applicable only to regions with similar atmospheric conditions. It is obviously desirable that the investigation be extended to other regions and other types of precipitation.

Approach to Problem

Data Used. Microfilm copies of hourly weather observation records for nine Illinois stations for the summers of 1951 and 1952 were the source of analytical data. These stations included Bradford, Joliet, Moline, Peoria, Quincy, Rockford, Springfield, Vandalia, and Chanute Field. Because night visibility observations are more subject to errors than daylight observations, the study was limited to the hours between 0500 and 1900. Because the object of the investigation was to determine the reduction in visibility due to

rainfall, cases were selected in which the visibility preceding rainfall was not restricted by fog, smoke, or haze. The study was further limited to the unstable types of rainshowers and thundershowers, which predominate during summer. The two-summer period provided a total of about 531 station-days of precipitation which met the preceding requirements for inclusion in the analysis.

Treatment of data. The rainfall data were divided into the four classes of intensities as defined by the U.S. Weather Bureau; very light, light, moderate, and heavy intensities. By definition, no accumulation occurs with very light rain, while light, moderate and heavy intensities correspond to rates of a trace to 0. 10 in./hr, 0. 11 to 0. 30 in./hr. and over 0. 30 in./hr, respectively.

In processing the data, visibility observations preceding and during each shower were tabulated. The percentage reduction in visibility due to rainfall was then calculated by dividing the difference between the visibility prior to and during rainfall by the visibility preceding precipitation, and multiplying by 100.

The data were first analysed using observations when no fog, haze, or smoke (visibility greater than six miles) was reported before the onset of precipitation, and none was reported during the occurrence of rainfall. These results, therefore, should represent the reduction in visibility due to rainfall. Later, a study was made of those cases where fog, haze, or smoke occurred during, but not preceding, rainfall. Such occurrences are representative of conditions under which extreme reductions in visibility may occur during precipitation. Unfortunately, insufficient data were available to complete the second study. It is complicated by the fact that the rain actually removed particles from the atmosphere previously restricting the visibility.

Results of Data Analysis

Mean Reduction in Visibility. Using 1951-1952 data for the nine Illinois stations, an average percentage reduction in visibility for each type and intensity of rainshower was computed for those cases in which no fog, haze, or smoke occurred prior to or during rainfall. The results have been expressed graphically in Figure 11.

Two results of particular interest are: first, the visibility reduction with thunderstorms is always greater than the corresponding rainshower intensity. Two possible explanations for this are suggested. The observer may consistently record the shower intensity according to the frequency of thunder rather than the rainfall rate; for example, thunderstorms having moderate rainfall rates may be recorded as light because of the infrequency of thunder. The other possibility is a variation in drop size, with smaller drops occurring with thunderstorms than with rainshowers of the same intensity. Small drops would reduce visibility more than large drops with equal amounts of liquid water content present in both cases.

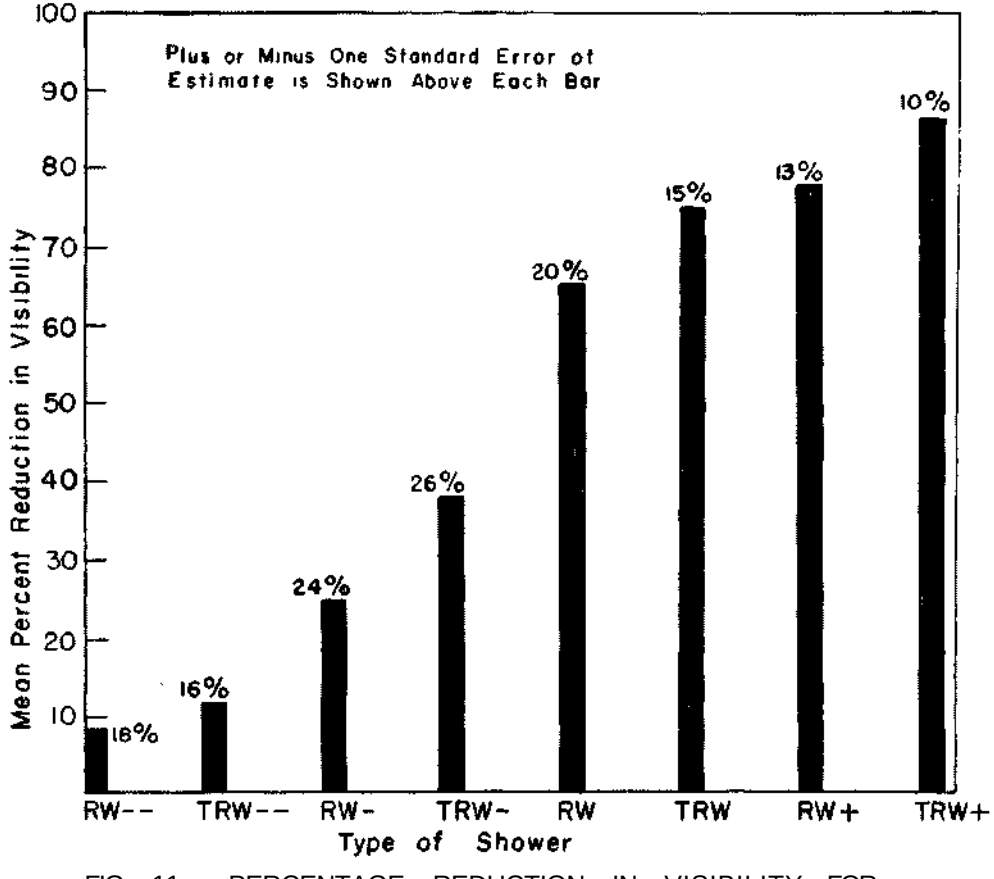

FIG 11 PERCENTAGE REDUCTION IN VISIBILITY FOR VARIOUS INTENSITIES OF SHOWERS.

Second result is the small increase in visibility reduction between moderate rainshowers and thundershowers and heavy ones. Drop size variation may also be an explanation for this; the visibility reduction due to the increase in liquid water content per unit volume may be partially offset by an increase in the ratio of large to small drops.

The above results are applicable only to areas of similar atmospheric conditions where the visibility ranges are about the same. The southwestern portion of the United States, where the turbidity is much less, would probably have greater visibility than Illinois during a shower of a given rainfall intensity.

Maximum Reduction in Visibility. As mentioned previously, the study of the maximum reductions in visibility to be expected when fog, haze, or smoke form during the precipitation period did not prove as fruitful as expected. The number of observations was very small, and the variations between observations were so large that it was decided not to include this phase of the study in this report. As expected, the results indicated an increase in visibility reduction for the lighter rainfall rates. During the two-year period studied, no fog, haze, or smoke formed during periods of heavy rainshowers or thundershowers.

Determination of Visibility Reduction by Radar

It is unlikely that very light showers will be detected by most radar sets except at short ranges. However, as shown by Figure 11, the average reduction in visibility during such storms is very small and, therefore, of little significance in the accomplishment of most fleet operations. For the preceding reasons, very light showers were not considered in developing techniques for ascertaining visibility reduction by radar.

The intensity of a radar echo (rainfall intensity) can be determined by use of automatic or manual gain reduction, as described under "Receiver Gain Controls". To make the results of Figure 11 applicable to radar analysis, the average percentage reductions in visibility for light, moderate, and heavy intensities were expressed in terms of rainfall intensity, using the U.S. Weather Bureau Circular N criteria for intensity. The results are shown in Table 3

Since the rainfall intensity can be determined from the radar echo intensity, the average percentage reduction in visibility during a shower due to raindrops can be estimated by entering Table 1 with the approximate intensity value. Since Weather Bureau records were used to develop the relation between rainshower intensity and visibility reduction (Figure 11), Table 1 is based upon the assumption that the classification of light, moderate, and heavy showers by Weather Bureau observers conforms with Circular N criteria for rainfall intensity. While the veracity of this assumption may be questionable, it represents the best estimate available at the present time.

TABLE 3

RELATION BETWEEN PERCENTAGE REDUCTION IN VISIBILITY AND RAINFALL INTENSITY FOR GIVEN TYPES AND INTENSITIES OF SHOWERS

Shower Type and Intensity	Average Percentage Reduction in Visibility	Circular N Criteria for Intensity in. /hr.
RW-	25	Trace to 0. 10
TRW-	38	" " "
RW	66	0. 11 to 0. 30
TRW	75	" " "
RW+	78	Over 0. 30
TRW+	87	" "

These percentage reductions in visibility have been entered in Figure 11, and the rainfall rates corresponding to light, moderate, and heavy showers have been shaded in„ This permits a direct estimation of the visibility reduction from the echo intensity,

Atlas' Equation for Determining Visibility From Rainfall Rate

The following unpublished equation by Atlas (18) for determining visibility during rainfall has received attention:

(Eq. 3) $V=12.\ 5R^{-.67}$, where V is visibility in Km and R is rainfall rate in mm/hr.

Recently Atlas has indicated changes in the values of the constants and exponent. Because only a few direct observations between radar echo intensity and visibility were available in this study, verification of the Atlas equation was not possible.

SQUALLY WIND DETERMINATIONS

Only a small amount of quantitative data has been available for the study of squally surface winds. A study was made of squally winds in connection with thunderstorms occurring at Weather Bureau first order stations in Illinois. The results indicate, as might be expected, that the average and peak gusts to be expected from heavy showers and thunderstorms are considerably higher than those from light or moderate intensities of showers and thundershowers.

Three aerovane recording wind systems have been operated for a short time on the Water Survey's Goose Creek raingage network. More records from these would be required in order to produce conclusive quantitative results. However, available information from the Thunderstorm Project (8) and data collected in this study does make it possible to draw helpful qualitative conclusions about squally winds associated with radar echoes.

Mechanisms Producing Squally Winds (8)

Squally surface winds associated with the passage of isolated air mass thunderstorms, frontal thunderstorms, or squall-line thunderstorms are produced primarily by the cold downdrafts of the thunderstorm cells that have reached maturity.

There are characteristic patterns in the wind velocity-divergence field associated with the various stages of the thunderstorm life cycle. During the early cumulus stage, even 20 to 30 minutes before the radar echo appears, the surface winds turn toward the areas of convection, where relatively weak convergence develops. The inflow, which is usually light, frequently extends over a radius of six to eight miles. When there are numerous cells in the vicinity, the outflow of one may so completely dominate the surface wind flow that it is impossible to detect the inflow field of another.

The cold downdraft is by far the most significant feature pertaining to squally surface winds. When the cold downdraft of a thunderstorm cell reaches the surface there is an immediate reversal from the inflow which was present during the cumulus stage of the cloud development. The outward flowing cold air underruns the warmer air and a discontinuity in the wind field is established.

In relatively slow-moving or stationary storms, the outflow is almost radial, and as it continues, an area of light winds develops immediately beneath the center of the downdraft area. However, in most cases, the outflow field is asymmetrical, with higher wind speeds on the downstream side. This is due to the reinforcement, or cancellation as the case may be, of the radial outflow by the prevailing air movement.

Often in the case of moving storms almost all of the cold downdraft air spreads out in the direction of cell movement, giving a strong wind discontinuity at the leading edge. A downward transport of relatively high horizontal momentum from upper levels reinforces the surface outflow wind speeds in the direction of the cloud movement and retards those in the opposite direction.

After the outflow has been spreading for 15 to 20 minutes, the discontinuity zone will have traveled about five or six miles from the cell center.

The surface winds near the discontinuity surface remain strong and gusty, but farther behind, inside the cold-air dome, the surface wind speeds decrease so that the strongest winds are no longer underneath the cell itself. This increase in wind speed as one approaches the discontinuity zone from the cold-air side results from a continued settling of the outflow air„ . The sharp increase in wind speed at the leading edge of the discontinuity has been termed "the first gust, " since it often appears as a first major gust of a period of high, gusty winds. After the cold air spreads outward, the wind speed near the boundary of this air decreases. The rate of decrease depends mainly upon the rate of spreading of the cold-air dome and thus the rate of dispersion of the downdraft energy.

Radar Echoes and Squally Winds

The Thunderstorm Project (8) found that the centers of downdrafts coincided with the cores of heaviest precipitation which are shown by PPI radar. This permits the determination of sources of strong surface wind gusts by the use of radar.

RHI radar can be used to determine the height of the base and tops of echoes and their vertical growth rates. The fastest growing and tallest echoes are likely to develop the strongest downdrafts and associated surface gusts.

Studies made by Jones (7) and American Airlines (9), revealed that the severest turbulence experienced by aircraft in flight was associated with steep gradients of radar echo contours. These steep gradients can be determined by the use of manual or automatic receiver-gain reduction devices.

Rules for Estimating Squally Winds from Radar Echoes

1. If a moving squall line or line of frontal thunderstorms is maintaining or increasing its intensity, then at any given time there will be some mature thunderstorm cells with well developed downdrafts. These downdrafts will afford a supply of energy for the surface wind gusts. Under such circumstances the echoes can usually be prognosticated to maintain their associated gust intensities as they reach stations in their future path.

2. Large and/or very intense, fast moving echoes will frequently produce gusts of 40 to 50 miles per hour. In general fast moving echoes produce the most intense gusts. Often the large intense echoes will appear as one cell rather than multicellular in structure.

3. The strongest squalls occur in the early mature stage before the energy of the downdraft has been widely dispersed through spreading of the cold-air dome. Strong echoes recently developed are the most dangerous.

4. Observations on numerous occasions have indicated that the most severe surface winds are associated with sharp discontinuites or wave appearances in the echo pattern. Figure 12 illustrates this type of echo. Gusts of 50 to 60 miles per hour have been observed with the passage of echoes of this shape.

5. High surface wind speeds and severe weather usually occur at the zone of intersection of two squall lines. This is in agreement with Tepper's theory (19) on the intersection of two pressure jump lines. (Figure 12d)

6. Large, fast moving thunderstorms in unstable air at sea should produce higher associated surface wind speeds than those of like, intensity on land because less surface friction occurs at sea to dispel the downdraft energy. The energy not dispelled by friction is available for creating higher surface gust speeds.

7. Pre-cold frontal and cold frontal squall lines and warm air mass thunderstorms usually have stronger associated surface wind gusts than high level thunderstorms above a warm frontal surface. The stability of the warm front tends to absorb some of the energy of downdrafts before they reach the earth's surface, leaving less downdraft energy for conversion into surface wind gusts. Synoptic information and RHI radar data can be used as aids in determining the likelihood that the thunderstorms are situated above a frontal surface. The case study of 23 July 1951, presented later, illustrates the use of synoptic information in determining whether the echoes are high based above a frontal surface.

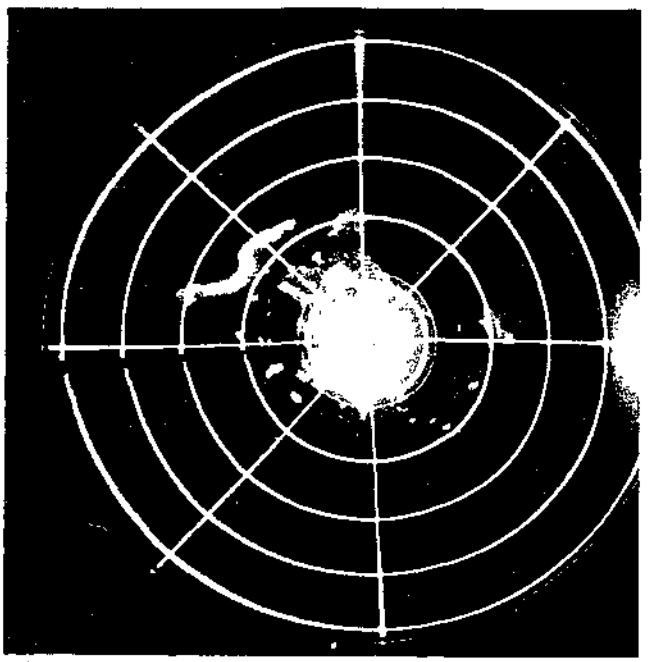

A. 1 JUNE 1953, 0905 CST.
WAVE PATTERN ON SQUALL LINE

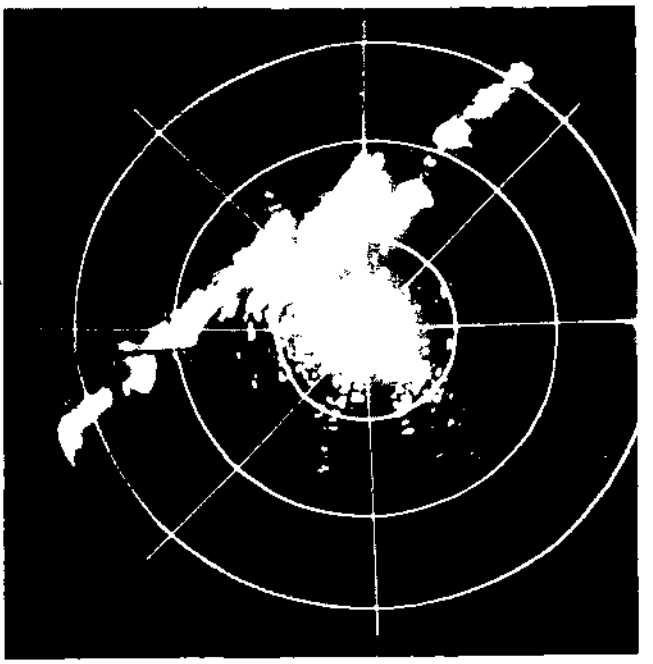

C. 5 JUNE 1953, 1705 CST.
TRIPLE SQUALL LINE

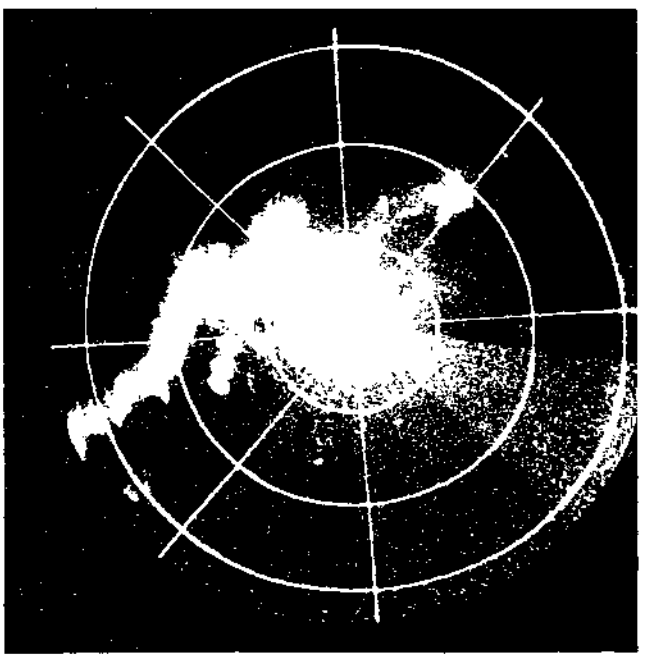

B. 5 JULY 1953, 2250 CST.
WAVE PATTERN ON SQUALL LINE

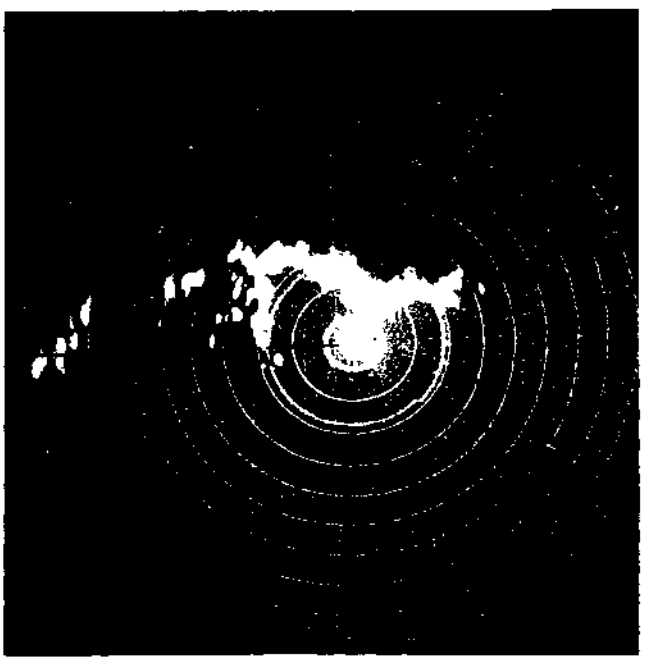

D. 8 JULY 1951, 2300 CST.
INTERSECTING SQUALL LINES

FIG. 12 ECHOES WITH SHARP DISCONTINUITIES OR WAVE PATTERNS ASSOCIATED WITH SQUALLY SURFACE WINDS

P ART III

CASE STUDIES

The following case studies are presented to illustrate to the aerologist both the usefulness and limitations of radar in short range forecasting. Several different meteorological phenomena are illustrated. The determination of visibility during the passage of echoes over the station has been ommitted due to the limited observational program conducted at the radar station. See Figure 5 for optimum operating range of the radar used in these studies.

The shipboard aerologist should make maximum use of the radar whenever surface hourly reports are available to confirm radar observations of echo intensity, visibility reduction, and beginning and ending of precipitation. In this way, he can thoroughly familiarize himself with the characteristics of the set he will use at sea where surface hourly reports are not available.

Time used is Central Standard Time (CST) and distance is expressed in nautical miles.

HIGH LEVEL SHOWERS AND THUNDERSTORMS DURING NIGHT OF 23-24 July 1951

This case illustrates the usefulness of radar in detecting unexpected weather in areas lacking surface reporting stations. The squall lines show quite rapid developments and changes in orientation that are of interest. Also, the usefulness of surface synoptic data as an aid in determining upper winds from PPI echoes is shown.

Synoptic Situation

At 1530* on 23 July 1951, a slow moving cold front was oriented east-west through northern Kentucky and southern Illinois (Figure 13). A post-frontal shower was reported at Louisville, and thundershowers were reported in the warm air south of the cold front at Jackson and Knoxville, Tennessee, Bowling Green, Kentucky, Maiden, Missouri and Little Rock, Arkansas. By 2130, the front had become stationary slightly south of its 1530 position. At 2130 thunderstorms were reported at Terre Haute, Indiana, Maiden, Missouri, Walnut Ridge, Arkansas, and at stations farther southwest in Oklahoma and Texas. Figure 14 shows the wind profile in the echo area as determined from streamline charts.

*Time used is Central Standard Time.

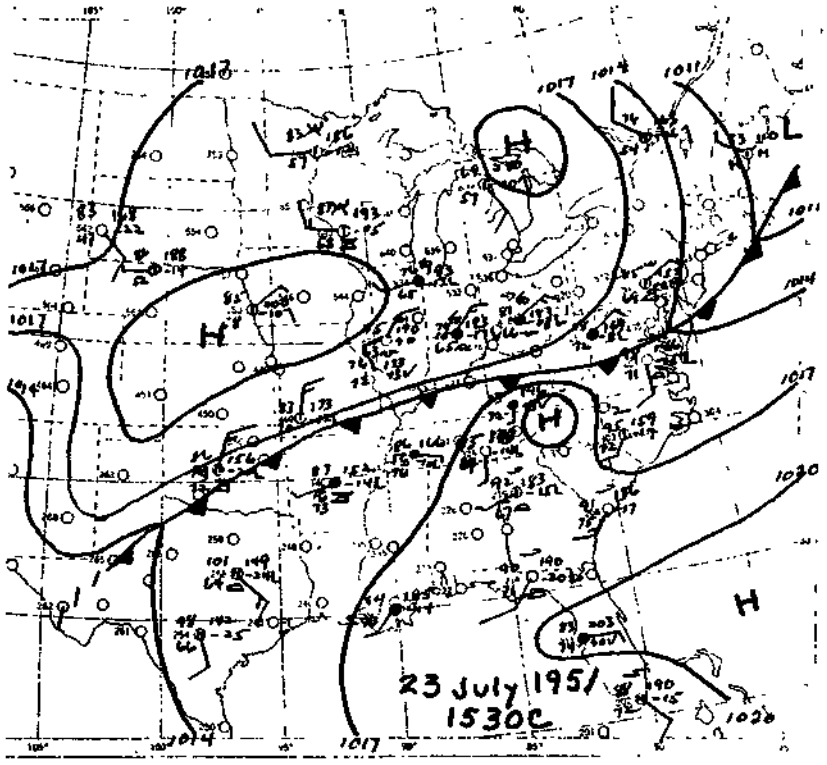

FIG. 13 23 JULY 1951 I530CST SYNOPTIC CHART

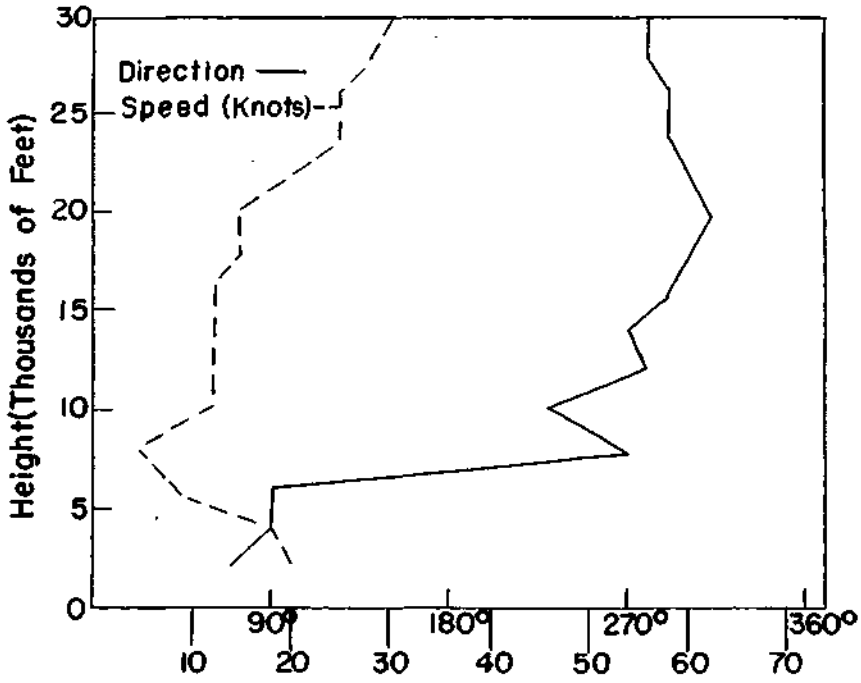

FIG. 14 23 JULY 1951 2100CST WIND PROFILE

Discussion of Radar and Synoptic Data

At 2011 (Figure 15a), the 3-cm radar showed developing showers west of Vandalia (VLA) Illinois, and over a large area from Terre Haute (HUF), Indiana, southward for 60 miles*. Surface reporting stations were lacking in this area. The echo pattern indicated the development of an ENE-WSW squall line just south of Terre Haute. By 2030 (Figure 15b), the radar showed a definite ENE-WSW squall line just north of Terre Haute. The Weather Bureau hourly total precipitation for Terre Haute between 2000 and 2100 was 0.21 inches. A few other echoes of lesser importance were still present west of Vandalia and 50 to 60 miles south-southwest of Terre Haute. At 2130 (Figure 15c), the isolated echoes west of Vandalia had increased in intensity. Two well-developed isolated echoes were situated in southeast Illinois about 50 miles southwest of Terre Haute. Most of the echoes appeared to develop along the surface position of the stationary front, 60 miles south of Terre Haute, and move northeastward up the frontal slope. Between 2100 and 2200, 0.25 inches of rain fell at Terre Haute.

By 2230 (Figure 15d), scattered echoes were situated to the north, west, and southwest of Vandalia, and the two intense isolated echoes had developed and moved toward a point 40 miles southwest of Terre Haute. The squall line north of Terre Haute was beginning to dissipate. Shortly after this, other echoes began to appear 40 miles southwest of Terre Haute. By 2300 (Figure 15e), an ESE-WNW squall line had developed and moved northeast to within 30 miles of that station. By 2330 (Figure 15f) the squall line was about 20 miles south of Terre Haute and had become oriented in a nearly E-W direction, possibly becoming linked with echoes to the north of Vandalia and with other echoes in Indiana, southeast of Terre Haute. The squall line had a total E-W extent of about 120 miles at this time. Some evidence of the older squall line north of Terre Haute was still present.

By 0030, 24 July, (Figure 15g), the heaviest portions of the E-W squall line had moved northward almost to Terre Haute. Most of the echoes northeast of Vandalia, on the west end of the line, had dissipated; also, most of the elements of the older squall line north of Terre Haute had dissipated. The individual elements of the major line moved from about 248° at 17 knots.

The Weather Bureau map for 0030, July 24 showed a thunderstorm at Evansville, 91 miles south of Terre Haute, and a rainshower at Indianapolis, Indiana, 6l miles east-northeast.of Terre Haute, with no indication of an E-W squall line along the frontal surface between these stations. However, the radar indicated a well-defined squall line at this hour.

At 0130 (Figure 15h), the major E-W squall line had moved northward to a position north of Terre Haute, and isolated echoes extended from Terre Haute southwest almost to Vandalia. Another line of echoes oriented ENE-WSW

*Distance is expressed in nautical miles.

had formed 40 miles to the northwest of the major squall line, at a position about 10 miles south of Danville (DAN), Illinois. Between 0100 and 0200, 0.28 inches of rain was recorded at Terre Haute as the squall line moved over that station.

By 0230 (Figure 15i), both squall lines had largely dissipated and smaller isolated echoes were scattered over the region. These slowly dissipated during the early morning hours.

Upper Winds

The upper wind pattern at 2100 (Figure 14) leaves little doubt that the echoes were high-based in the warm air mass above the frontal surface and steered by the higher level winds. The winds at 2000 ft and 4000 ft in the echo area were from 70° to 90° at 18 to 20 knots. At 6000 ft, the winds were still from an easterly direction but were very light. Between 6000 and 8000 ft, the winds veered to the southwest and remained light. Above 8000 ft, the southwesterly flow began to increase in strength from 12 knots at 10, 000 ft to 30 knots at 30, 000 ft.

Since the echoes moved from about 248° at 17 knots, they must have been high based in the southwesterly current above the frontal surface. RHI radar would have shown the base and tops of these echoes. However , in the absence of such radars, surface synoptic data, as illustrated here, can provide supplementary information to the PPI radar for determining the approximate base of echoes. Due to the high base of these echoes, they are best suited for determining the layer mean winds for 6000-30, 000 ft. The use of the nomograms for determining winds from the echo movements gave a mean wind of 255° at 23 knots for the layer. The actual observed mean wind for this layer at 2100, as taken from streamline charts, was 268° at 17 knots.

Conclusions

This is a typical example in which radar detects unexpected weather developments in rather passive synoptic situations and over areas lacking surface reporting stations. Also, it illustrates the usefulness of radar for upper-wind determinations and shows how available surface synoptic data should be taken into consideration in selecting the layer of best correlation.

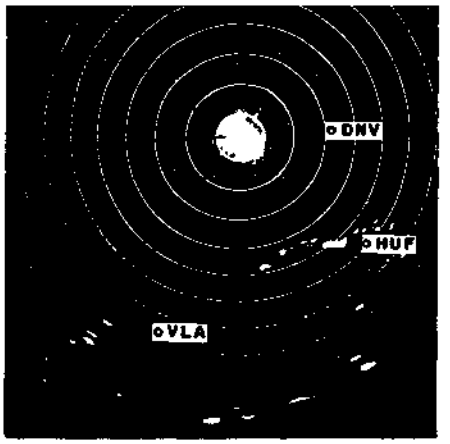

A. 2011 CST

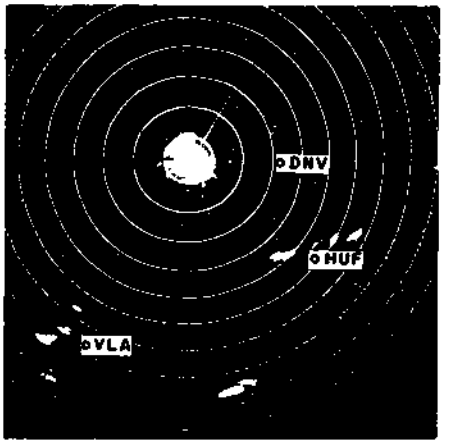

C. 2130 CST

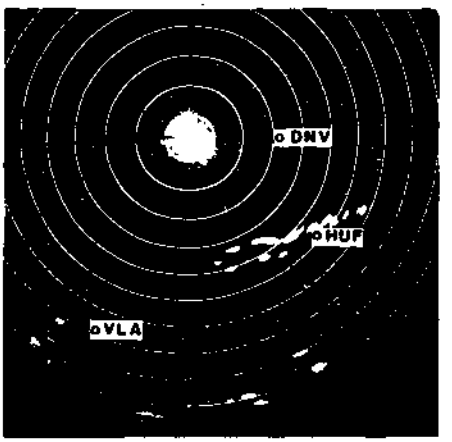

B. 2030 CST

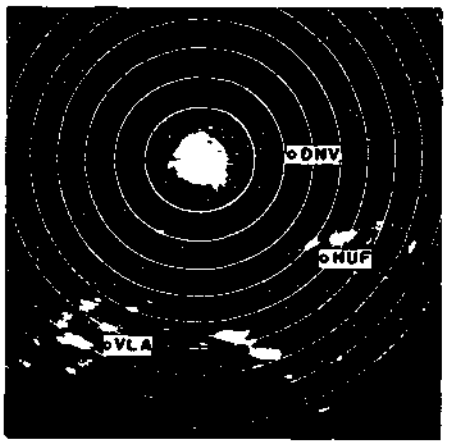

D. 2230 CST

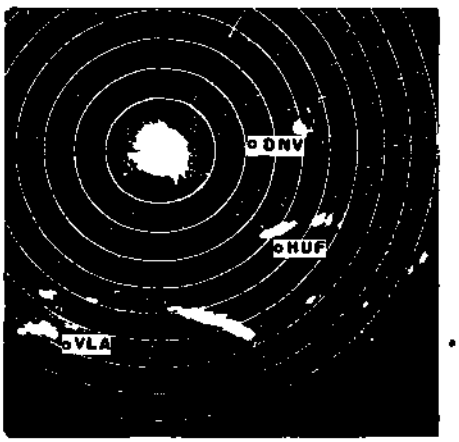

E. 2300 CST

FIG. 15 HIGH LEVEL SHOWERS AND THUNDERSTORMS DURING NIGHT OF 23-24 JULY 1951
(10-MILE RANGE MARKERS)

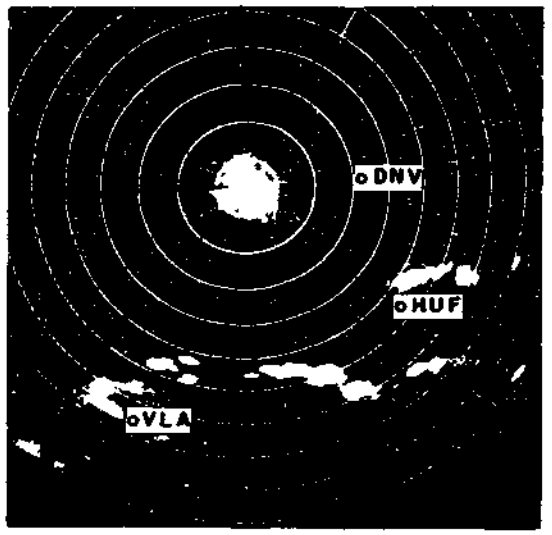

F. 2330 CST

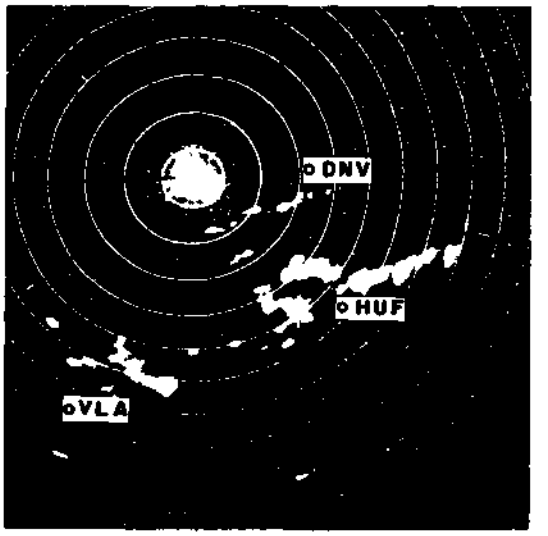

H. 0130 CST

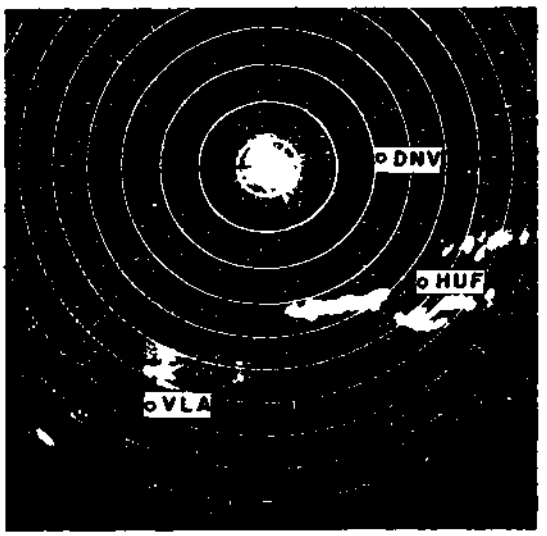

G. 0030 CST

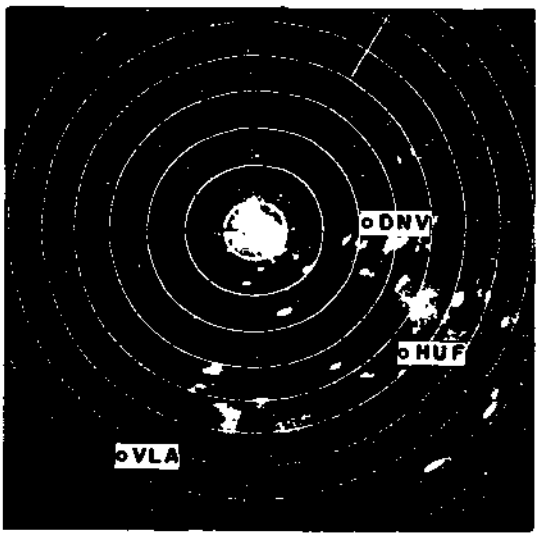

I 0230 CST

FIG. 15 HIGH LEVEL SHOWERS AND THUNDERSHOWERS DURING NIGHT OF 23-24 JULY 1951 (10-MILE RANGE MARKERS)

PRE-FRONTAL SQUALL LINE OF 12 SEPTEMBER 1951

This case illustrates the utility of 3-cm radar in detecting squall lines and tracking such storms for a period of several hours. Limitations in the detection of light showers and in determining the depth and intensity of precipitation zones due to range and precipitation attenuation are also illustrated.

Synoptic Situation

The 0930 weather map drawn from hourly reports, (Figure 16), showed a cold front extending south-southwestward from a major low in Canada through eastern Minnesota, then through a weak low in northeast Iowa, and into southeastern Kansas and central Oklahoma.

An analysis of synoptic conditions indicated that the cold front would pass the station by 2200 with thunderstorms and rainshowers in advance of the front.

Discussion of Radar and Synoptic Data

The radar was turned on at 1435 (Figure 18a) and three groups of echoes were observed on the radar scope. One group was 80 to 100 miles northwest of the station, while two groups were located southeast of the station, one at 40 to 60 miles and the other at 90 miles.

Shortly thereafter, more echoes appeared in the northwest. By 1522 (Figure 18b) they were arranged in a N-S band about 110 miles long. The echoes to the southeast had become arranged into a NNW-SSE line about 70 miles long. but were not increasing in intensity.

The 1530 hourly reports indicated light showers in progress at Peoria (PIA) and Springfield, (SPI); precipitation beginning at Peoria at 1500 and at Springfield at 1528. The shower at Peoria was visible on the radar but the shower at Springfield was not. However, a later examination of the raingage trace at Springfield indicated a rainfall rate of only 0. 02 in./hr. , too light to be detected by the radar at that range due to attenuation. The raingage chart at Peoria was not available for comparison with the rainfall rates.

By 1602 (Figure 18c), the squall line to the southeast had almost completely disappeared from the scope, probably due to range attenuation. There were no radar echoes over Peoria or Springfield at this time, but the 1630 hourly reports indicated light showers still in progress at both stations. Both range and precipitation attenuation of the low-powered 3-cm radar could have been the reason for not seeing this rainfall, since there were echoes between both stations and the radar station.

The forward movement of the squall line at this time was from 285, at 25 knots. With the continuation of this speed and direction of movement,

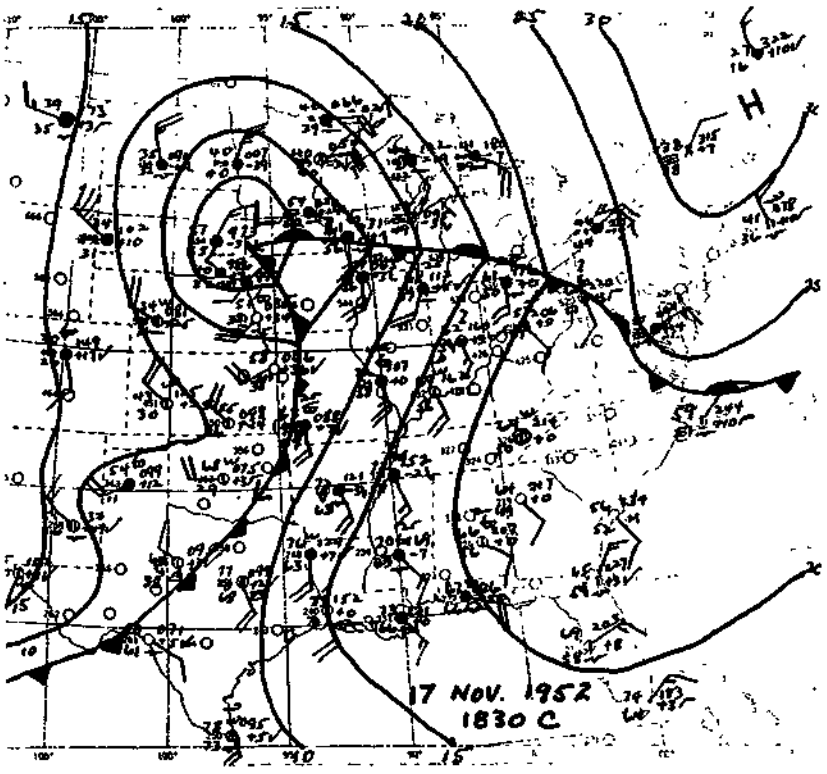

FIG. 26 17 NOV. 1952 I830CST SYNOPTIC CHART

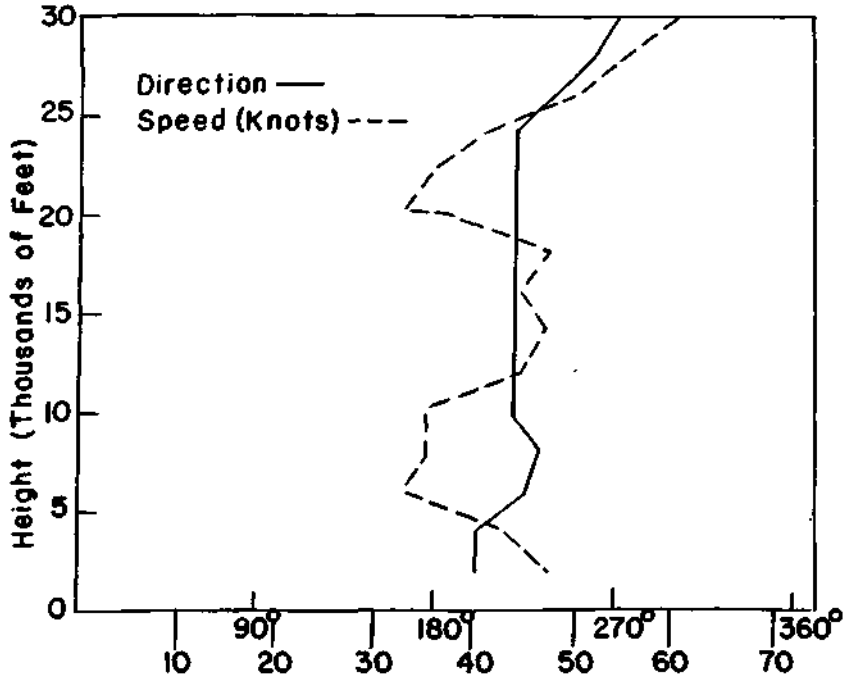

FIG. 27 17 NOV. 1952 2I00CST WIND PROFILE

moderately heavy precipitation was expected to begin in Champaign in two hours, or about 1800.

The movement of the cells within the squall line was from 215° at 46 knots. This was compared with 0900 pibals (Figure 17). The wind velocity was very uniform between 2000 ft and 30, 000 ft, the direction varying between 200º and 215º , and the speed varying between 35 and 45 knots. Consequently, the mean winds for all three layers were approximately 207° at 41 knots.

Two adjacent squall lines became distinctly visible by 1640 (Figure 18d). As the first line approached the station, more echoes became visible to the rear indicating that the precipitation area probably extended over a relatively broad zone.

The range of the radar was reduced to 30 miles at 1645 to permit a detailed study of the echoes as they passed over the dense raingage network centered 18 miles west-northwest of the station. By 1720 (Figure 18e), the echoes were only 15 miles west of Champaign. Precipitation began in northwest Champaign at 1755 as a large echo developed to the west southwest (Figure 18f). At 1750 a wind shift with gusts of 34 mph was recorded at the Water Survey's weather station in Champaign.

Rainfall continued for a period of about two hours at Champaign, and was light except for the initial burst at 1755. As mentioned previously, the appearance of a second squall line at 1640 was indicative of the presence of a broad rainfall zone. Because of the attenuation factors involved, the intensity of the precipitation echoes to the rear of the first squall line and the exact depth of the rainfall zone could not be reliably ascertained with the APS-15 (3-cm) radar. With a more powerful 3-cm set, such as the CPS-9 more detailed information on the depth and intensity of the rainfall zone could have been obtained. Furthermore, the presence of a broad rainfall zone might have become apparent at an earlier time with a more powerful set.

Conclusions

Although attentuation factors masked the intensity and depth of the squall zone in this case, the ability of the radar to detect and track the forward edge of this zone for several hours would have provided valuable information for flight planning or other operations affected by such weather phenomena, In analyzing such situations, knowledge of radar limitations due to attenuation factors is important to the forecaster in order to make maximum utilization of the available data.

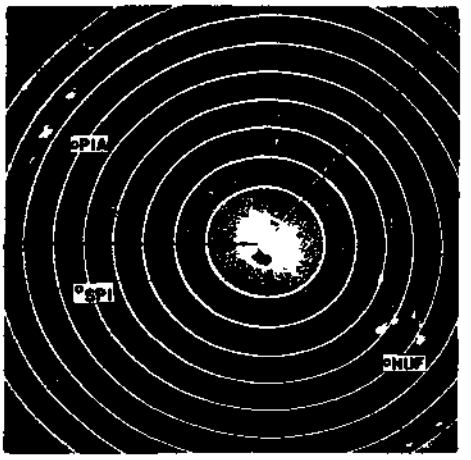

a. 1435 CST

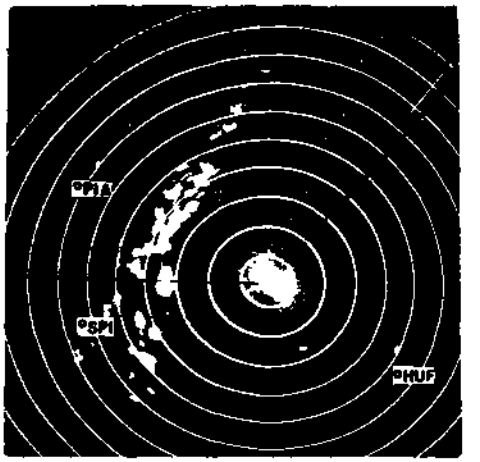

d. 1640 CST

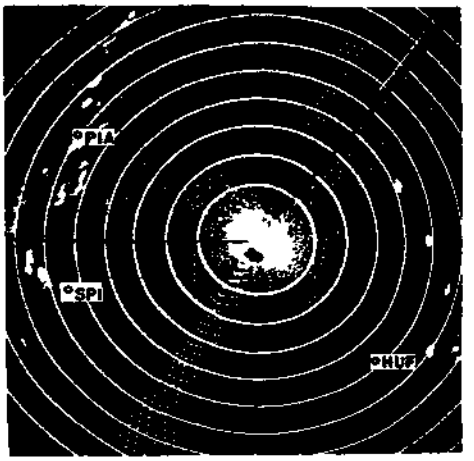

b. 1522 CST

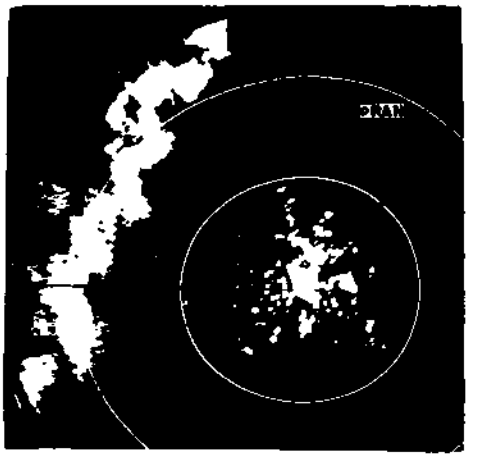

e. 1720 CST

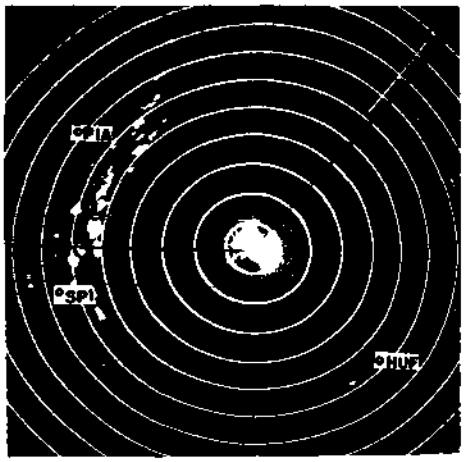

c. 1602 CST

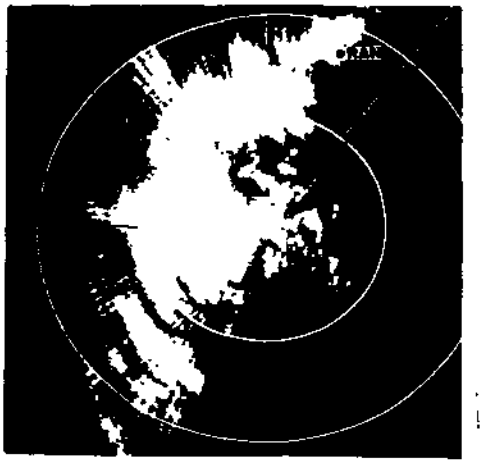

f. 1758 CST

FIG. 18 PREFRONTAL SQUALL LINE OF 12 SEPTEMBER 1951 (10-MILE RANGE MARKERS)

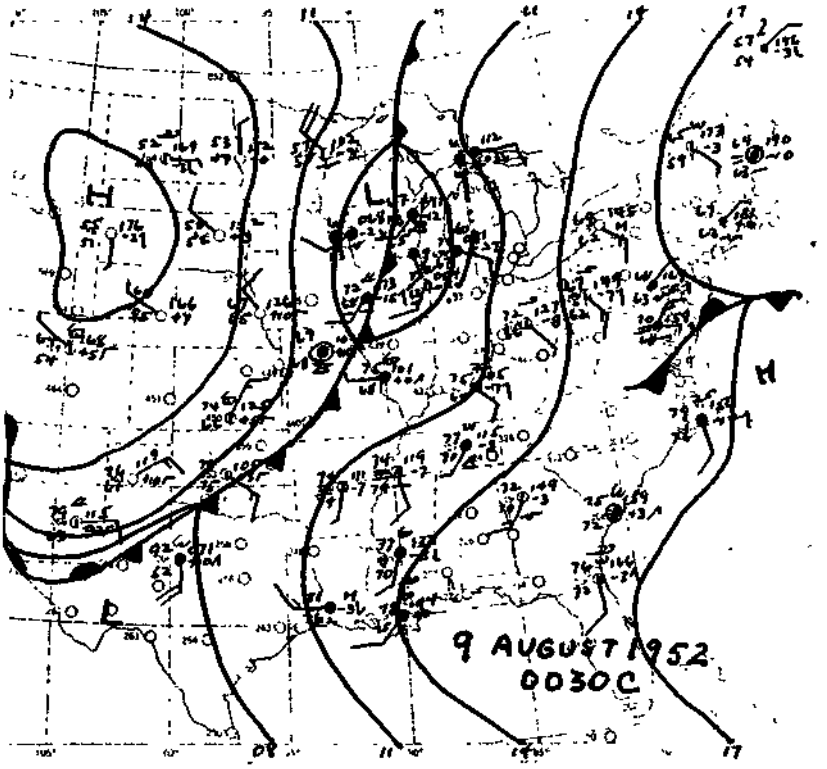

FIG. 19 9 AUGUST 1952 0030CST SYNOPTIC CHART

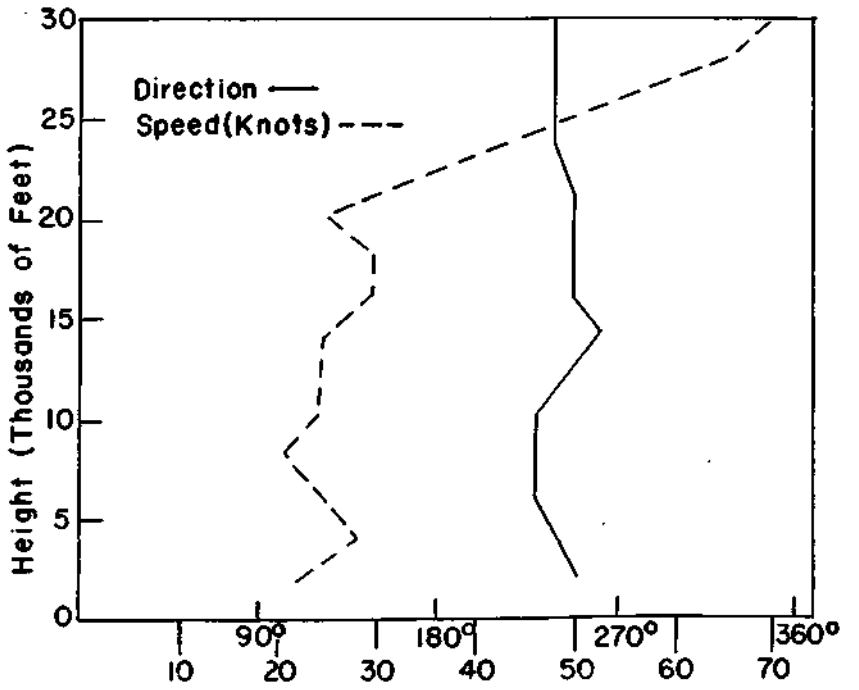

FIG. 20 9 AUGUST 1952 0300CST WIND PROFILE

PRE-FRONTAL SQUALL LINE OF 8-9 AUGUST 1952

This case illustrates the growth and dissipation of a squall line as observed by radar and the effects of this formation on anomalous propagation that was occurring prior to the formation. The radar was also useful in locating an area of lighter winds in southern Illinois and indicated large openings in the squall line.

Synoptic Situation and Weather Forecast

There was a weak low center located in central Wisconsin and a cold front extended south-southwestward from this low through extreme western Illinois and central Missouri at 0030 on 9 August (Figure 19). Some squall line activity had been associated with this cold front in extreme northern Illinois, and, the previous evening, very light shower activity occurred in central Illinois.

The cold front was expected to pass the station about 1000 on the 9th with scattered showers in advance of the cold front.

Radar Data

The first precipitation echoes became visible about 2255 on the 8th (Figure 21a) at a range of 90 to 100 miles northwest of the station. There was an excessive amount of ground clutter with some targets visible as far as 45 miles from the station. The precipitation echoes were quite strong, indicating a rather intense thunderstorm in progress.

By 0008 of the 9th (Figure 21b) the intensity of the echoes had decreased, and were located 70 to 100 miles northwest of the station. The ground pattern had begun to change shape, with fewer ground targets visible to the northwest. Convergence into the thunderstorm area was destroying the inversion that produced the trapping. However, it was still difficult to distinguish the ground targets from the precipitation echoes except by use of the "A" scope.

More echoes began to appear and at 0057 (Figure 21 c), three groups of echoes were present. By 0128 (Figure 21 d), a general intensification of the echoes was easily noticeable. All signs of anomalous propagation were gone by this time, indicating a rather wide area of convergence in the thunderstorm area.

By 0210 (Figure 21e), the central portion of the squall line had developed considerably, with the southern end only 35 miles west of the station. There was no appreciable change in intensity of the echoes to the north, but the echoes in the southwest had begun to dissipate. A few light echoes were visible to the east and south. The movement of the cells in the center portion was from 255° at 24 knots. More development at the southern end of the line would be necessary

before a precipitation forecast for the station would be required, since the east-northeasterly movement of these cells would take them north of the station.

The range of the radar set was reduced to 30 miles at this time to study the detail of the showers as they passed over the Water Survey's raingage network, centered 18 miles west-northwest of the station.

The echoes were located only 20 miles west of the station at 0237 (Figure 2 If) and no new development.had occurred that would cause rain - at the station.

The echoes passed to the north about 0345 without any rain occurring at the radar station. When the radar range was increased to 100 miles at 0422 (Figure 21g), the squall line had lost most of its characteristics and appeared as a circular area of showers. The intensity of the echoes continued to decrease as they moved away from the station, probably a result of range attenuation. By 0534 (Figure 21h), they had become a small area of showers. A few isolated showers continued until about 0730.

The computed movement of the cells in the center portion, 255° at 24 knots at 0210, was compared with the 0300 Pibals (Figure 20). The wind direction was fairly constant between 2000 ft and 30, 000 ft, varying between 230° and 260°. The wind speeds ranged Between 20 and 30 knots up to 20, 000 ft, then increased rapidly to 70 knots at 30, 000 ft. The 2, 000-26, 000-ft layer or the 2000-20, 000-ft layer should yield equally satisfactory results for correlation purposes since there was no frontal surface aloft, and the echoes probably did not extend above 20,000 or 25, 000 ft. Using nomograms presented in the wind study, the wind velocity from the movement of the echoes should be 250° at 27 knots for the 2000-26, 000-ft layer, and 245° at 22 knots for the 2000-20, 000-ft layer. The observed mean winds for the layers were 243° at 29 knots and 244° at 25 knots respectively. The 10, 000-ft level wind determined from the nomogram was 253° at 21 knots, while the observed wind was 230° at 23 knots.

The echoes to the south of Springfield were moving in the same direction as those in the center portion, but 6 knots slower, at a speed of only 18' knots. The Pibal reports indicated that lighter winds did exist in southern Illinois.

Conclusions

This case illustrates the utility of radar in detecting and tracking echoes for determination of the general wind field, echo intensity, storm movement and changes in atmospheric stability. It was also possible to detect an area of lighter winds by noting differences in the speed of movement of echoes. The aerologist should exercise judgment in doing this, however, since differences in the speed of movement of echoes may be a result of vertical extent rather than actual differences in the wind field.

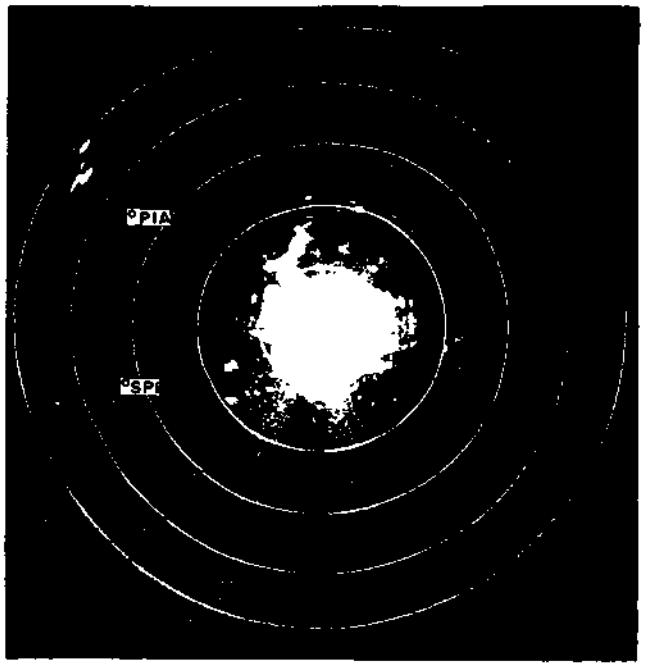

a. 2255 CST (8 AUG 52)

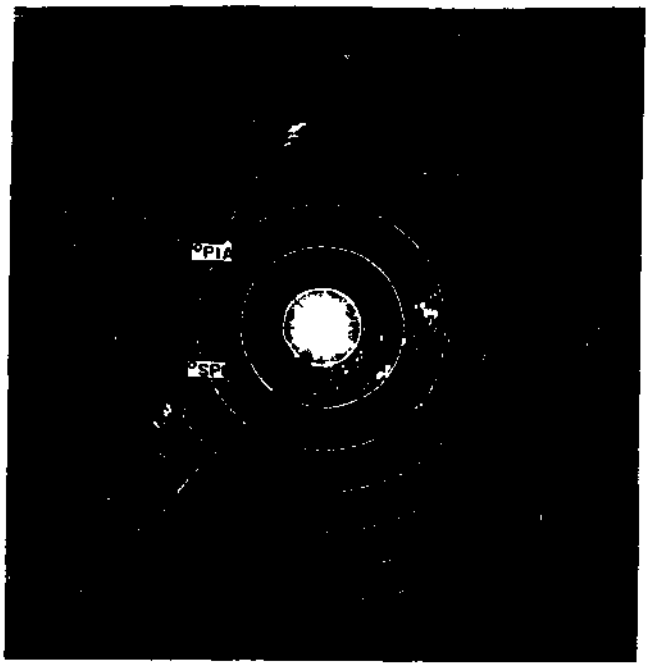

c. 0057 CST

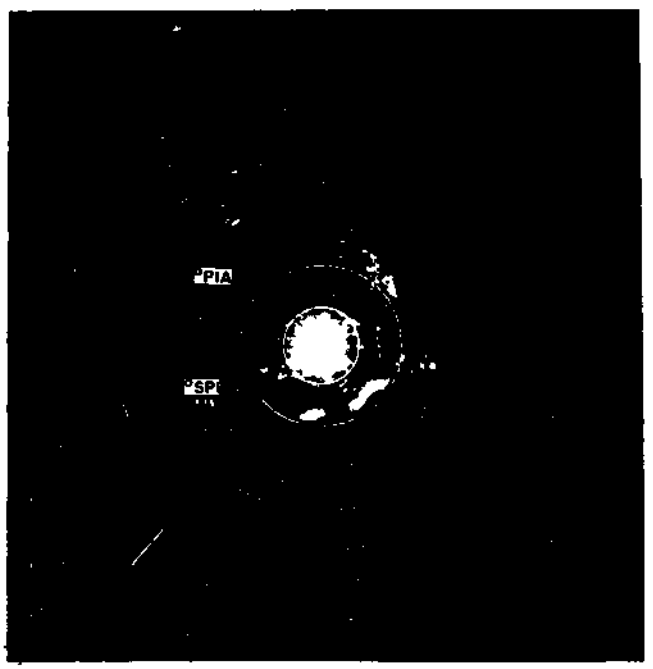

b. 0008 CST

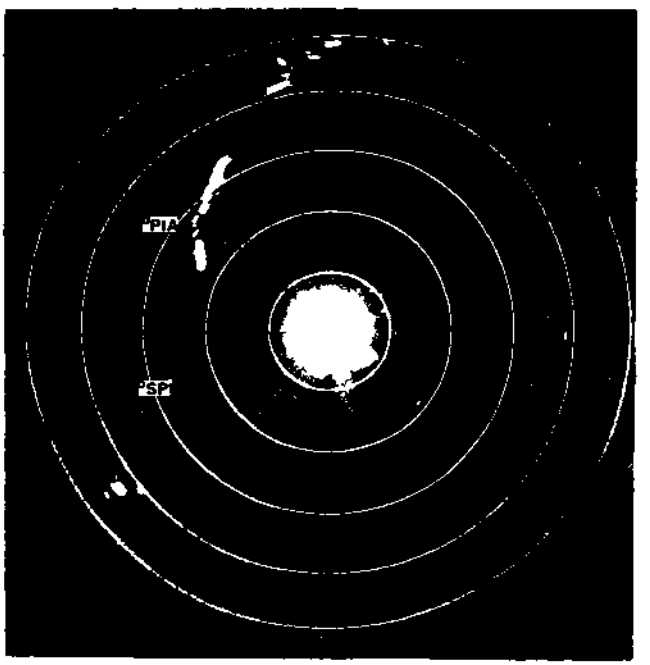

d. 0128 CST

FIG. 21 PREFRONTAL SQUALL LINE OF 8-9 AUGUST 1952
(20-MILE RANGE MARKERS)

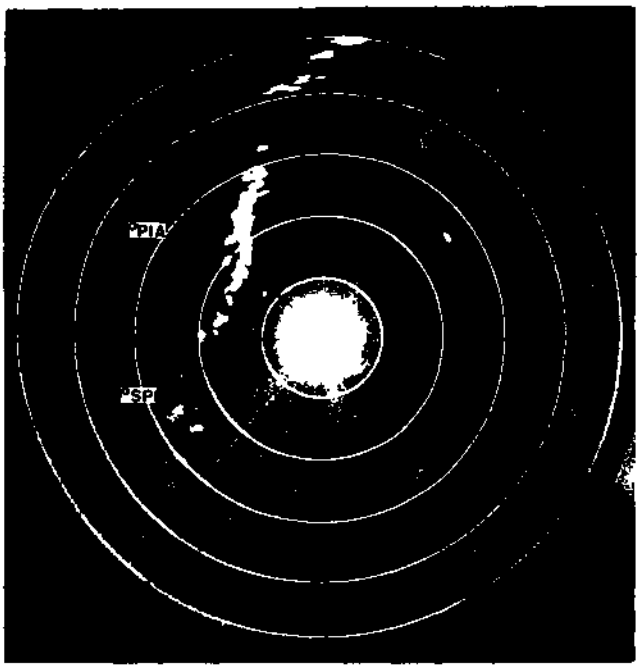

e. 0210 CST

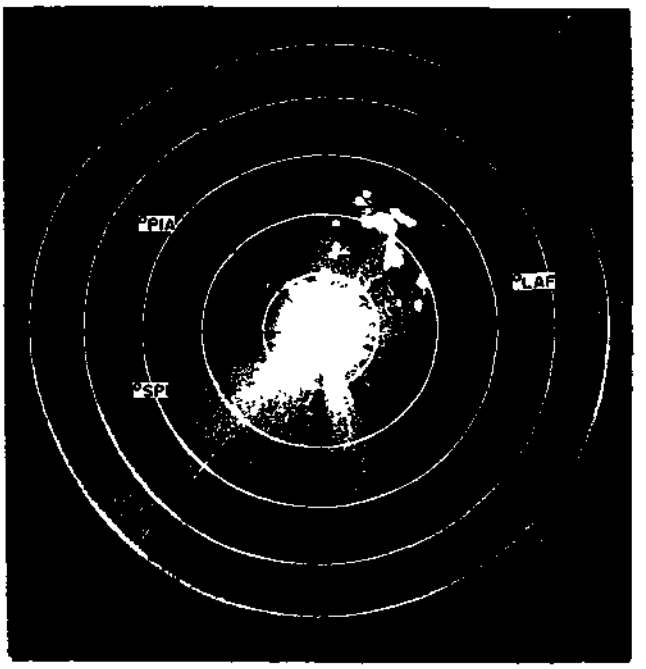

g. 0422 CST

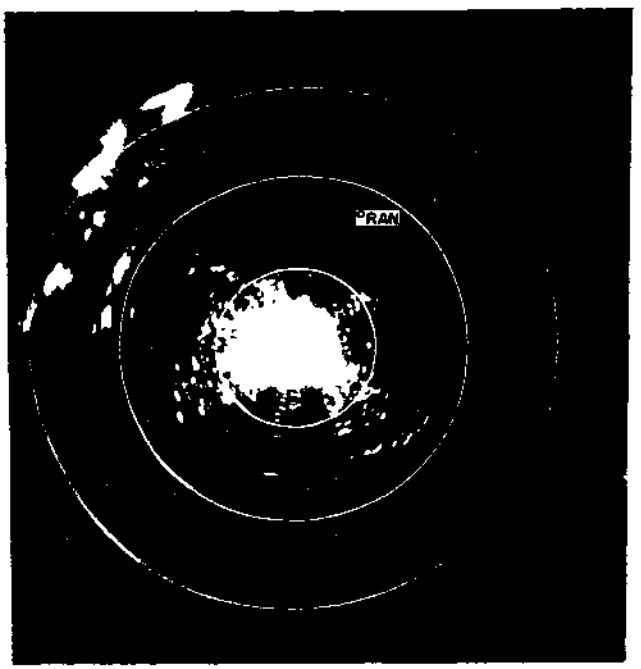

f. 0237 CST (10 MILE MARKERS)

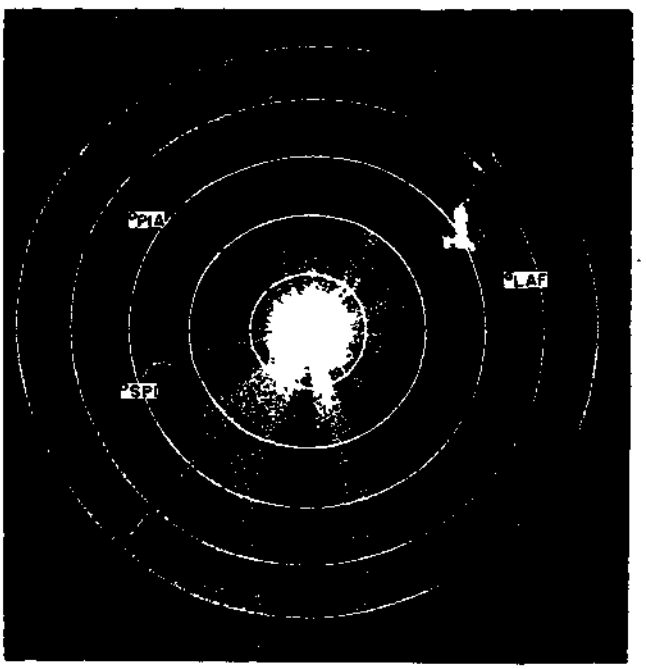

h. 0534 CST

FIG. 21 PREFRONTAL SQUALL LINE OF 8-9 AUGUST 1952
(20-MILE RANGE MARKERS UNLESS OTHERWISE INDICATED)

SHOWER FORMATIONS ON A STATIONARY FRONT

14 OCTOBER 1952

This case illustrates another situation where RHI data or supplementary surface synoptic data are needed in conjunction with PPI data to select the layer of best correlation for upper wind determinations. A large echo with severe surface weather conditions was detected as it passed over Decatur, Illinois. The utility of radar in ascertaining changing storm characteristics is shown. The detection and tracking of relatively intense precipitation zones' within areas of light rainfall is demonstrated, and the necessity for avoiding use of echoes in such zones for determining upper winds is illustrated.

Synoptic Situation and Weather Forecast

The weather map at 0630 (Figure 22) indicated a stationary front located along the Ohio River Valley. This front had passed the station the night before as a slow-moving cold front. The only precipitation with the front on the 0630 map was a past shower at Indianapolis, Indiana, but the Weather Bureau forecast called for occasional light rain showers and scattered light thundershowers for soutitern and central Illinois.

Discussion of Radar and Synoptic Data

The radar scope at 0815 showed no echoes. The radar was turned on again at 0930 and several echoes had developed in an E-W line, 40 to 95 miles southeast of the station (Figure 25a). By 0947 (Figure 25b), the number of showers had increased and spread westward, and a zone of showers extended from 40 miles south-southeast of the radar station to 20 miles west of Indianapolis (Ind.). There also was an echo 20 miles south of Springfield (SPI), and an echo only 25 miles southwest of the radar station (Figure 25b).

For determination of the direction and speed of upper winds, the 6000-30, 000-ft layer should correlate best in this case, since the slow-moving cold front had passed the station the night before, and a frontal surface should have been present aloft with the echoes based above this surface. RHI radar would have been very useful here for determining the cloud base, especially if nothing had been known about the synoptic situation. The movement of the echoes was from 240* at 37 knots. The use of the nomograms presented in the wind study gave a 6000-30, 000-ft layer mean wind of 250° at 38 knots. The mean wind velocity (Figure 23) for the 6000-30, 000-ft layer as determined from winds aloft charts was 249º at 43 knots, or a difference of 10° and 5 knots between the mean wind determined from echo movement and the observed mean wind. Neither of the two other layers or three levels gave good wind correlationa. The observed mean velocity for the 2000-20, 000-ft layer was 219° at 30 knots; the mean velocity for the 2000-26, 000-ft layer was 225° at 35 knots.

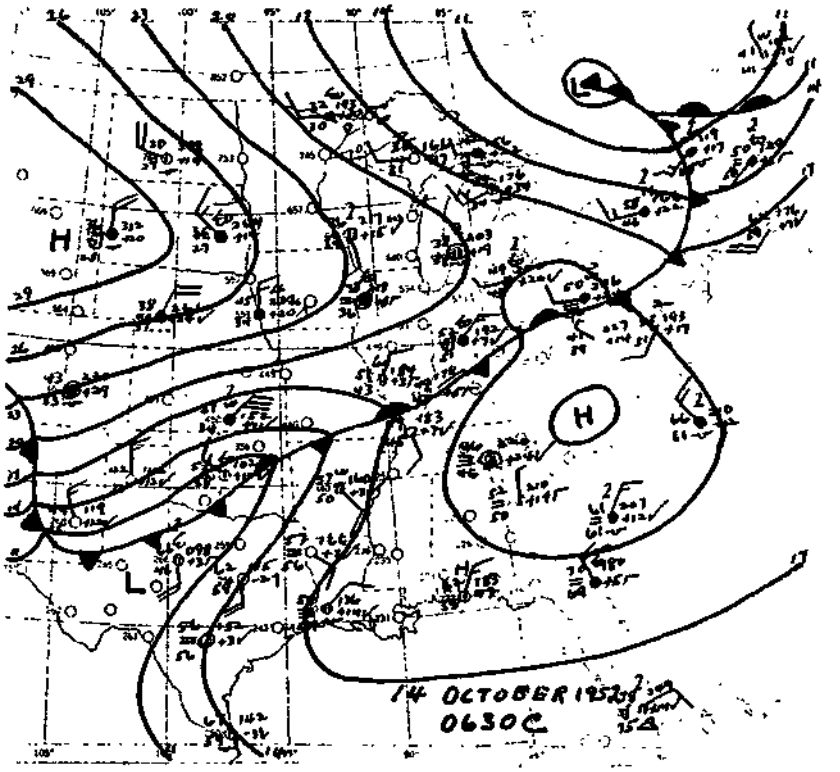

FIG. 22 14 OCTOBER 1952 0630CST SYNOPTIC CHART

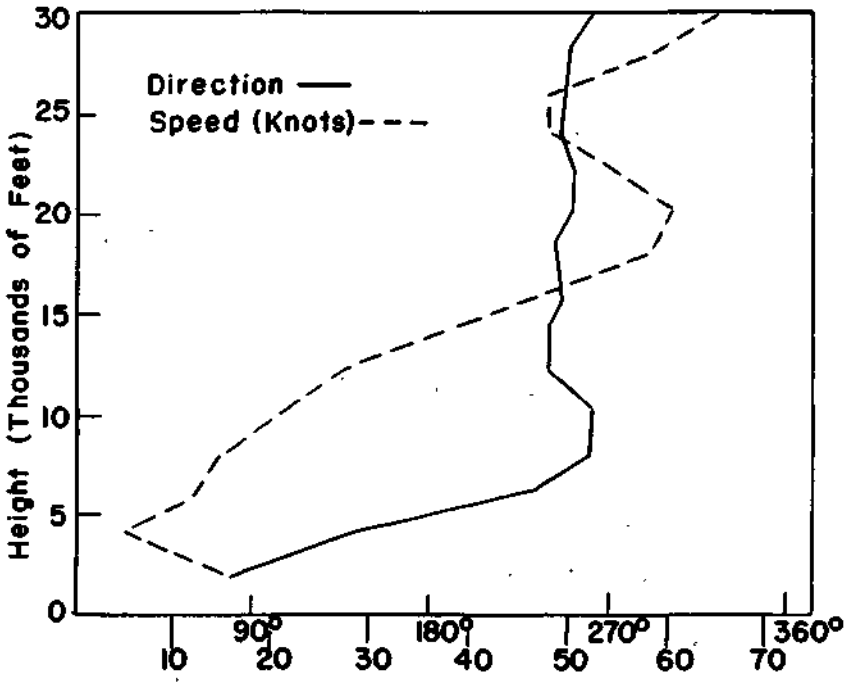

FIG. 23 14 OCTOBER 1952 0900CST WIND PROFILE

The time of arrival for the shower located 25 miles southwest of the station was computed to be 1020. Since the echo was very weak, the rainfall was expected to be very light. A brief shower did occur between 1015 and 1030, with only a trace of precipitation being recorded at the radar station. At 1057", the zone of showers, as indicated by the radar, was about 140 miles long and extended from 20 miles west of Springfield, to 20 miles north-northeast of Terre Haute (HUF), Indiana (Figure 25c). Another echo had developed only 15 miles southwest of the radar station, and it was computed that the center would pass a little northwest of the station. Light precipitation was expected to begin again at 1115.

The radar antenna was tilted to 15° elevation at 1058 and was left there until 1140 to collect echo data at close range. The maximum range at this elevation angle is about 20 miles, the center of the beam being about 30, 000 ft high at this range.

A light thundershower began at the station at 1112 and lasted until 1135 with 0. 02 in. of rain falling at the radar station. Quincy and Springfield reported a light rainshower and a light thundershower, respectively, on the 1130 hourly weather sequence, and Indianapolis reported a rainshower ending at 1101.

At 1140 (Figure 25d) the antenna was again lowered to zero elevation, and a large intense echo was located 30 miles west of the station, extending southward over Decatur (DEC), Illinois. The echo was about 40 miles long and eight miles deep, and larger in areal extent than most echoes produced by shower-type precipitation.

The automatic gain-reduction device indicated only one cell present in the southern half of this echo. Usually there are two or three cells within thunderstorms so that the existence of only one large cell may have been an indication of the storm intensity. The stepping switch also revealed a rather steep gradient of only three miles between the leading edge of the echo and the center of the cell, as shown by the radar. Attenuation of the radar beam prevented an accurate determination of the gradient on the trailing edge.

Studies made by Jones (7) and American Airlines (9), revealed that the severest turbulence was associated with steep gradients of radar echo contours, so that flight forecasts could have been issued to avoid this area. The Weather Bureau cooperative observer reported hail as the echo passed over Decatur. There was no recording raingage at Decatur to determine the storm rainfall rate but 0. 94 in. fell during the day.

As the same echo center passed the radar station, a pressure rise of 0. 17 in. was recorded, and a gust of 22 mph occurred with a preceding mean wind speed of 10 mph. The rainfall rate was 1. 5 in./hr with a total rainfall of 0. 26 in.

The ability to isolate storm areas and to determine changing characteristics was illustrated later in the day. Echoes continued to form in central Illinois and spread northward. During the late afternoon and evening, the character of the radar echoes changed from well-defined, shower-type echoes to poorly-defined echoes (Figure 25e), and finally merged into an area of general light rain with interdispersed heavier portions. The general rain was verified with 2030 reports. The precipitation area at that time covered central and northern Illinois and northern Indiana.

Several more intense areas were visible within the precipitation area. Between 2130 and 2215, a fairly well-defined line of echoes passed to the northwest of the station (Figure 25f). The computed echo movement was from 244° at 72 knots.

The 2100 Pibal reports (Figure 24) indicated veering winds from 010° at 24 knots at 2000 ft to 090° at 13 knots at 6000 ft. Above 6000 ft the wind direction was southwesterly. The wind speed did not reach 70 knots until the 16, 000-ft level, so that the echo speed must have been related to the winds near this level. The cloud base was probably at about 6000 ft where the frontal surface was located.

As mentioned in the wind study, natural seeding from high clouds may produce areas of more intense precipitation within areas of light rain. Natural seeding from clouds at or about 16, 000 ft could have been the reason for the fast movement of this line of echoes (11)(12).

The correlation of echo velocities and mean upper wind velocities for this line of echoes was very poor since the echo movement was related to the winds at a high level. However, it was pointed out in the wind study that cores of more intense precipitation within areas of light rain should be avoided for correlation purposes.

Conclusions

This case illustrates the use of radar in routine shortrange forecasting. Two unusual phenomena occurred: a severe thunderstorm and the rapid movement of a line of echoes. The movement of this line of echoes was related to the winds at 16, 000 ft.

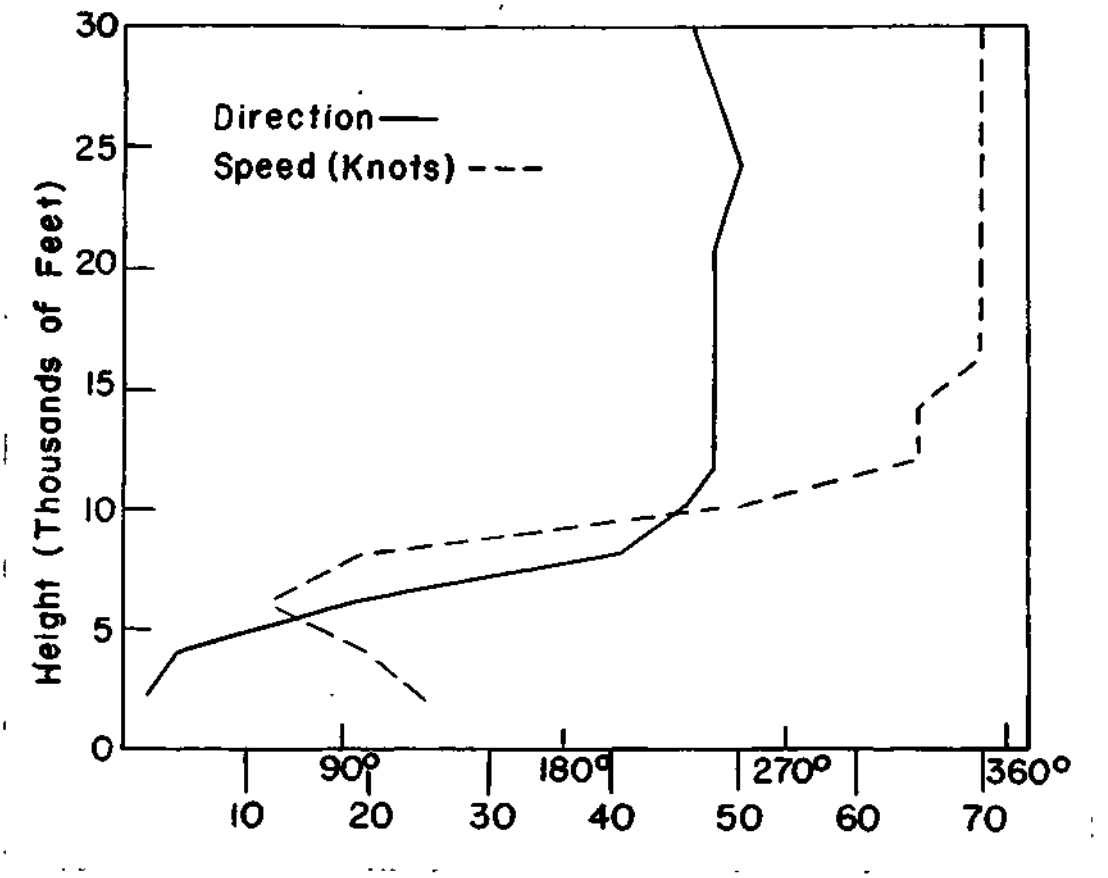

FIG. 24 14 OCTOBER 1952 2100CST WIND PROFILE

a. 0930 CST

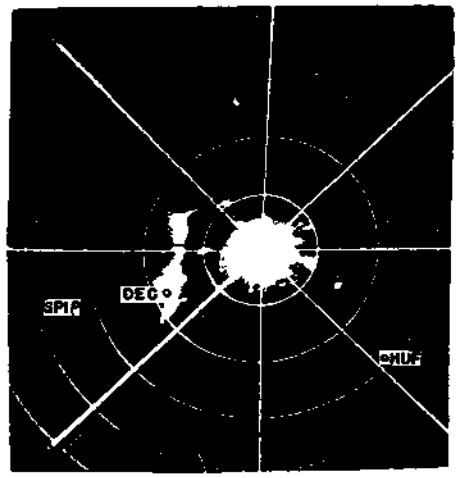

d. 1140 CST

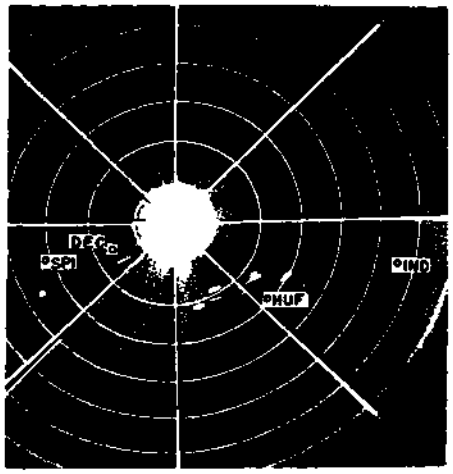

b. 0947 CST

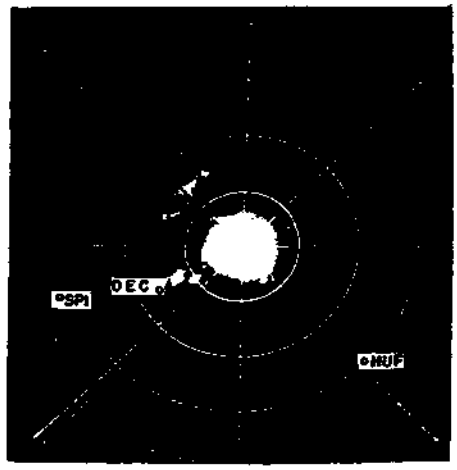

e. 2015 CST

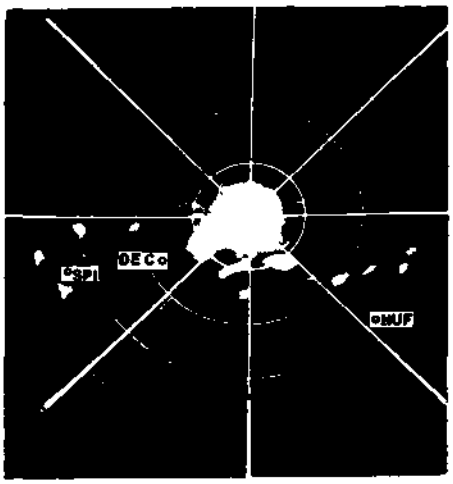

c. 1057 CST

f. 2150 CST (60 MILE MARKERS)

FIG. 25 SHOWER FORMATIONS ON A STATIONARY FRONT, 14 OCTOBER 1952 (20-MILE RANGE MARKERS UNLESS OTHERWISE INDICATED)

SQUALL LINE OF 17 NOVEMBER 1952 SHOWING EFFECTS OF ATTENUATION

This case is presented as an example of the effects of attenuation on low-powered, 3-cm radar equipment. An examination of hourly weather reports showed that what appeared to be an innocent-looking squall line was actually an area of widespread shower activity with only the leading edge visible. The movement of the squall line was very erratic and it dissipated as it moved into a low-level jet stream.

Synoptic Situation and Weather Forecast

The 1830 weather map of 17 November (Figure 26) showed a well-developed low center in eastern South Dakota with a warm front running eastward into central Wisconsin, and extending east-southeastward into Pennsylvania as a quasi-stationary front. A slow moving cold front was located southeastward from the low center through central Iowa, then south southwestward into western Missouri, through a weak low in eastern Oklahoma and into central Texas. This cold front was expected to move into western Illinois by 0630 of 18 November. Figure 27 gives the upper wind profile at 2100.

The weather Bureau 1600 forecast called for scattered light rainshowers and occasional light thundershowers spreading eastward through Illinois. Some locally heavy thunderstorms were also expected.

Discussion of Radar and Synoptic Data

A very weak echo, located 118 miles west of the station, appeared at 1650 (Figure 29a). The movement at 1726 (Figure 29b) was northeastward at about 45 knots. A definite velocity could not be determined due to the long range and weak intensity of the echo. More echoes formed and continued to develop, resulting in a squall line with a N-S orientation. By 1818, this squall line had reached its greatest length and intensity (Figure 29c). A new echo appeared at this time and was located 105 miles west of the station.

On the 1830 weather reports, Peoria (PIA) reported lightning in the west, Quincy, reported a light thunderstorm in progress, and Burlington, Iowa, reported a light rainshower.

The original squall line to the northwest showed definite signs of dissipation by 1836, while the new echo to the west had developed into another N-S squall line (Figure 29d). The new squall line continued to grow, and at 1905 the line was 70 miles long and very narrow, while the original squall line had almost completely dissipated (Figure 29e).

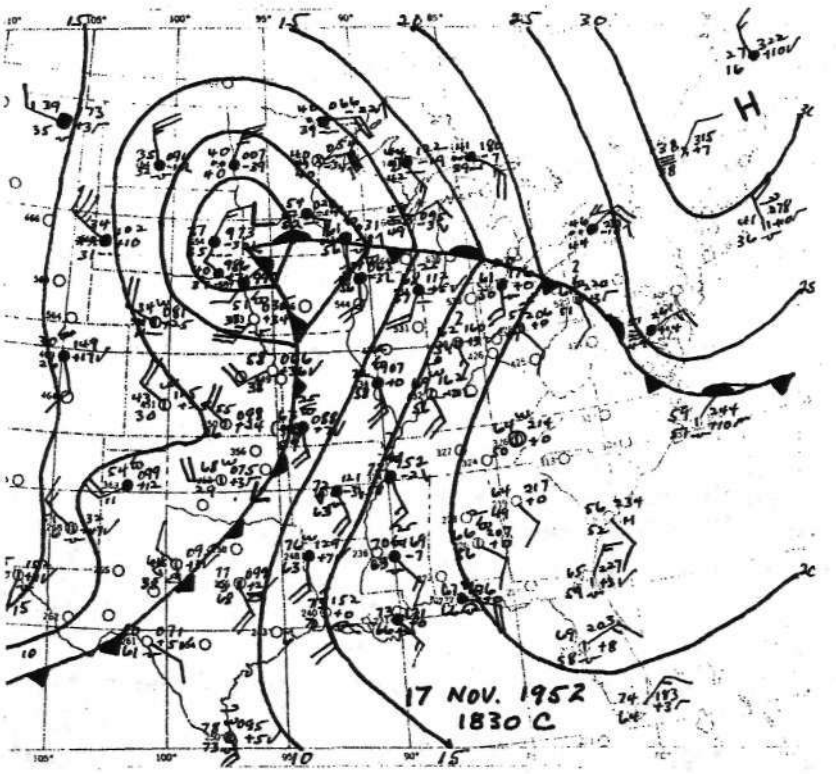

FIG. 26 17 NOV. 1952 I830CST SYNOPTIC CHART

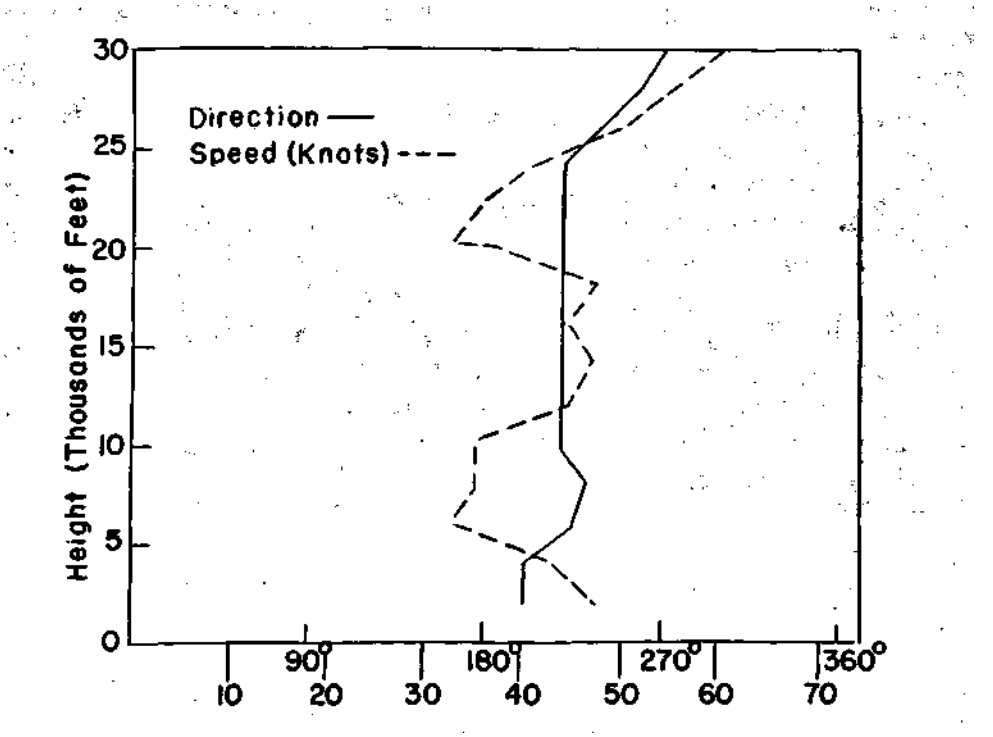

FIG. 27 17 NOV. 1952 2100CST WIND PROFILE

The computed movement of the individual cells of the new squall line was from 240° at 40 knots. The movement of the squall line was from 280° at 25 knots. Based upon these movements, the time of arrival of precipitation at the station was expected to be about 2210.

The areal extent of the squall line continued to increase as it approached the station, and the storm reached an overall length of 140 miles about 2020 (Figure 29f).

Although the radar indicated only a narrow band of precipitation, all the stations in Illinois west of this line reported light to moderate showers and thunder showers in progress on the 2030 weather sequence reports.

The showers in the leading edge attenuated the radar beam so that the showers to the rear were not visible. If low-powered, 3-cm equipment is used, as in this case, the absence of echoes behind a squall line does not necessarily indicate that showers are not occurring.

At 2122, the squall line was still located 30 to 40 miles west of the station, but was beginning to show a slight decrease inarealex tent(Figure 29g). The thunderstorms within the squall line were very distinct. It became apparent at this time that the movement of the squall line was becoming very erratic, having moved 40 miles between 1905 and 2020, but only 10 miles between 2020 and 2122, so that a definite forecast of the time of arrival could not be established. However, the utility of the radar was still appreciable since the exact position and intensity of the leading squall line and any changes in its characteristics were still easy to determine,,

The movement of the cells was computed to be 214° at 37 knots, a more southerly direction than the previously computed direction of 240° . The speed of movement of the individual cells was about the same as before. The decrease in speed of movement of the squall line and the resultant increase in the effect of the wind field on the cell movement probably is the explanation.

The range of the radar was reduced to 30 miles at this time to increase the detail of the showers within the squall line as they passed over the Illinois State Water Survey's network of 50 raingages. By 2150 (Figure 29h), the intensity of the echoes west of the station showed some signs of decreasing, and most of the squall line structure had dissipated by 2215 (Figure 29i). The nearest echo was only 12 miles west of the station. At this point, without any apparent reason the squall line ceased to advance.

Echoes were located around the station at 2353 (Figure 29j) and precipitation began shortly after in the form of light rainshowers and continued through the night with a total accumulation of 0. 44 in.

The computed movement of the cells at 2130 (214°, 37 knots) was compared with the 2100 Pibal reports (Figure 27). The variation in wind velocity through the first 25, 000 ft was such that the correlation of the direction and speed of movement of the cells and the mean winds was equally satisfactory for all three of the layers mentioned in the wind study. The average wind velocity for all three layers was about 220", 41 knots.

Isotachs (lines of equal wind speed) drawn on the 2000-ft (Figure 28) and 4000-ft level streamline charts indicated an area of maximum wind speed extending from southeastern Illinois into northwestern Indiana and central lower Michigan. The wind direction at these levels was parallel to the orientation of the squall line. It has been thought by some meteorologists that areas to the west of a northward-flowing, low-level jet are conducive to squall line formation because of the presence of cyclonic vorticity, and that squall lines would dissipate after they crossed the major axis of the jet because of the anticyclonic vorticity to the east. From this analysis it appears that this particular squall line dissipated as it moved into the center of the low-level jet.

Conclusions

This case indicates a number of interesting meteorological conditions. First, a weak squall dissipated while a second one developed and dissipated as they moved into the center of the low-level jet. Further studies are recommended to determine the exact influence of the low-level jet upon precipitation. Pronounced attenuation is present as surface reporting stations indicate rainfall while the radar did not detect such. A forecast of the time of arrival of rainfall was impossible due to the changing direction of movement of the cells and the deceleration and dissipation of the squall line. However, a forecaster without radar would not have had knowledge of this changing situation.

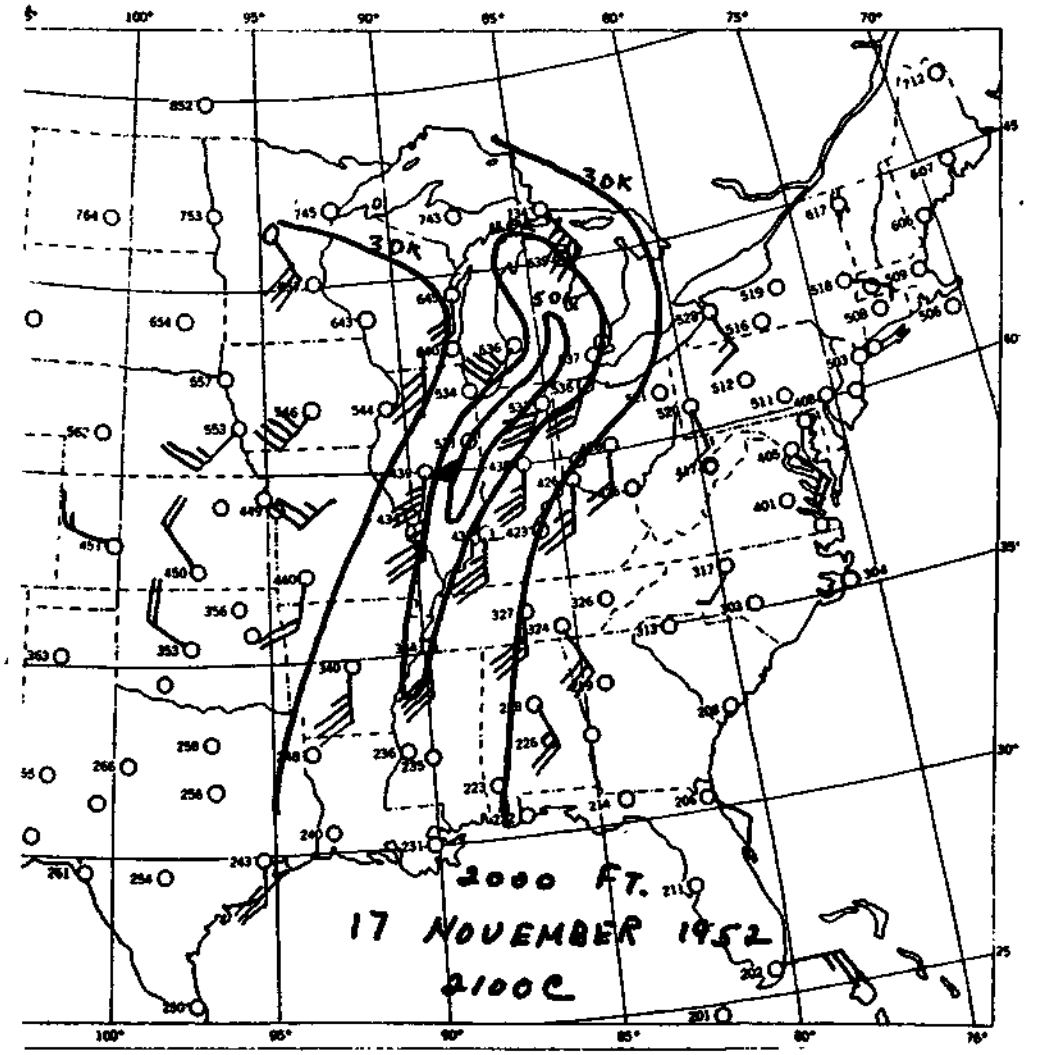

FIG. 28 17 NOV. 1952 2000-FT. WINDS 2100CST

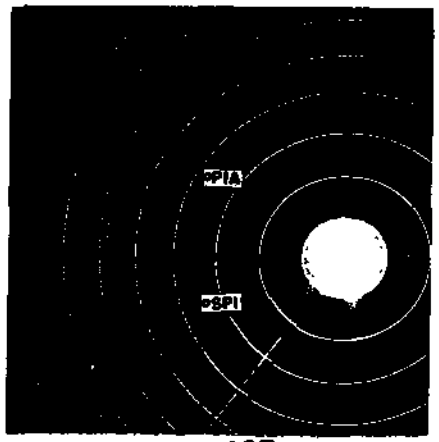

a. 1650 CST

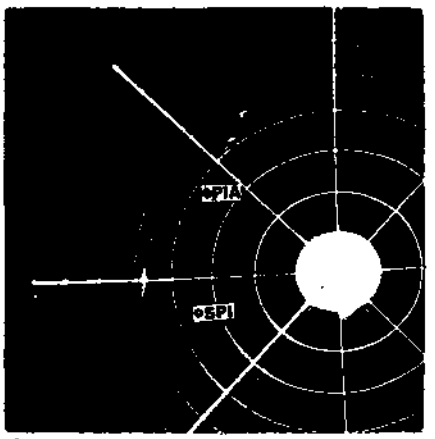

d. 1836 CST

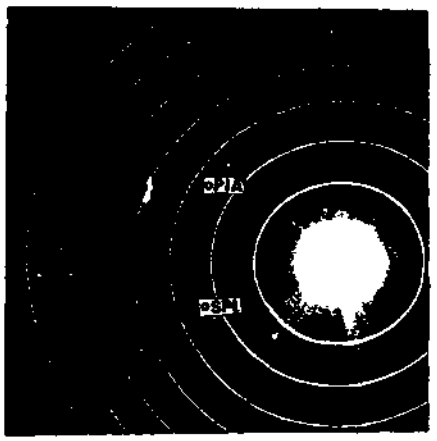

b. 1726 CST

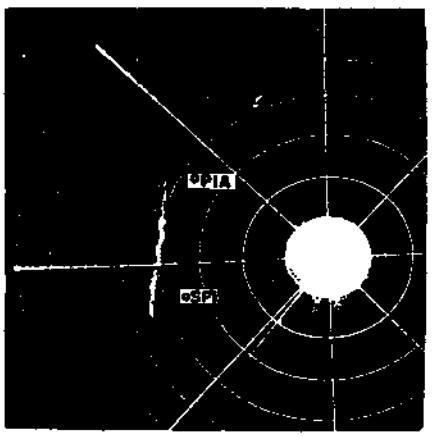

e. 1905 CST

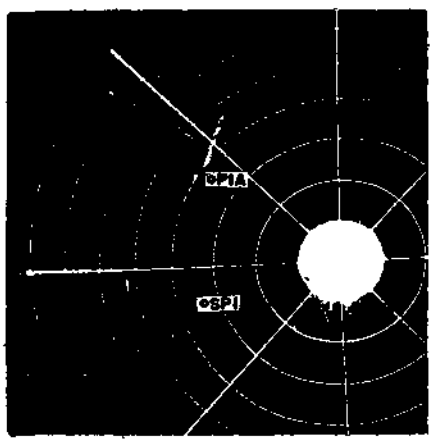

c 1818 CST

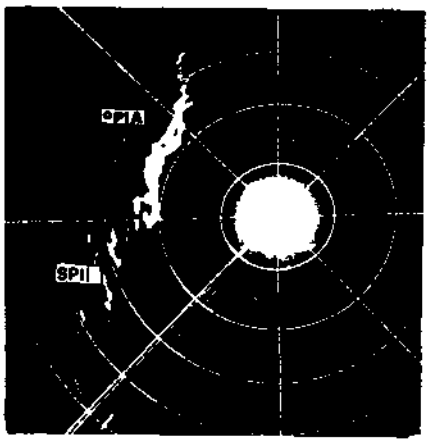

f. 2020 CST

FIG. 29 SQUALL LINE OF 17 NOVEMBER 1952, SHOWING EFFECT OF ATTENUATION (20-MILE RANGE MARKERS UNLESS OTHERWISE INDICATED)

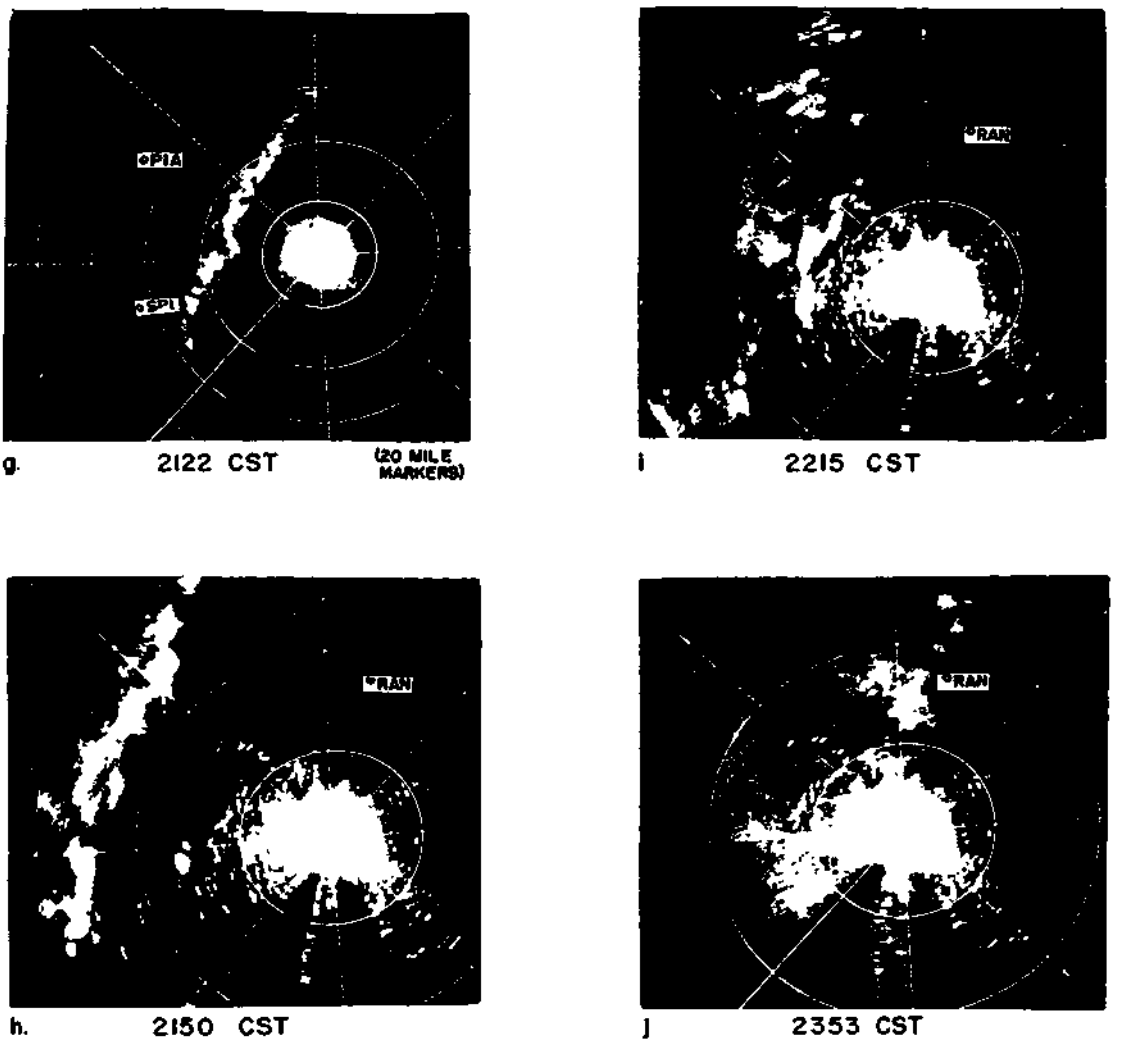

g. 2122 CST (20 MILE MARKERS)

i 2215 CST

h. 2150 CST

j 2353 CST

FIG. 29 SQUALL LINE OF 17 NOVEMBER 1952, SHOWING EFFECT OF ATTENUATION (10-MILE RANGE MARKERS UNLESS OTHERWISE INDICATED)

RADAR OBSERVATION OF A TORNADO OF 9 APRIL 1953

On 9 April 1953, the Illinois State Water Survey was fortunate to observe by radar the development, growth, and partial decay of a tornado that caused three million dollars in property damage and two fatalities.

Synoptic Situation

The surface weather map drawn from hourly sequence reports indicated a cold front lying about 70 miles west of the area of tornado formation in east central Illinois (Figure 30). The front was moving eastward at 25-30 knots. A low of 995 mb was located in the vicinity of Bradford, Illinois, about 100 miles northwest of the area where the tornado was first observed. A warm front extended eastward from the low across northern Illinois. The low center was deepening, moving rapidly northeastward, and occlusion was beginning to take place. Figure 31 gives the upper wind profile at 1500.

The tornado, which moved east-northeastward at about 45 knots, appeared to be associated with a squall zone in advance of the front. Reports from Weather Bureau stations and interrogation of residents in the tornado area indicated that rain and hail were occurring to the north of the tornado path, but no precipitation was falling in the immediate vicinity of the tornado.

The Chanute Air Force Base Weather Station, about eight miles north of the tornado, reported a heavy thundershower with hail.

Radar Data

The photographs in Figure 32 summarize the history of the tornado from its detection until it crossed the Indiana state line. All except the last photograph are on 30-mile range with 10-mile range markers.

The first photograph (1644) shows the radar precipitation echo of the cloud with which the tornado was associated, 15 minutes prior to the first detection of the tornado formation. The first appearance of an appendage on the southwest edge of the mother cloud is faintly visible in the second photo at 1700. The radar beam extended from the surface to an elevation of about 2000 ft at this time.

The next two photographs taken at 1705 and 1710 show progressive development of the tornado. In the photograph at 1713, taken about 13 minutes after the initial detection, development of a cyclonic curl becomes clearly evident at the south end of the appendage. Further cyclonic development is illustrated in the photographs at 1716 and 1719, and the appearance of an "eye" in the storm is discernible in the latter photograph. Observers

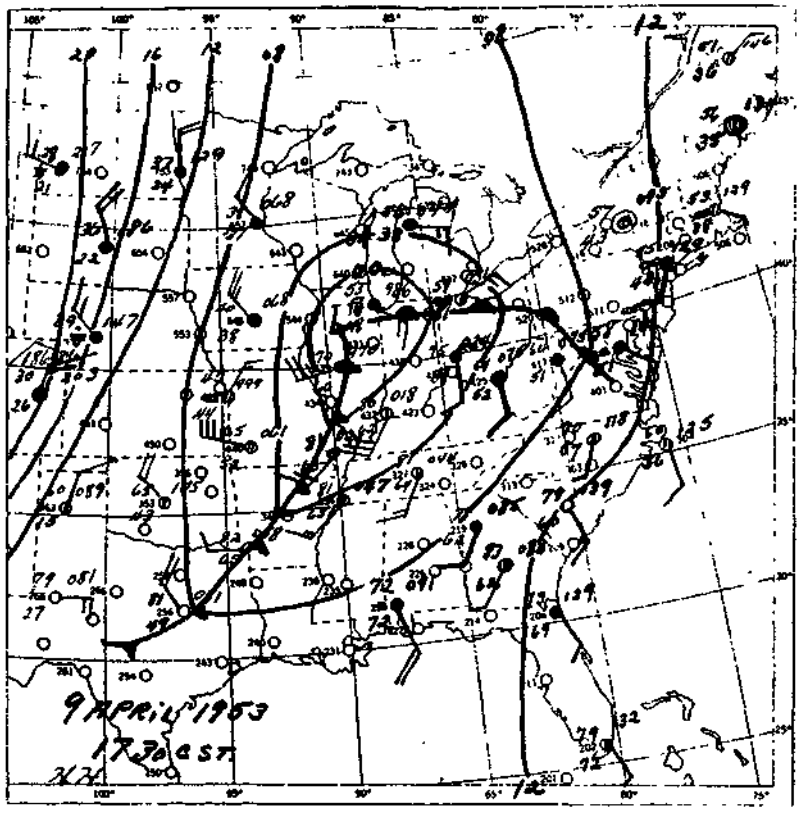

FIG. 30 9 APRIL 1953 I730CST SYNOPTIC CHART

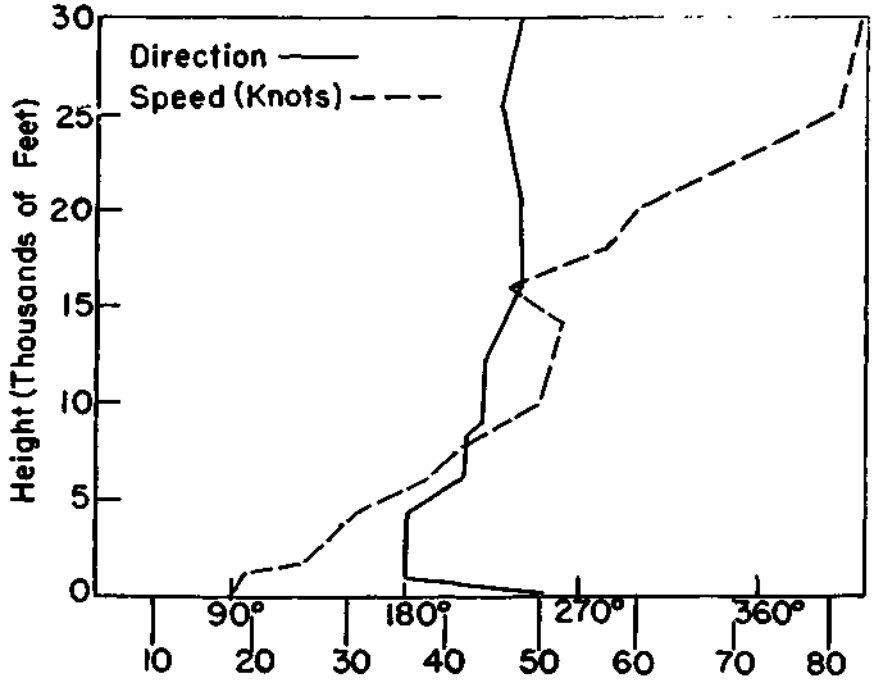

FIG. 31 9 APRIL 1953 I500CST WIND PROFILE

reported seeing the tornado extend from a cloud base straight to the ground. The position of this cloud was determined to have approximately coincided with the south end of the appendage seen on the radar.

The photograph at 1735 indicates that the mother cloud has decreased in size and has developed a spiral appearance. Meanwhile, the tornado echo has increased in areal extent. The photograph at 1738 is similar to 1735. At about this time (1738), the tornado was causing its greatest property damage in Illinois. The width and length of the tornado path was greater than reported for most tornadoes.

The last photo at 1800 shows 100-mile range with 20-mile range markers. Other precipitation echoes in the surrounding area are shown. The tornado was about 35 miles from the radar station at the time of this photograph.

The size of the cyclonic circulation, as shown by radar, and the width and nature of the path of destruction indicate that there may have been a tornado cyclone, as proposed by Brooks (20), having one or more funnels within. This small intense cyclonic circulation may have developed alongside the mother cloud and continued to grow until it began to envelop the mother cloud in its later stages.

Conclusions

This case shows that radar can detect tornadoes and show their development and movement, provided they are of sufficient size or have a peculiar circulation pattern of the above described type associated with them. Some smaller, less destructive tornadoes may also have circulation patterns associated with them that would be detectable with radar.

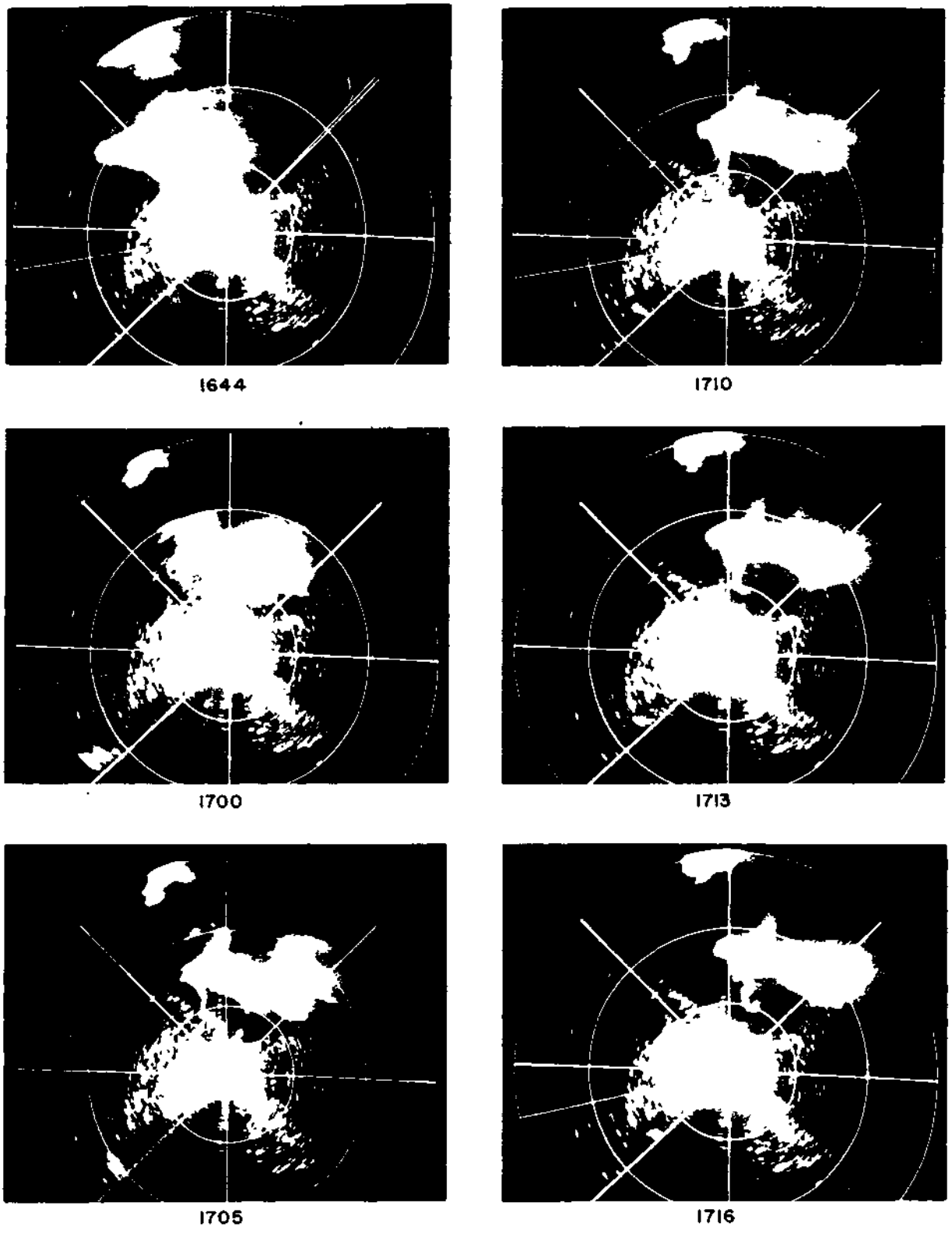

FIG.32 RADAR PPI PHOTOS WITH 10-MILE RANGE MARKERS; ILLUSTRATING TORNADO DEVELOPMENT ON 9 APRIL 1953.

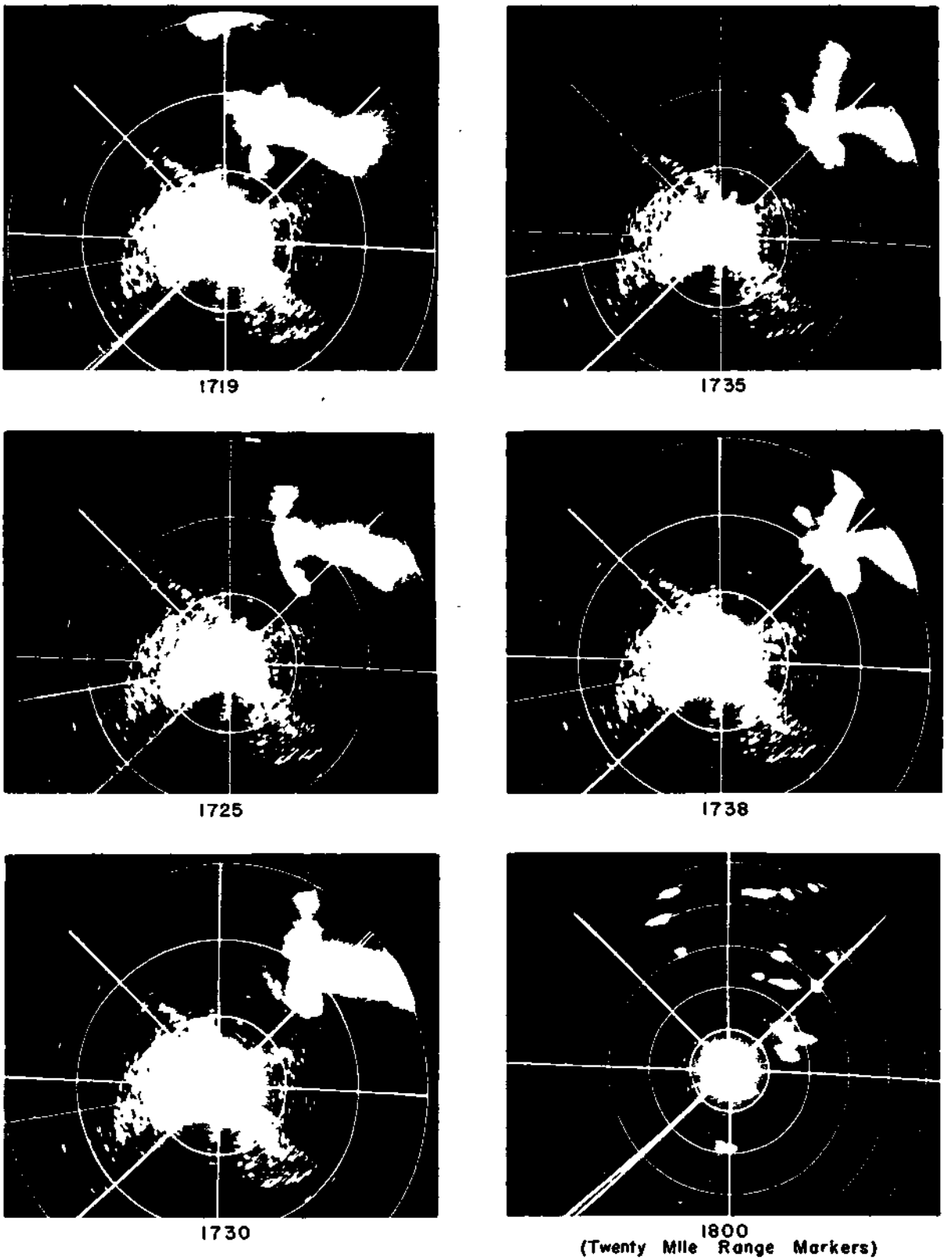

FIG. 32 CONTINUED DEVELOPMENT AND EAST-NORTHEAST MOVEMENT AT 45 MPH.

PARALLEL PRECIPITATION BANDS OF 17 APRIL 1953

This case illustrates the utility of radar for micro-synoptic studies by showing the structural features of precipitation as produced by upslope motion on a stationary front.

Synoptic Situation and Weather Forecast

The weather map at 0630, on 17 April (Figure 33) showed a major low center located between Lake Superior and James Bay. The cold front from this low extended across central Ohio, southern Indiana, and southern Illinois into a flat wave in southeast Kansas and then into another low center in the Texas Panhandle. The cold front had passed the radar station about midnight. Intermittent light snow and rain occurred at the radar station during most of the day.

The 1000 Weather Bureau regional forecast called for light snow showers and occasional sleet in portions of central Illinois and spreading eastward into central and southern Indiana and Ohio.

By 1230 the front had become quasi-stationary across the southern tip of Illinois and southern Indiana. A weak wave was present in southeast Kansas and southwest Missouri. Most of the stations in Illinois and Indiana were reporting light snow, light rain, or light freezing rain.

Discussion of Radar and Synoptic Data

The Chanute Field rawin and Springfield pibal for 0900 were not available. It was determined from the streamline charts that a shear zone at lower levels existed acr.oss central Illinois. This shear zone plus the absence of the above two wind observations, made it difficult to determine accurate wind computations, in the vicinity of the echoes, from the streamline charts. The mean winds, estimated from the streamline charts, for the layers 2000-20, 000 ft and 2000-26, 000 ft were 270º at 40 knots and 272º at 47 knots, respectively (Figure 34).

The radar set was turned on at 0955. There were some light, ill-defined echoes around the station to a distance of 30 miles. The precipitation was mostly in the form of light snow showers and located mainly to the south of the radar station. By 1024 (Figure 35a) the precipitation had formed WNW-ESE bands and was moving from 240º at about 28 knots, as computed from plots made at short intervals of time.

As mentioned in the wind study, such echoes in widespread areas of stable precipitation are not ideally suited for upper wind determinations unless the base and top of the echoes can be measured with RHI radar or estimated from synoptic conditions. In this case, the Chanute Field 0900

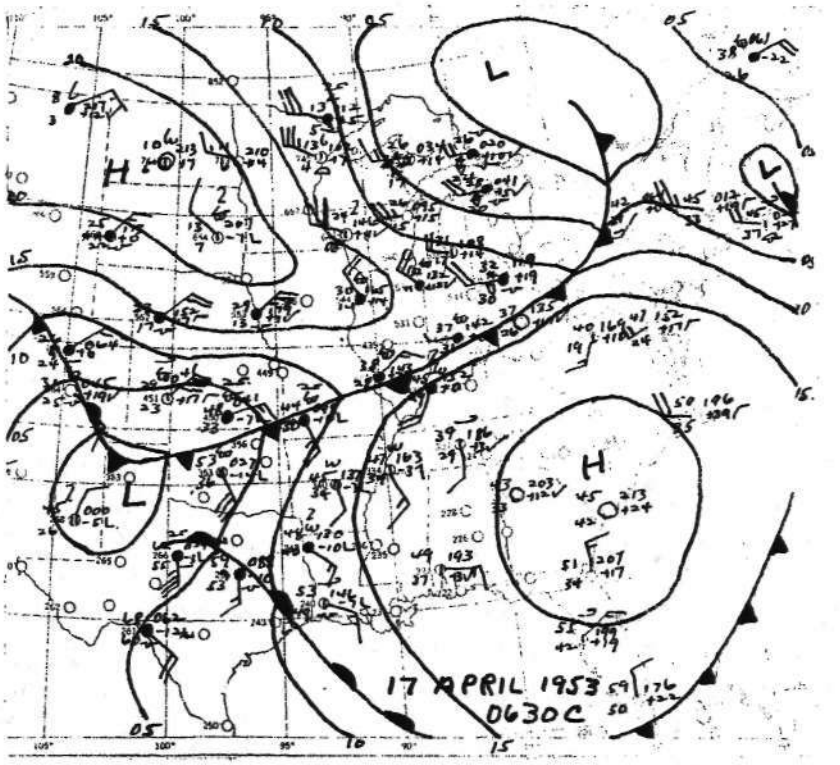

FIG. 33 17 APRIL 1953 0630CST SYNOPTIC CHART

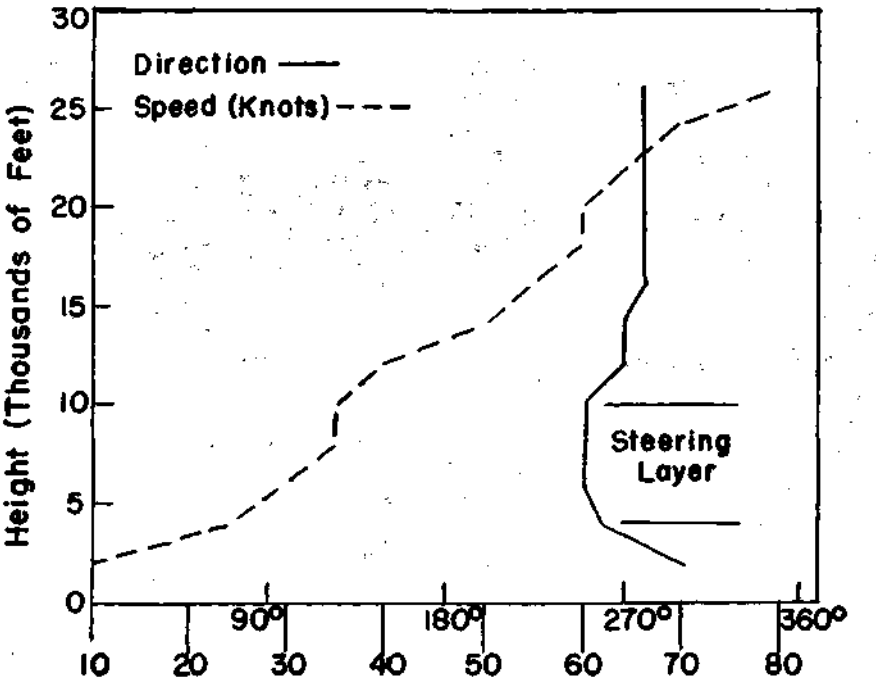

FIG. 34 17 APRIL 1953 0900CST WIND PROFILE

radiosonde showed the base of the frontal surface to be at about 3500 ft above sea level. The echoes were apparently in the warm air mass above this frontal surface. Although the streamline charts are questionable for the layer 4000-10, 000 ft, there are indications that the winds in this "steering" layer did agree with the echo movement. On the 1030 weather sequence, stations to the north and northeast, not reporting precipitation, were carrying ceilings of 6000-10, 000 ft. The WBAN facsimile weather charts showed the front to be located about 50 miles north of Chanute Field on the 850 mb chart and just south of Joliet, Illinois, on the 700 mb chart. This is further evidence that the cloud deck producing the precipitation was just above the frontal surface and sloped with it upward to the north and northeast.

In Figures 35a, b, and c, there may have been other WNW-ESE bands farther southwest of the station that were not visible due to attenuation by precipitation at radar station. It is interesting to note that the bands were oriented nearly perpendicular to the winds just above the frontal surface, and at an angle of about 40° to the frontal surface as seen in a horizontal plane projection. These bands may therefore be produced by wind-generated gravity waves on the frontal surface. A maximum of precipitation should occur near the crest of the waves and a minimum near the lowest points. It was not possible to prove this with the available weather records.

As the day progressed, the precipitation bands, as shown on the radar, began to shift slowly to an E-W orientation (Figures 35 d, e, f, g, and h) and finally shifted to a ENE-WSW orientation and decreased in speed by 2200 (Figure 35 i, j, k, and 1). This change in orientation agrees with the change in the winds above the frontal surface. By 2100, the winds for the layer 4000-8000 ft over southern and central Illinois had backed to a southerly or south-southeasterly direction and decreased in speed. By late evening the 4000-8000 ft winds were blowing nearly perpendicular to the stationary front, and the bands were oriented nearly parallel to the front and perpendicular to the winds.

A pilot report, 40 miles southeast of Vichy, Missouri, and 240 miles southwest of the radar station, gave the top of the overcast as 10, 000 ft at 1540. This agrees with the radar and wind data, indicating that the cloud decks did not extend to great heights, in which case, they would have been influenced by the strong westerly winds above 10, 000 ft.

Figure 35 i, j, k, and 1 indicates that the bands were moving slowly or nearly stationary. Also, early in the day the bands appeared to move slower than the winds blowing perpendicular to them. If wind-generated gravity waves on the frontal surface were responsible for the banded precipitation, then it is likely that the ripples were in the nature of standing waves and drifted downstream slowing rather than moving with the wind.

As mentioned ealier, the winds above the frontal surface decreased in speed in the same manner that the echoes decreased in speed. However, at all times the echoes appeared to move slower than the winds.

Conclusions

This case presents the effects of winds in a "steering layer" upon the echo movement. Parallel bands of precipitation aire shown to exist approximately perpendicular to the winds in the steering layer. These bands are explained by wind-generated gravity waves on the frontal surface, which drift downwind at a speed less than that of the winds. A changing of orientation of these precipitation bands' is shown to agree with the slowly backing winds. This case particularly illustrates how synoptic and radar data can supplement one another.

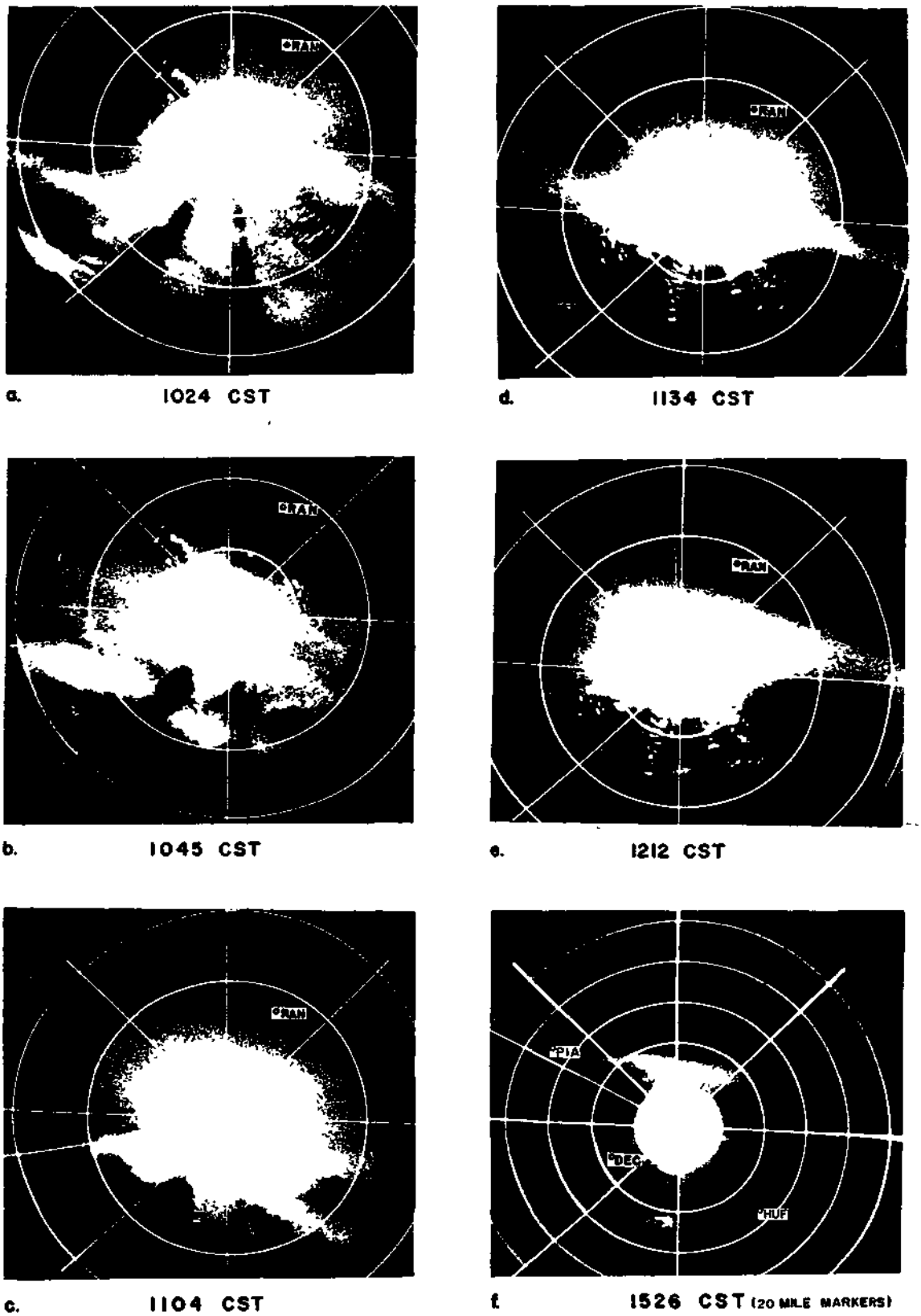

FIG. 35 PARALLEL PRECIPITATION BANDS OF 17 APRIL 1953
(10-MILE RANGE MARKERS UNLESS OTHERWISE INDICATED)

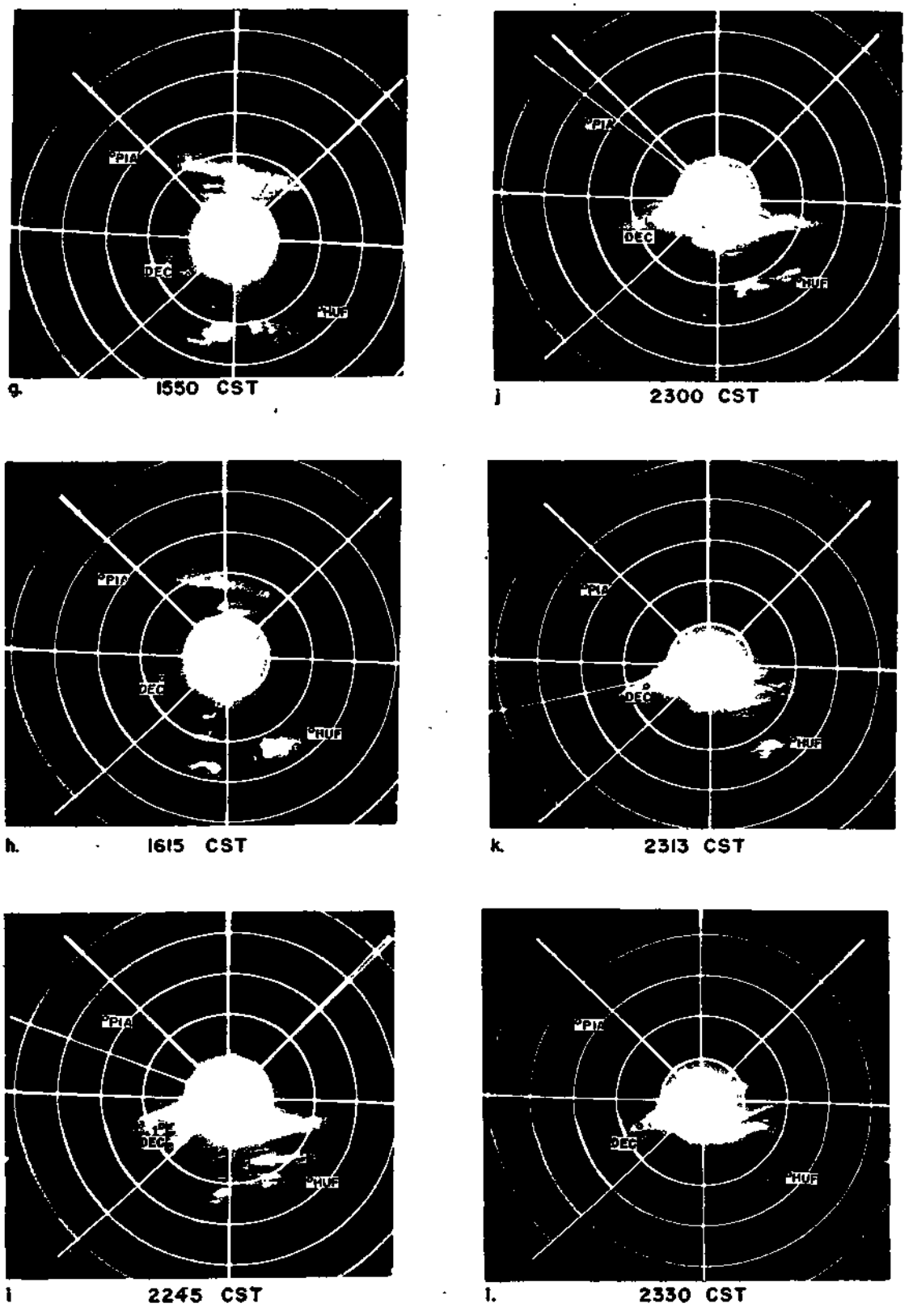

FIG. 35 PARALLEL PRECIPITATION BANDS OF 17 APRIL 1953
(20-MILE RANGE MARKERS)

LIST OF REFERENCES

1. Wexler, R., "Theory and Observation of Radar Storm Detection," Compendium of Meteorology, 1951, pp. 1283-1289..

2. Wexler, R. and Swingle, D.M., "Radar Storm Detection, " Bulletin American Meteorological Society, 1947, 28:159-167.

3. Ligda, Myron G. H., "Radar Storm Observation, " Compendium of Meteorology, 1951, pp. 1265-1282.

4. Wexler, R., "Rain Intensities by Radar, " Journal of Meteorology, Vol. 5, No. 4, August 1948, pp. 171-173.

5. Lawson, J. L. and Uhlenbeck, G. E., Threshold Signals, Massachusetts Institute of Technology Radiation Laboratory Series, McGraw-Hill Book Company, Inc., New York, Vol. 25, 1950, p. 142.

6. Coons, Richard D., "Guided Propagation of Radar in Thunderstorm Conditions, " Bulletin American Meteorological Society, Vol. 28, No. 7, September 1947, pp. 324-329.

7. Jones, R. F., The Relation between the Radar Echoes from Cumulus and Cumulonimbus Clouds and the Turbulence Within Those Clouds, Meteorological Research Paper 484, British Air Ministry Meteorological Office, 14 April 1949.

8. Byers, H. R. and Collaborators, The Thunderstorm. U. S. Government Printing Office, Washington, D. C., June 1949.

9. Ayer, R. W., White, F. C., Armstrong, L. W., The Development of an Airborne Radar Method of Avoiding Severe Turbulence and Heavy Precipitation in the Precipitation Areas of Thunderstorms and Line Squalls, American Airlines, 1949, BuAer Contract NDa(s)-9006.

10. Stout, G„ E., Neill, J. C., and Farnsworth, G. W., Rainfall-Radar Studies of 1951, State Water Survey, Report of Investigation No. 19, "1953".

11. Rex, Daniel F., "An Operational Use of Weather Radar, " Proceedings of the Third Radar Weather Conference, Montreal, Canada, 15-17 September 1952, pp. C17-C20.

12. Hiser, H. W. and Bigler, S. G., Wind Data from Radar Echoes,. Technical Report No. 1, under Navy BuAer contract No. 189s-88l64 with Illinois State Water Survey, Urbana, Illinois, 26 March 1953.

13. Brooks, H. B„ , "Summary of Some Radar Thunderstorm Observations," Bulletin American Meteorological Society, Vol. 72, No. 10 December 1946, pp. 557-563.

14. Ligda, Myron G. H. , "Horizontal Motion of Small Precipitation Areas as Observed by Radar", Proceedings of the Third Radar Weather Conference, Montreal, Canada, 15-17 September 1952, pp. D41-D48.

15. Cunningham, R. M. , "Some Observations of Natural Precipitation Processes, " Bulletin American Meteorological Society, Vol. 32, No. 9, November 1951, pp. 334-343.

16. Hudson, H. E., Jr. , Stout, G. E., and Huff, F. A. . Studies of Thunderstorm Rainfall with Dense Raingage Networks and Radar, State Water Survey, Report of Investigation No. 13, 1952.

17. Spilhaus, A. F. , "Drop Size, Intensity, and Radar Echo of Rain, " Journal of Meteorology, Vol. 5, No. 4, August 1948, pp. 161-164.

18. Private communication between the Project's Group Leader and David Atlas, Geophysical Research Directorate, Cambridge Air Force Research Center, Cambridge, Massachusetts.

19. Tepper, M. , "A Proposed Mechanism of Squall Lines - The Pressure Jump Line, " Journal of Meteorology, Vol. 7, No. 1, 1950, pp. 21-29.

20. Brooks, E. M. , "Tornadoes and Related Phenomena, " Compendium of Meteorology, 1951, pp. 673-680.